WashU

Based on I. Bigaran, B. Dev, **DLG**, P. Machado [2406.20067; PRD **111**, 113004 (2025)]

Tau Tridents at Accelerator Neutrino Facilities

Multi-Particle Reactions Workshop

University of California Berkeley

July 30, 2025

Diego Lopez Gutierrez

What are neutrino tridents and why do we care?

Neutrino Tridents $\nu_\ell N \to \nu_{\ell'} \ell \ell' N$

Neutrino Tridents $\nu_\ell N \to \nu_{\ell'} \ell \ell' N$

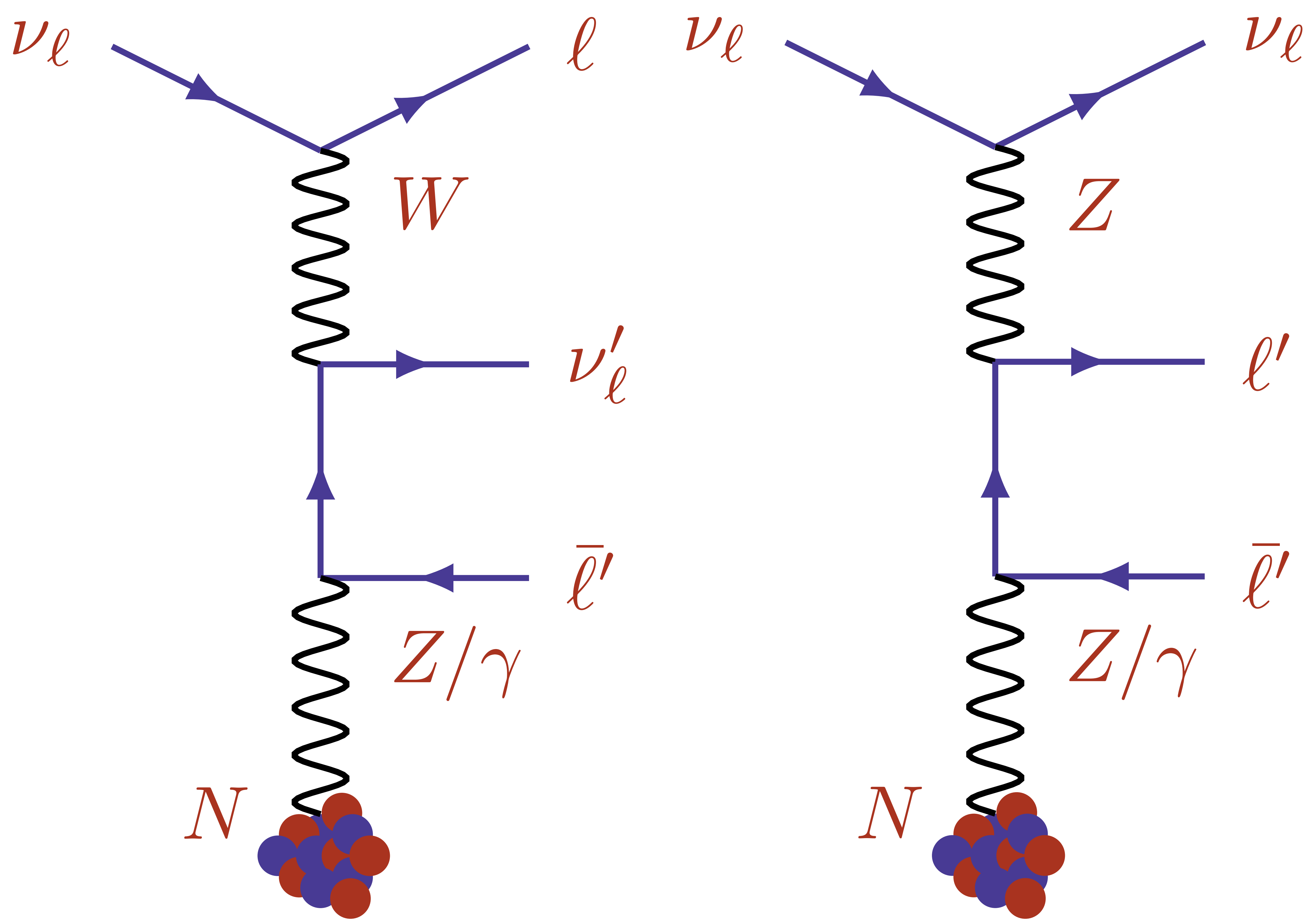

Charged Current **Neutral Current**

Precision test of the electroweak sector

Neutrino Tridents $\nu_\ell N \to \nu_{\ell'} \ell \ell' N$

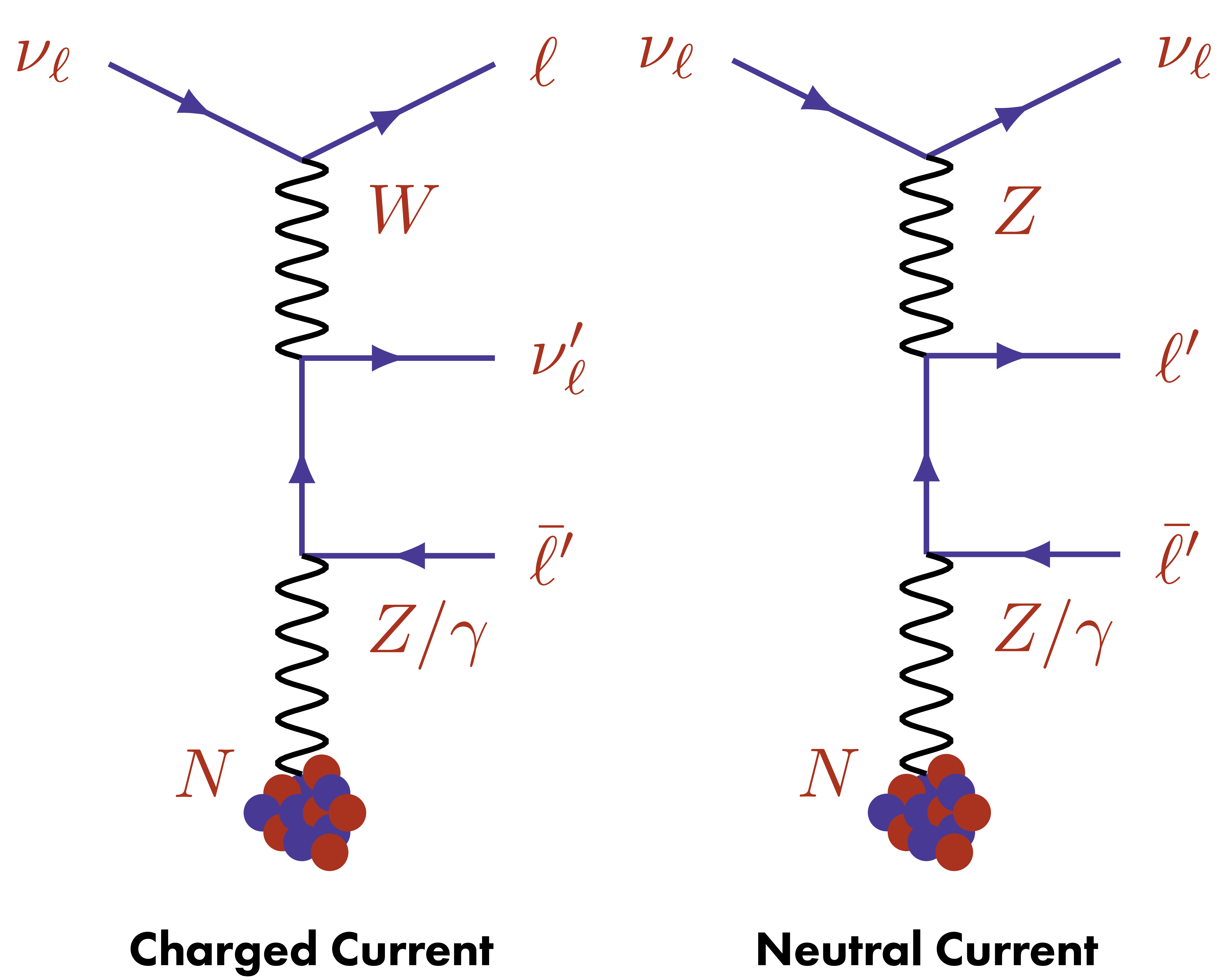

Precision test of the electroweak sector

$\nu_\mu N \to \nu_\mu \mu^+ \mu^- N$: Charm-II (~55), CCFR (~37); NuTeV. Consistent with SM. No e or τ tridents ever observed!

Neutrino Tridents $\nu_\ell N \to \nu_{\ell'} \ell \ell' N$

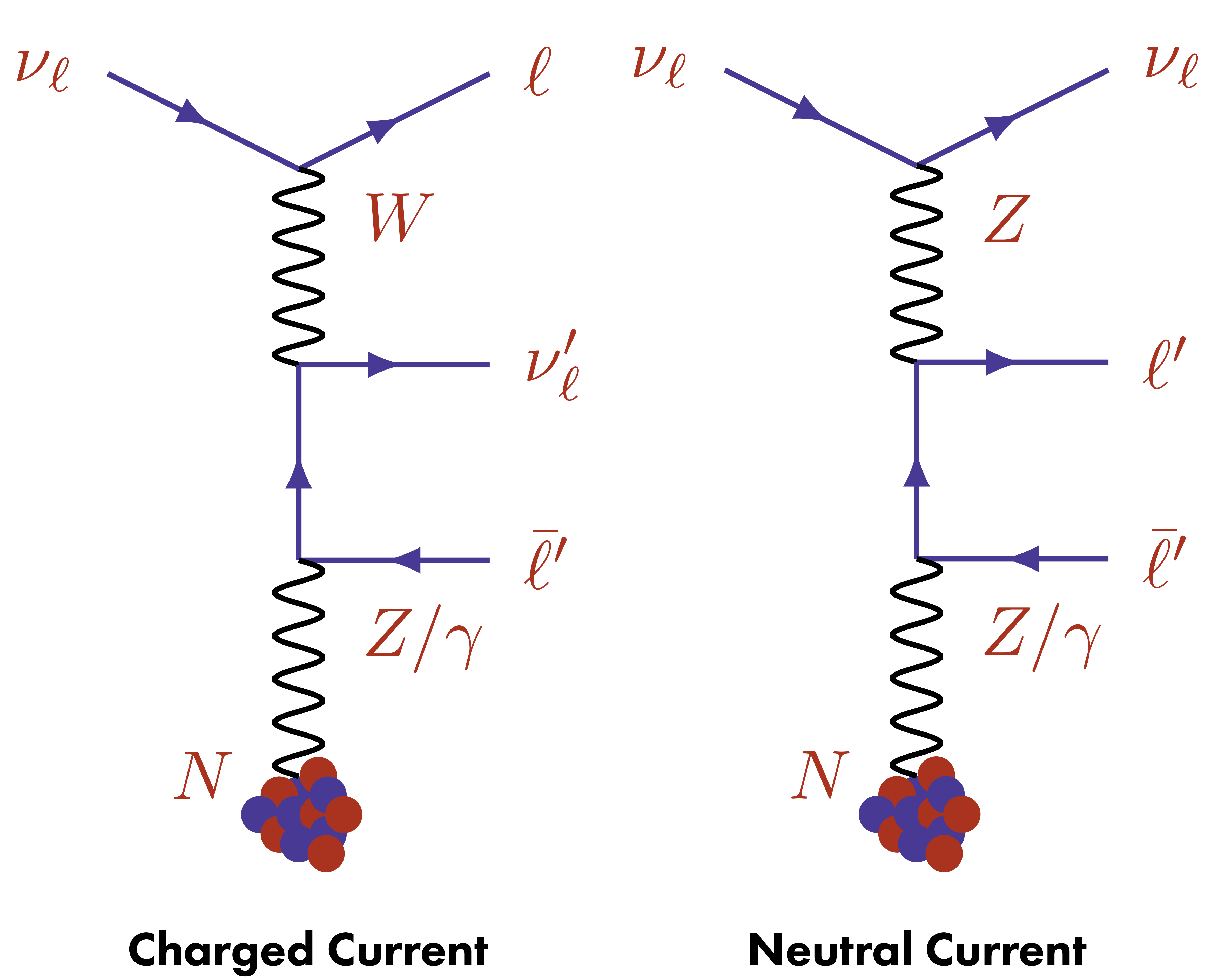

Precision test of the electroweak sector

$\nu_\mu N \to \nu_\mu \mu^+ \mu^- N$: Charm-II (~55), CCFR (~37); NuTeV. Consistent with SM. No e or τ tridents ever observed!

Standard Model

- ν_τ: DONuT (~9), OPERA (~10).
- τ in SM: D meson decay or ν-oscillations. *Anomalous* for DUNE ND.
- τ tridents as "new" source.

Neutrino Tridents $\nu_\ell N \to \nu_{\ell'} \ell \ell' N$

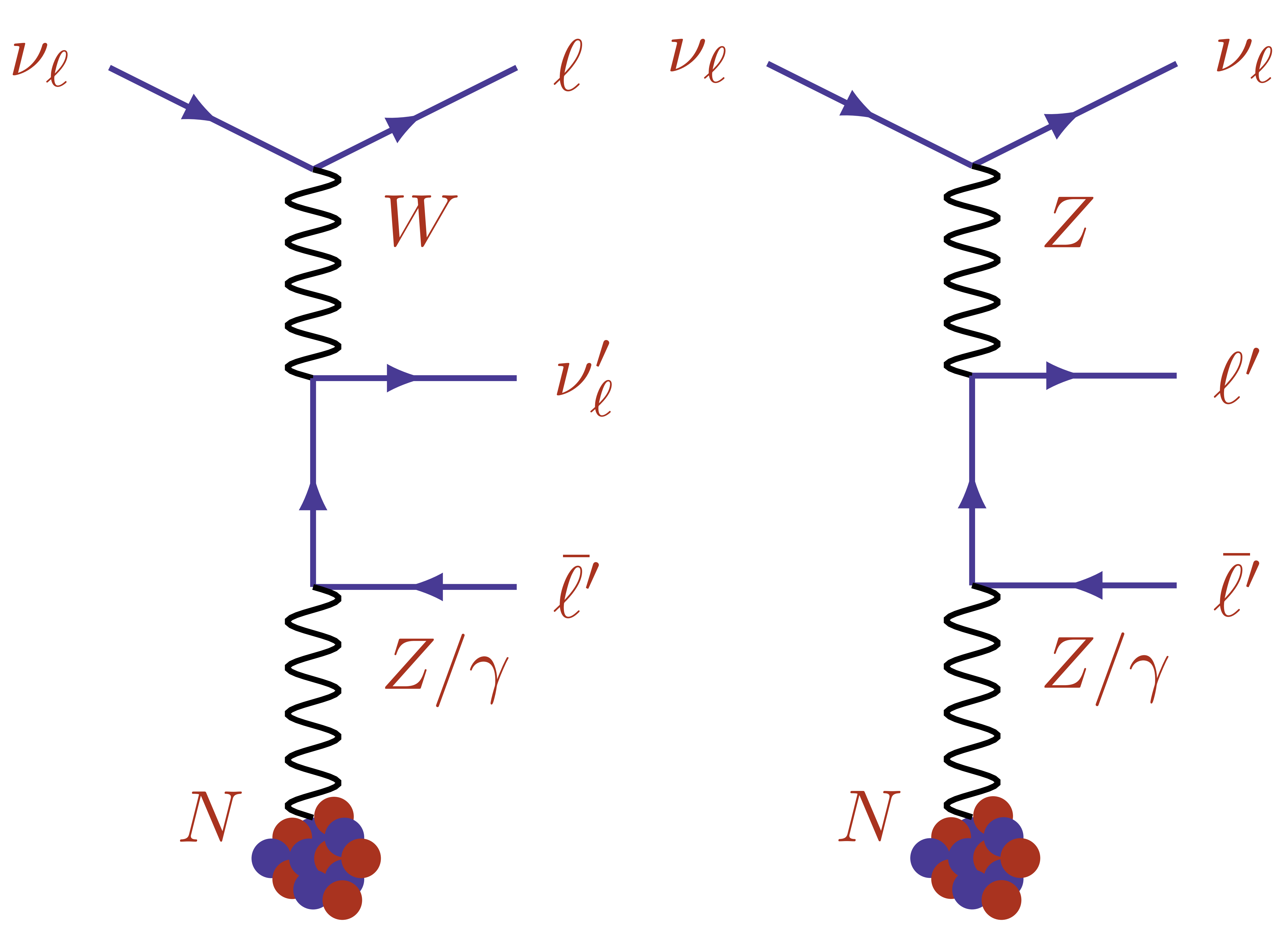

Charged Current **Neutral Current**

Precision test of the electroweak sector

$\nu_\mu N \to \nu_\mu \mu^+ \mu^- N$: Charm-II (~55), CCFR (~37); NuTeV. Consistent with SM. No e or τ tridents ever observed!

Standard Model

- ν_τ: DONuT (~9), OPERA (~10).
- τ in SM: D meson decay or ν-oscillations. *Anomalous* for DUNE ND.
- τ tridents as "new" source.

Beyond the Standard Model

- Charged LFV: Tridents with $\ell \neq \ell'$ as backgrounds.
- Final-state ν_τ in BSM: $L_\mu - L_\tau$, $B - L$, Z', ν_s -oscillations.

Trident Calculation

Based on [1902.06765]

Trident Calculation

Based on [1902.06765]

Accelerator ν experiments: $Q_\nu^2 \ll M_{W/Z}^2$

Trident Calculation

Based on [1902.06765]

Accelerator ν experiments: $Q_\nu^2 \ll M_{W/Z}^2$

γN dominant for $E_\nu < 10^8$ GeV

Trident Calculation

Based on [1902.06765]

Accelerator ν experiments: $Q_\nu^2 \ll M_{W/Z}^2$

γN dominant for $E_\nu < 10^8$ GeV

Avoid Equivalent Photon Approximation

Trident Calculation

Based on [1902.06765]

Accelerator ν experiments: $Q_\nu^2 \ll M_{W/Z}^2$

γN dominant for $E_\nu < 10^8$ GeV

Avoid Equivalent Photon Approximation

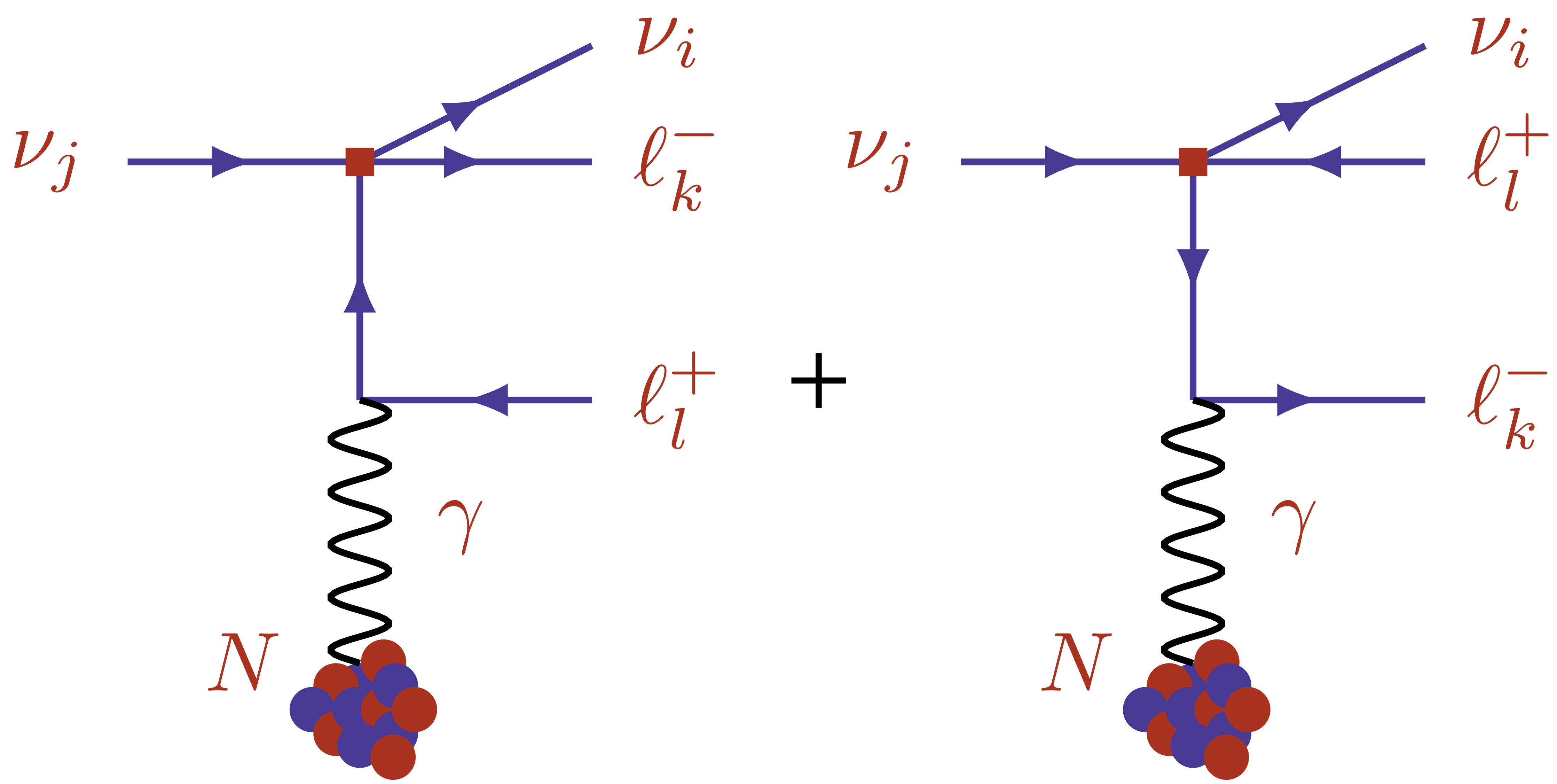

Trident Calculation

Based on [1902.06765]

Accelerator ν experiments: $Q_\nu^2 \ll M_{W/Z}^2$

γN dominant for $E_\nu < 10^8$ GeV

Avoid Equivalent Photon Approximation

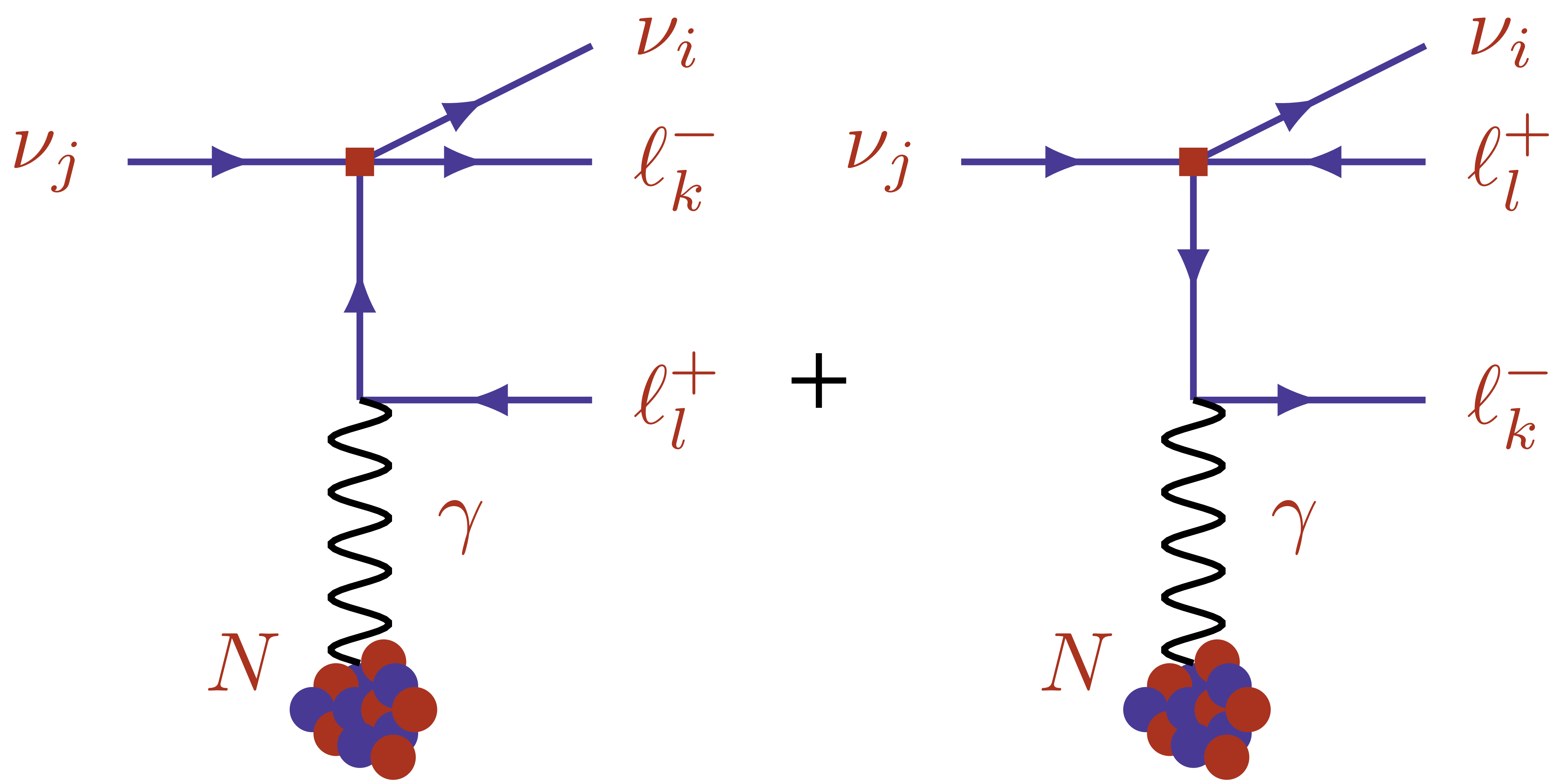

Coherent Scattering

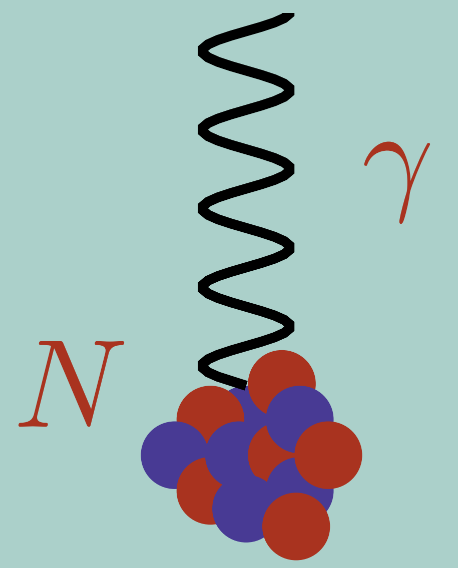

- Nuclear form factor.
- Z^2 scaling.
- $\ell^+\ell'^-$ final state.

Trident Calculation

Based on [1902.06765]

Accelerator ν experiments: $Q_\nu^2 \ll M_{W/Z}^2$

γN dominant for $E_\nu < 10^8$ GeV

Avoid Equivalent Photon Approximation

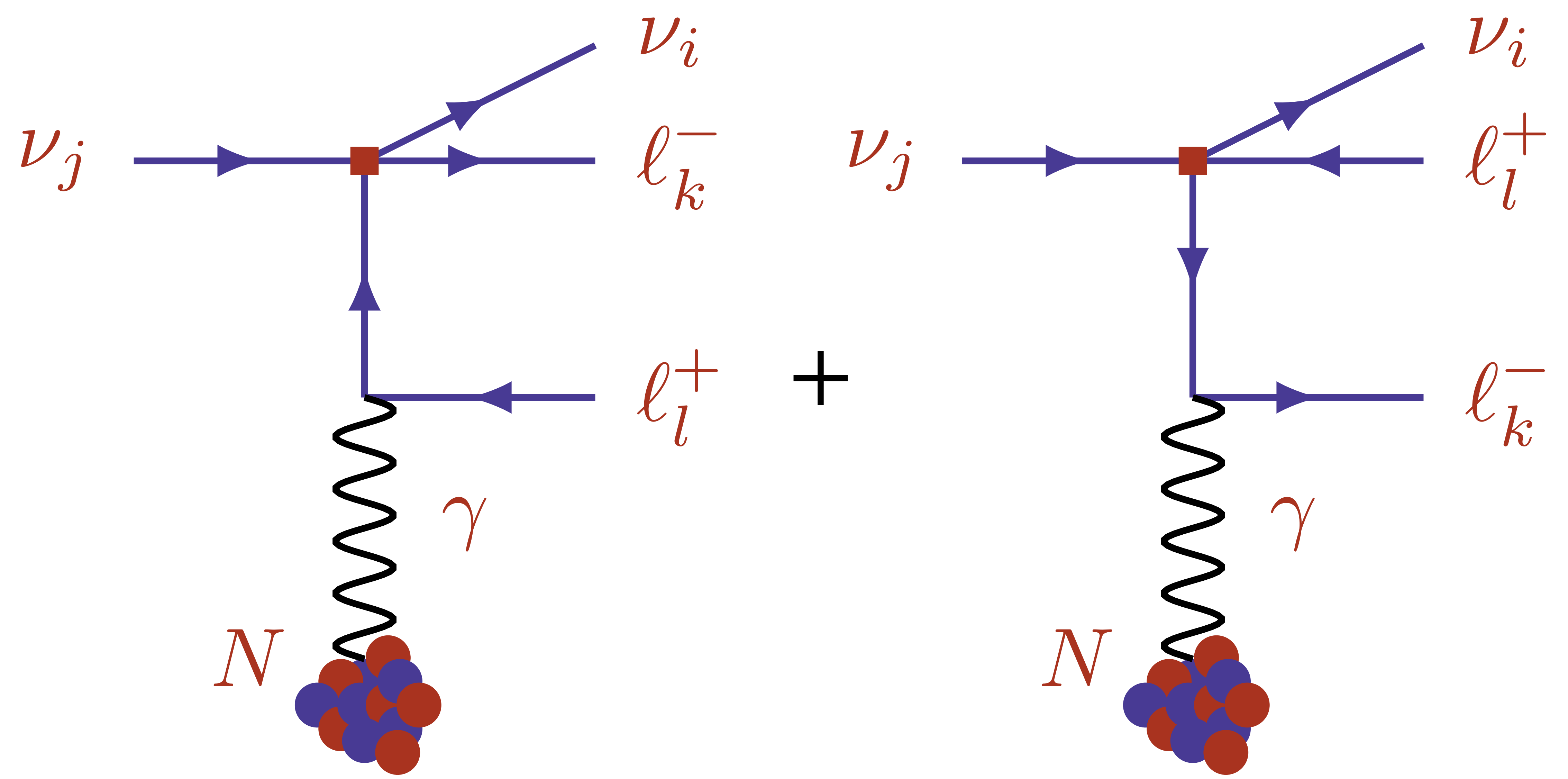

Coherent Scattering

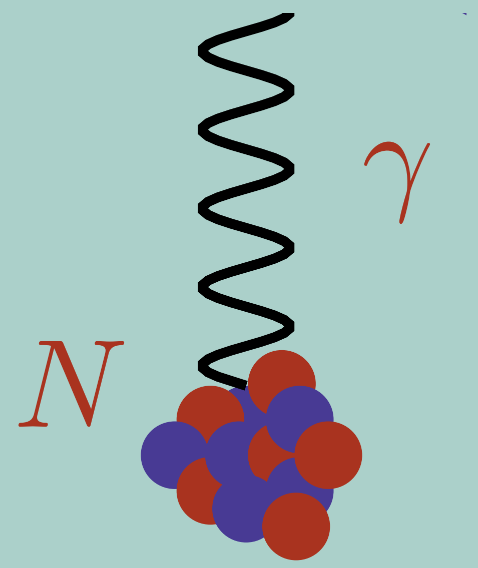

- Nuclear form factor.
- Z^2 scaling.
- $\ell^+\ell'^-$ final state.

Incoherent (diffractive) Scattering

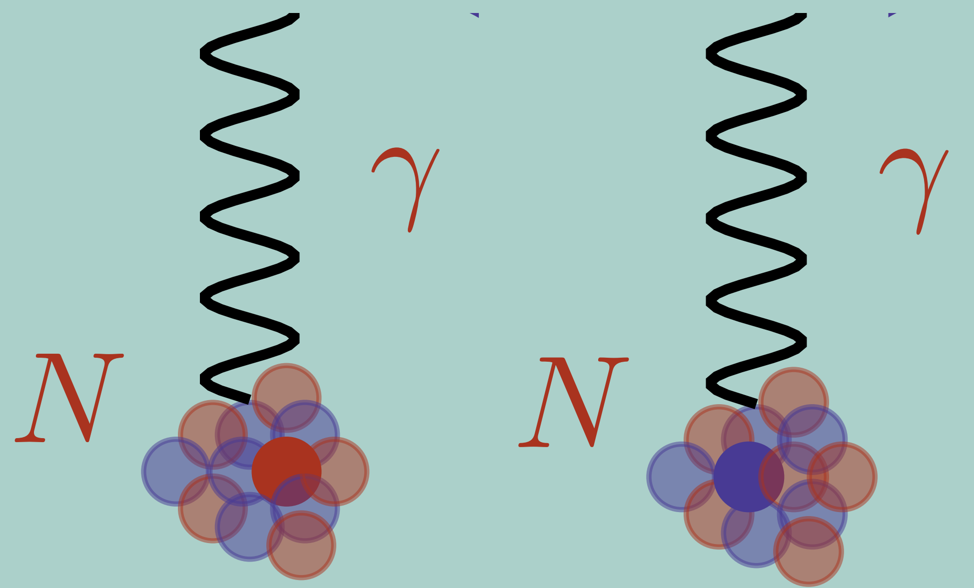

- Nucleon form factors.
- $2Z$ scaling.
- $\ell^+\ell'^- + p(n)$ final state.
- Fermi gas with Pauli blocking

Coherent Trident Cross Section

$$\mathrm{d}\sigma_{\mathrm{coh}} = \frac{Z^2 \alpha_{\mathrm{EM}}^2 G_F^2}{128\pi^6} \frac{1}{m_N E_\nu} \frac{\mathrm{d}^3 k'}{2E_{k'}} \frac{\mathrm{d}^3 p_+}{2E_+} \frac{\mathrm{d}^3 p_-}{2E_-} \frac{\mathrm{d}^3 P'}{2E_{P'}} \frac{H_N^{\alpha\beta} L_{\alpha\beta}}{q^4} \delta^4(k - k' - p_+ - p_- + q)$$

Coherent Trident Cross Section

$$d\sigma_{\text{coh}} = \frac{Z^2\alpha_{\text{EM}}^2 G_F^2}{128\pi^6}\frac{1}{m_N E_\nu}\frac{d^3k'}{2E_{k'}}\frac{d^3p_+}{2E_+}\frac{d^3p_-}{2E_-}\frac{d^3P'}{2E_{P'}}\frac{H_N^{\alpha\beta}L_{\alpha\beta}}{q^4}\delta^4(k-k'-p_+-p_-+q)$$

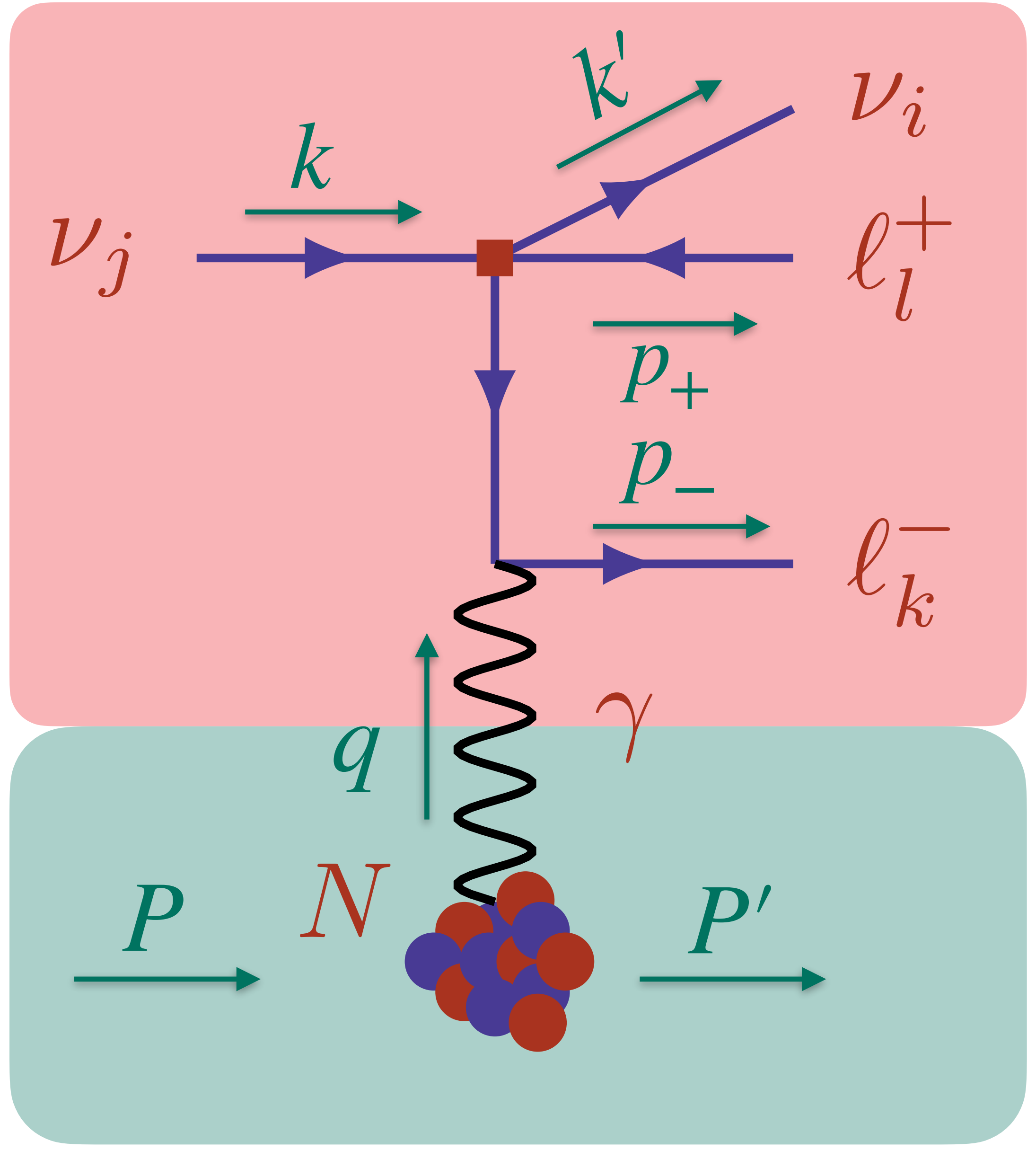

Coherent Trident Cross Section

$$d\sigma_{\rm coh} = \frac{Z^2\alpha_{\rm EM}^2 G_F^2}{128\pi^6}\frac{1}{m_N E_\nu}\frac{d^3k'}{2E_{k'}}\frac{d^3p_+}{2E_+}\frac{d^3p_-}{2E_-}\frac{d^3P'}{2E_{P'}}\frac{H_N^{\alpha\beta}L_{\alpha\beta}}{q^4}\delta^4(k-k'-p_+-p_-+q)$$

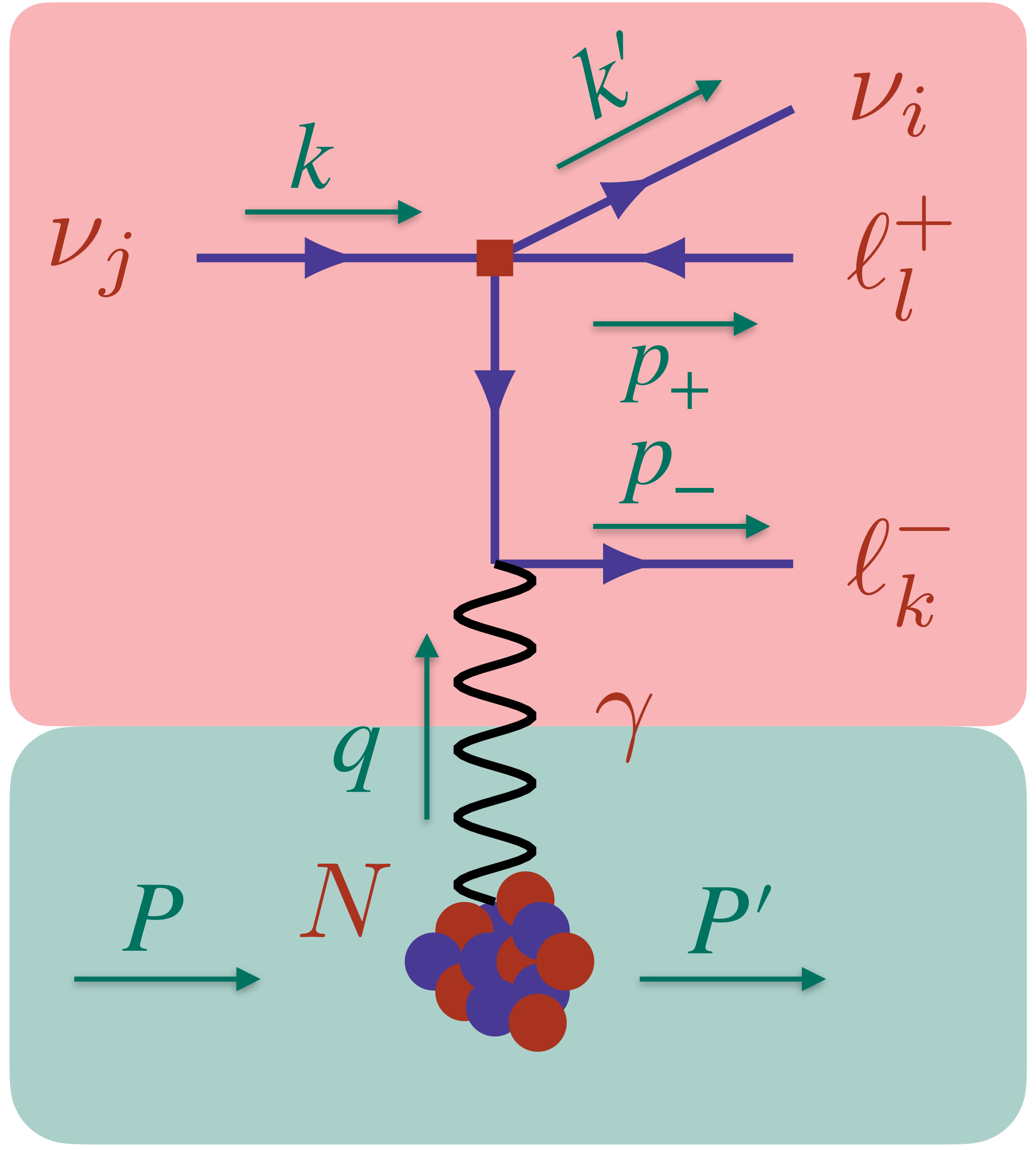

$$L_{\alpha\beta} = \sum_{s,s',s_+,s_-} A_\alpha A_\beta^\dagger$$

$$A_\alpha = (\bar{u}'\gamma_\mu P_L u)\left(\bar{u}_-\left[\gamma_\alpha\frac{(p_- - q)\cdot\gamma + m_-}{(p_- - q)^2 - m_-^2}\gamma^\mu(g^V_{ijkl} + g^A_{ijkl}\gamma_5) - \gamma^\mu(g^V_{ijkl} + g^A_{ijkl}\gamma_5)\frac{(p_+ - q)\cdot\gamma + m_+}{(p_+ - q)^2 - m_+^2}\gamma_\alpha\right]v_+\right)$$

Coherent Trident Cross Section

$$d\sigma_{\text{coh}} = \frac{Z^2\alpha_{\text{EM}}^2 G_F^2}{128\pi^6}\frac{1}{m_N E_\nu}\frac{d^3k'}{2E_{k'}}\frac{d^3p_+}{2E_+}\frac{d^3p_-}{2E_-}\frac{d^3P'}{2E_{P'}}\frac{H_N^{\alpha\beta}L_{\alpha\beta}}{q^4}\delta^4(k-k'-p_+-p_-+q)$$

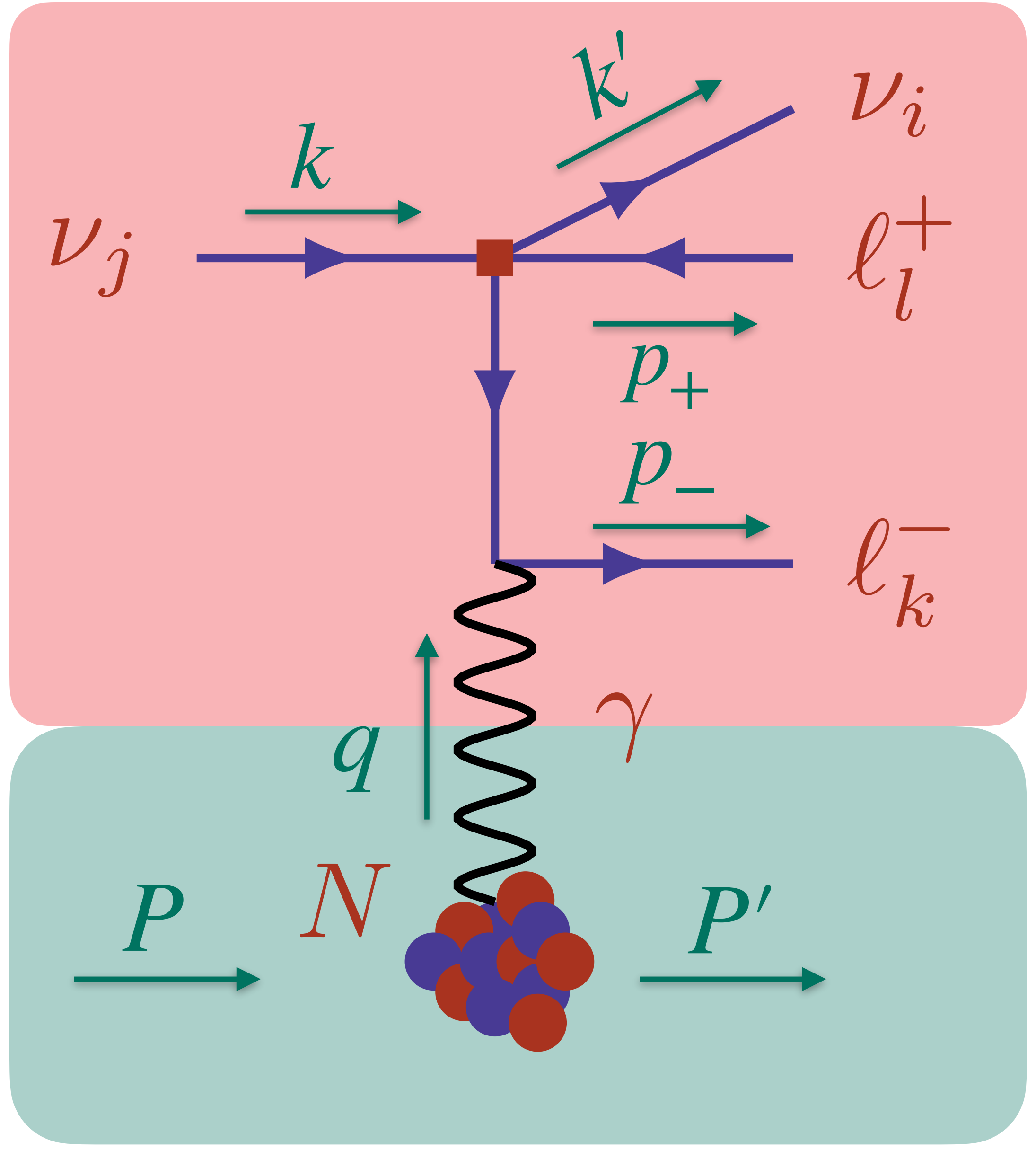

$$H_N^{\alpha\beta} = 4P^\alpha P^\beta [F_N(q^2)]^2$$

Form Factor: Woods-Saxon parametrization

$$F_N(Q^2) = \int dr r^2 \frac{\sin(qr)}{qr}\rho_N(r)$$

Charge Distribution: 3-parameter Fermi parametrization

$$\rho_N(r) = \frac{\mathcal{N}\left(1 + w\frac{r^2}{r_0^2}\right)}{1+\exp\left(\frac{r-r_0}{\sigma}\right)}$$

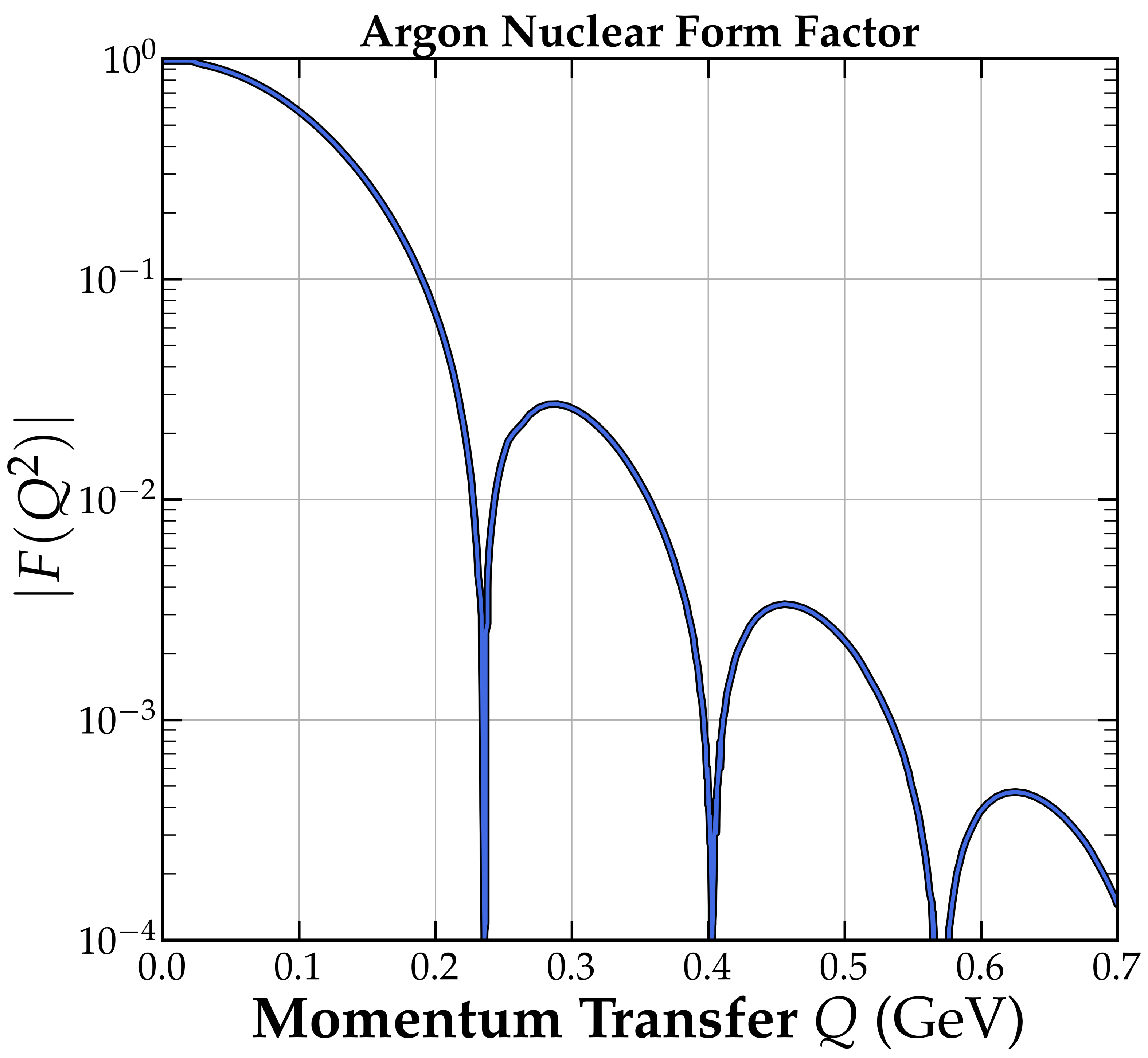

Incoherent Trident Cross Section

$$\mathrm{d}\sigma_{p(n)} = \frac{\alpha_{\mathrm{EM}}^2 G_F^2}{128\pi^6} \frac{1}{m_{p(n)} E_\nu} \frac{\mathrm{d}^3 k'}{2E_{k'}} \frac{\mathrm{d}^3 p_+}{2E_+} \frac{\mathrm{d}^3 p_-}{2E_-} \frac{\mathrm{d}^3 P'}{2E_{P'}} \frac{H_{p(n)}^{\alpha\beta} L_{\alpha\beta}}{q^4} \delta^4(k - k' - p_+ - p_- + q)$$

Incoherent Trident Cross Section

$$\mathrm{d}\sigma_{p(n)} = \frac{\alpha_{\mathrm{EM}}^2 G_F^2}{128\pi^6}\frac{1}{m_{p(n)}E_\nu}\frac{\mathrm{d}^3k'}{2E_{k'}}\frac{\mathrm{d}^3p_+}{2E_+}\frac{\mathrm{d}^3p_-}{2E_-}\frac{\mathrm{d}^3P'}{2E_{P'}}\frac{H^{\alpha\beta}_{p(n)}L_{\alpha\beta}}{q^4}\delta^4(k-k'-p_+-p_-+q)$$

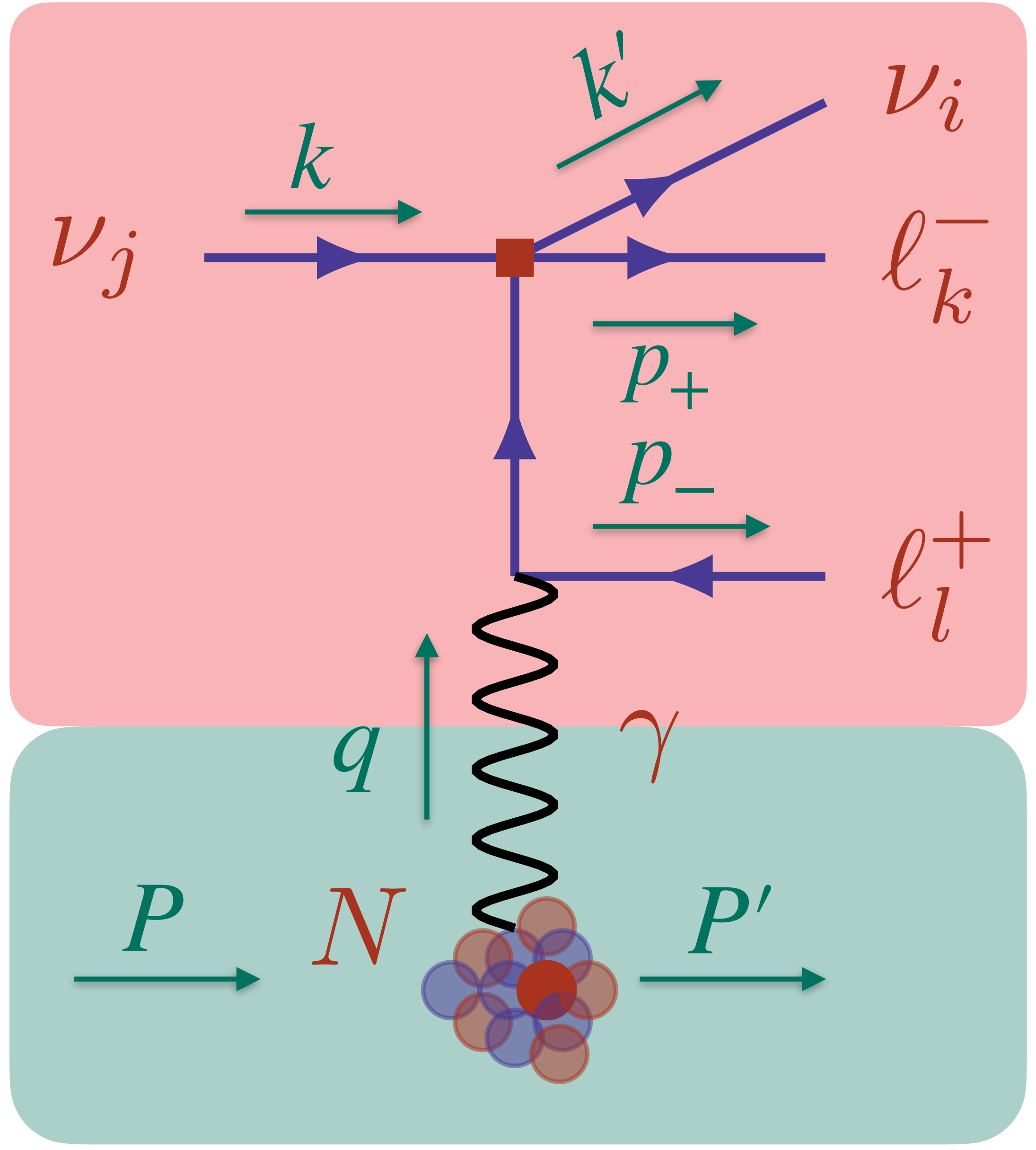

$$H^{\alpha\beta}_{p(n)} = 4P^\alpha P^\beta\left(\frac{4m^2_{p(n)}[G_E^{p(n)}(Q^2)]^2}{Q^2+4m^2_{p(n)}} + \frac{Q^2[G_M^{p(n)}(Q^2)]^2}{Q^2+4m^2_{p(n)}} + g^{\alpha\beta}Q^2[G_M^{p(n)}(Q^2)]^2\right)$$

Proton: electron-proton elastic scattering

Neutron: electron-nucleus (deuterium and ^{3}He) scattering

[arXiv:0812.3539]

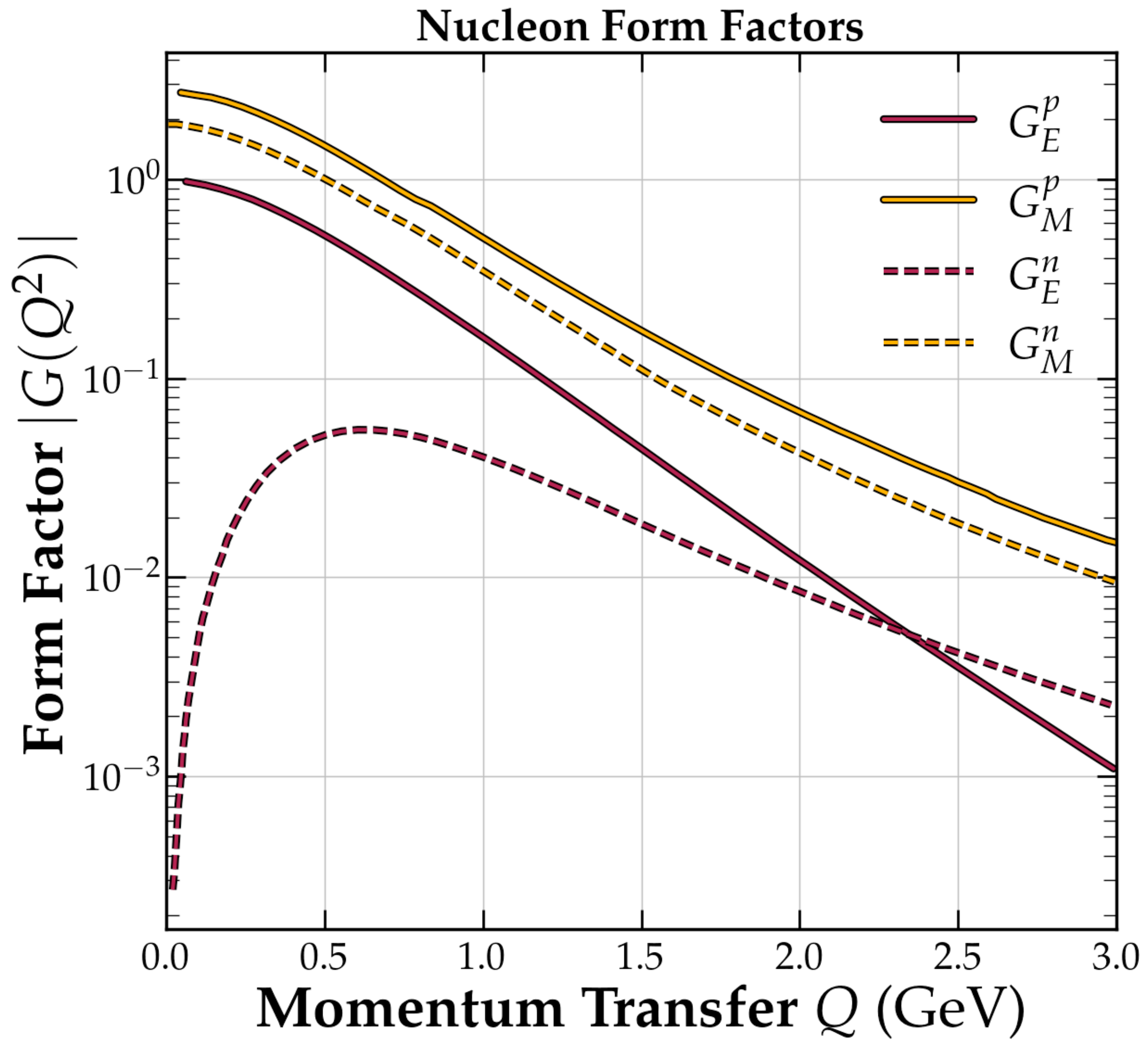

Incoherent Trident Cross Section

$$d\sigma_{p(n)} = \frac{\alpha_{EM}^2 G_F^2}{128\pi^6}\frac{1}{m_{p(n)}E_\nu}\frac{d^3k'}{2E_{k'}}\frac{d^3p_+}{2E_+}\frac{d^3p_-}{2E_-}\frac{d^3P'}{2E_{P'}}\frac{H^{\alpha\beta}_{p(n)}L_{\alpha\beta}}{q^4}\delta^4(k-k'-p_+-p_-+q)$$

$$d\sigma_{incoh} = \Theta(|\mathbf{q}|)(Zd\sigma_p + (A-Z)d\sigma_n)$$

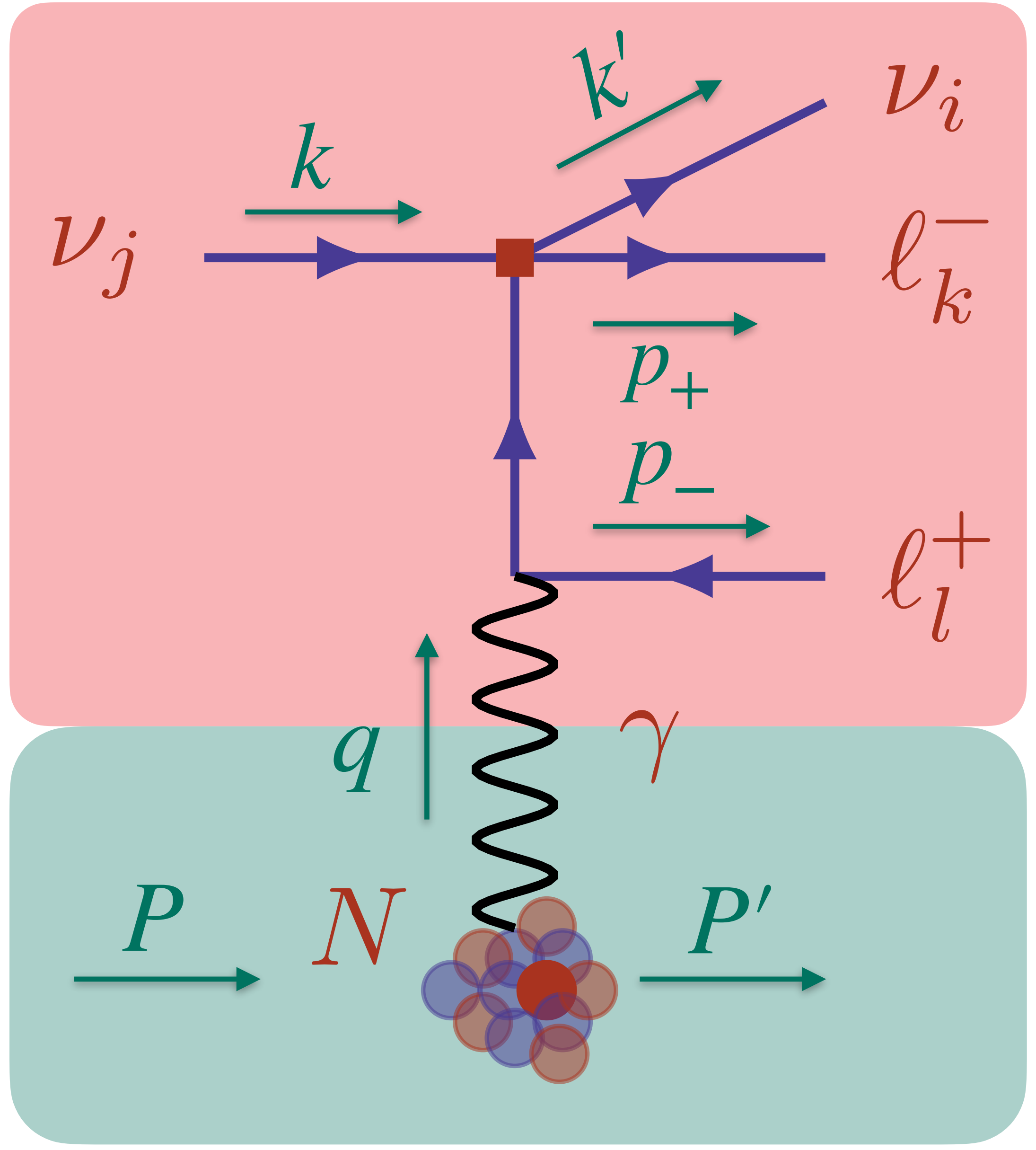

$$H^{\alpha\beta}_{p(n)} = 4P^\alpha P^\beta\left(\frac{4m^2_{p(n)}[G_E^{p(n)}(Q^2)]^2}{Q^2+4m^2_{p(n)}} + \frac{Q^2[G_M^{p(n)}(Q^2)]^2}{Q^2+4m^2_{p(n)}}\right) + g^{\alpha\beta}Q^2[G_M^{p(n)}(Q^2)]^2$$

$$\Theta(|\mathbf{q}|) = \begin{cases} \frac{3}{4}\frac{|\mathbf{q}|}{p_F} - \frac{|\mathbf{q}|^3}{16p_F^3} & \text{for } |\mathbf{q}| < 2p_F \\ 1 & \text{for } |\mathbf{q}| > 2p_F \end{cases}$$

$$p_F = 235 \text{ MeV}$$

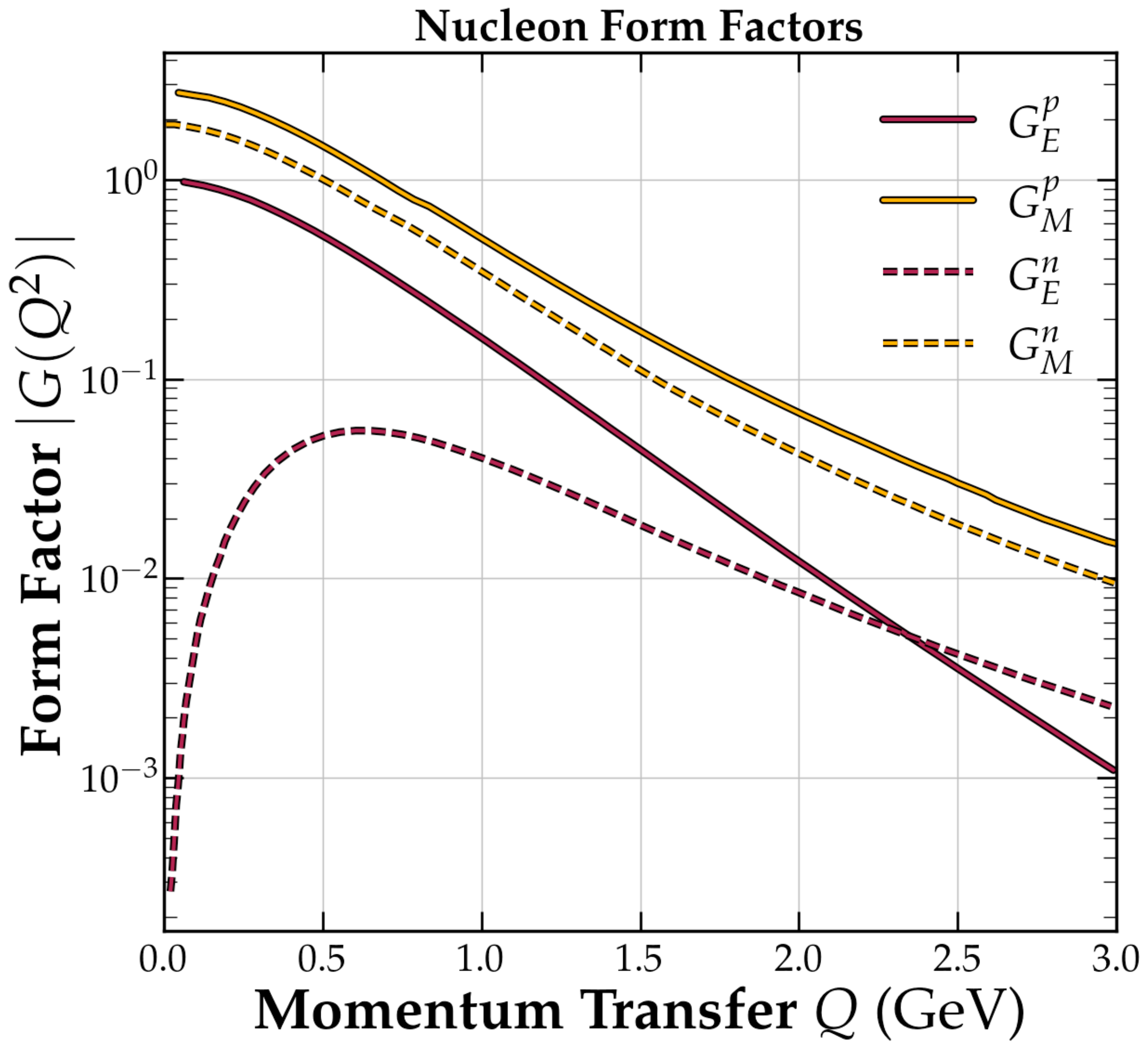

Cross Sections

Cross Sections

Trident process	$E_\nu^{\rm th}$ (GeV) Incoherent (proton)	Coherent ^{40}Ar	^{184}W	^{56}Fe
$\nu_i N \to \nu_i N e^+ e^-$	0.001	0.001	0.001	0.001
$\nu_i N \to \nu_i N \mu^+ \mu^-$	0.24	0.21	0.21	0.21
$\nu_i N \to \nu_i N \tau^+ \tau^-$	10	3.7	3.6	3.7
$\nu_\mu N \to \nu_e N e^- \mu^+$	0.11	0.11	0.11	0.11
$\nu_\mu N \to \nu_\tau N \tau^- \mu^+$	3.8	1.9	1.9	1.9
$\nu_e N \to \nu_\tau N \tau^- e^+$	3.5	1.8	1.8	1.8

$$E_\nu^{\rm th} \approx \frac{(m_\ell + m'_\ell + M_{\rm tgt})^2 - M_{\rm tgt}}{2M_{\rm tgt}}$$

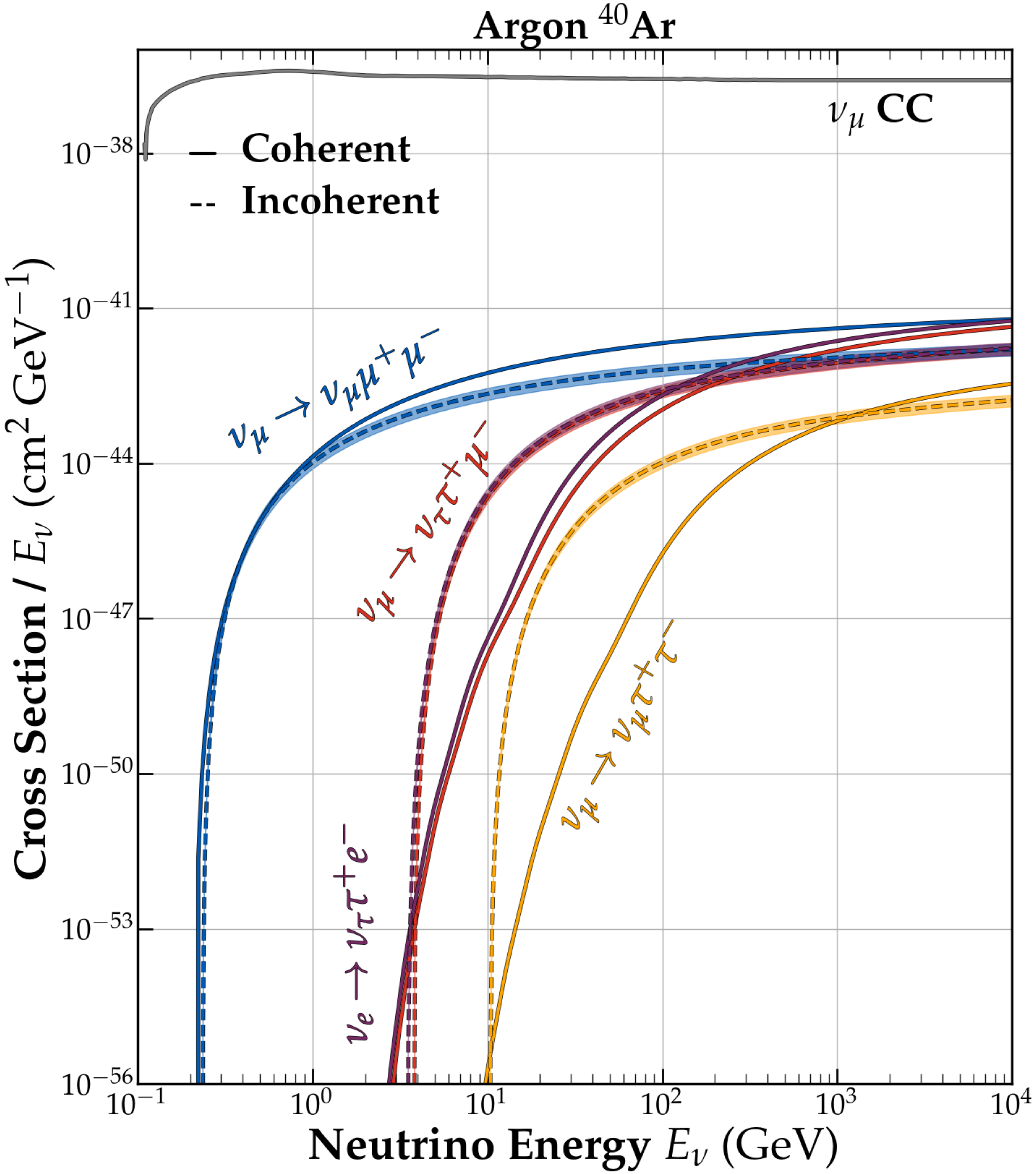

Cross Sections

Trident process	$E_\nu^{\rm th}$ (GeV)			
	Incoherent (proton)	Coherent ^{40}Ar	Coherent ^{184}W	Coherent ^{56}Fe
$\nu_i N \to \nu_i N e^+ e^-$	0.001	0.001	0.001	0.001
$\nu_i N \to \nu_i N \mu^+ \mu^-$	0.24	0.21	0.21	0.21
$\nu_i N \to \nu_i N \tau^+ \tau^-$	10	3.7	3.6	3.7
$\nu_\mu N \to \nu_e N e^- \mu^+$	0.11	0.11	0.11	0.11
$\nu_\mu N \to \nu_\tau N \tau^- \mu^+$	3.8	1.9	1.9	1.9
$\nu_e N \to \nu_\tau N \tau^- e^+$	3.5	1.8	1.8	1.8

$$E_\nu^{\rm th} \approx \frac{(m_\ell + m'_\ell + M_{\rm tgt})^2 - M_{\rm tgt}}{2M_{\rm tgt}}$$

*Uncertainty quantification of nuclear effects is work in progress

Uncertainty	Coherent	Incoherent
Higher order QED	3%	3%
Higher order EW	5%	5%
Form factors *	1%	3%
Nuclear modeling *	-	30%
TOTAL	6%	31%

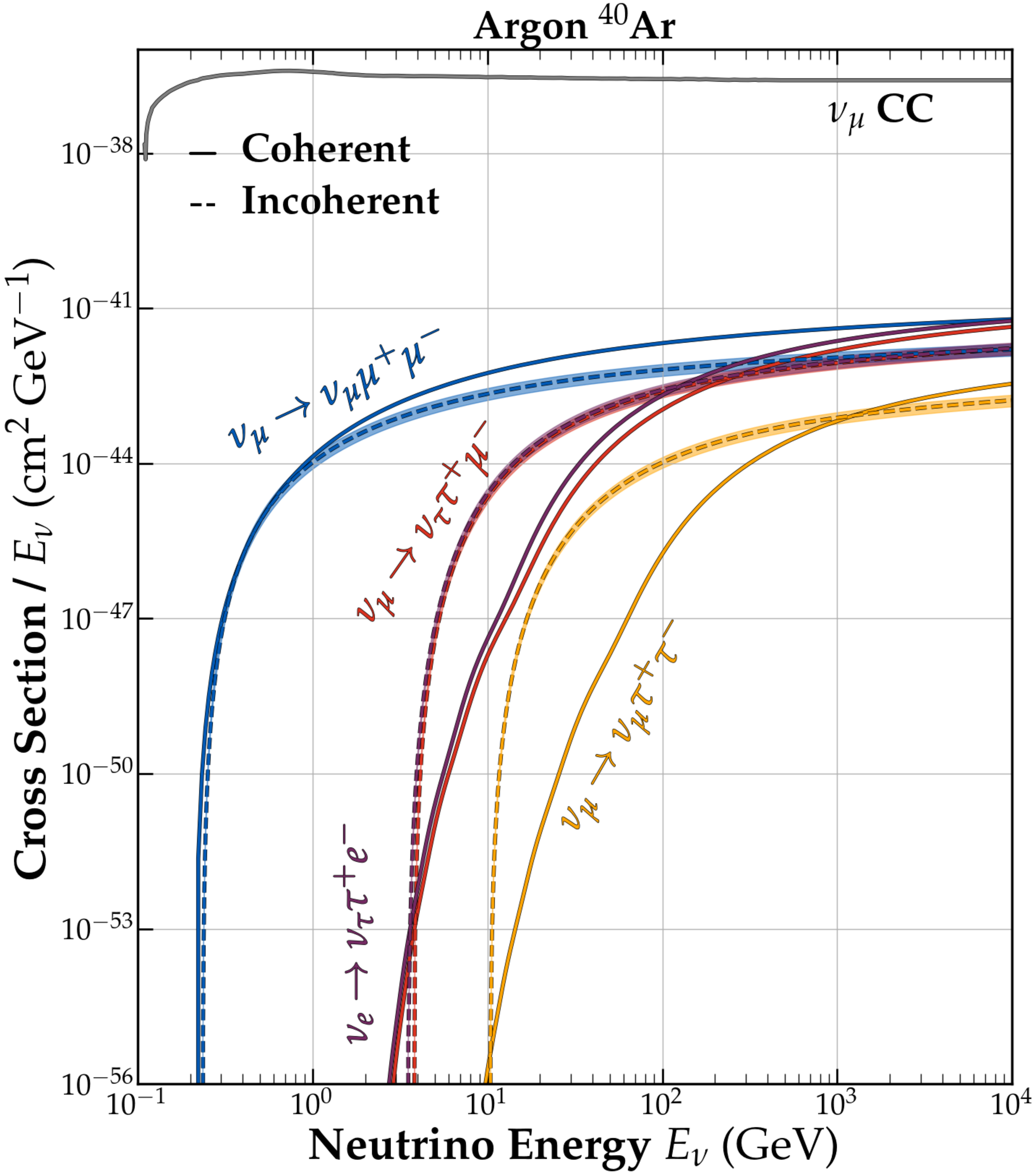

Cross Sections

Trident process	E_ν^{th} (GeV)			
	Incoherent (proton)	Coherent		
		^{40}Ar	^{184}W	^{56}Fe
$\nu_i N \to \nu_i N e^+ e^-$	0.001	0.001	0.001	0.001
$\nu_i N \to \nu_i N \mu^+ \mu^-$	0.24	0.21	0.21	0.21
$\nu_i N \to \nu_i N \tau^+ \tau^-$	10	3.7	3.6	3.7
$\nu_\mu N \to \nu_e N e^- \mu^+$	0.11	0.11	0.11	0.11
$\nu_\mu N \to \nu_\tau N \tau^- \mu^+$	3.8	1.9	1.9	1.9
$\nu_e N \to \nu_\tau N \tau^- e^+$	3.5	1.8	1.8	1.8

$$E_\nu^{th} \approx \frac{(m_\ell + m'_\ell + M_{tgt})^2 - M_{tgt}}{2M_{tgt}}$$

*Uncertainty quantification of nuclear effects is work in progress

Uncertainty	Coherent	Incoherent
Higher order QED	3%	3%
Higher order EW	5%	5%
Form factors *	1%	3%
Nuclear modeling *	-	30%
Total	6%	31%

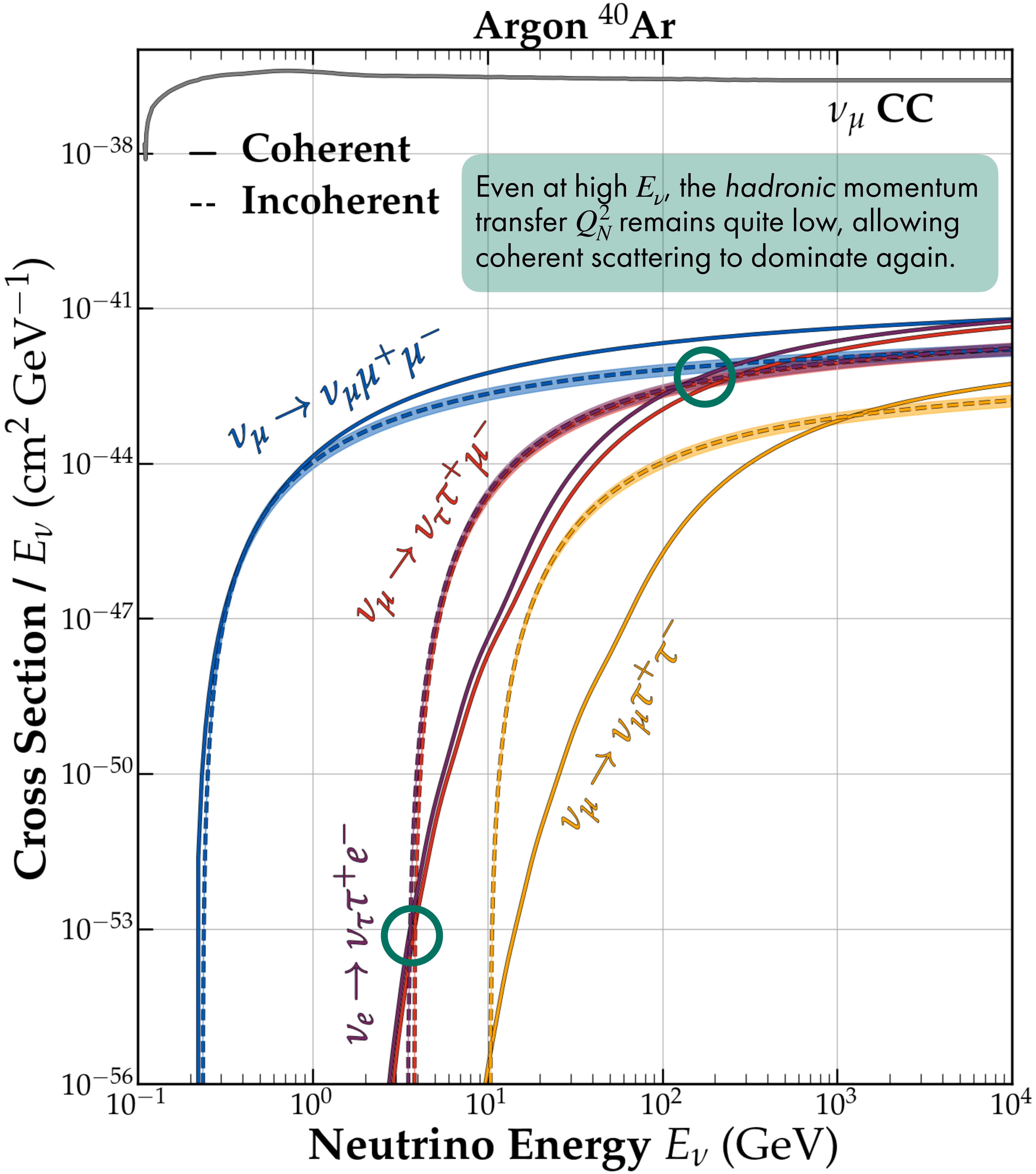

Can we see tridents at DUNE?

Deep Underground Neutrino Experiment

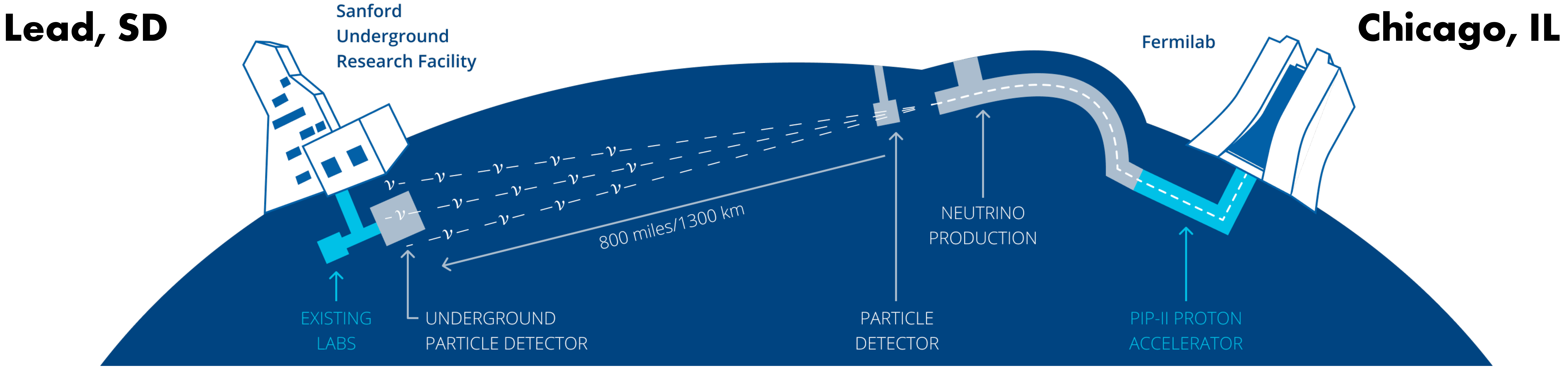

Deep Underground Neutrino Experiment

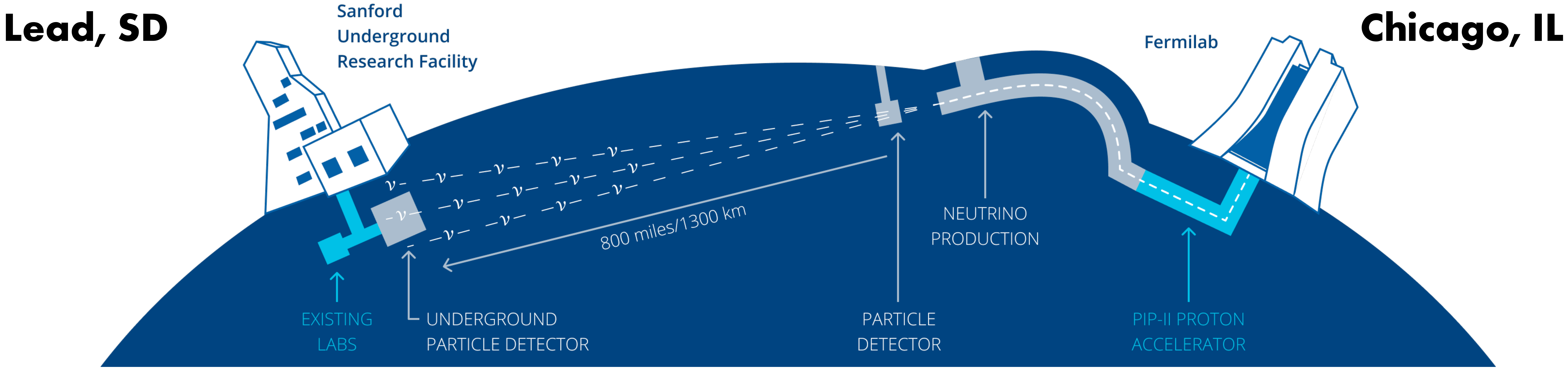

- Long-baseline liquid argon (LAr) time projection chamber (TPC).
  - Near Detector (ND): 574 m, 67 tonnes of argon
  - Far Detector (FD): 1300 km, 4 modules each with 40k tonnes of argon
- Focus on DUNE ND: 10^6 ν events / (GeV·ton·MW·year).

DUNE ND Flux

DUNE ND Flux

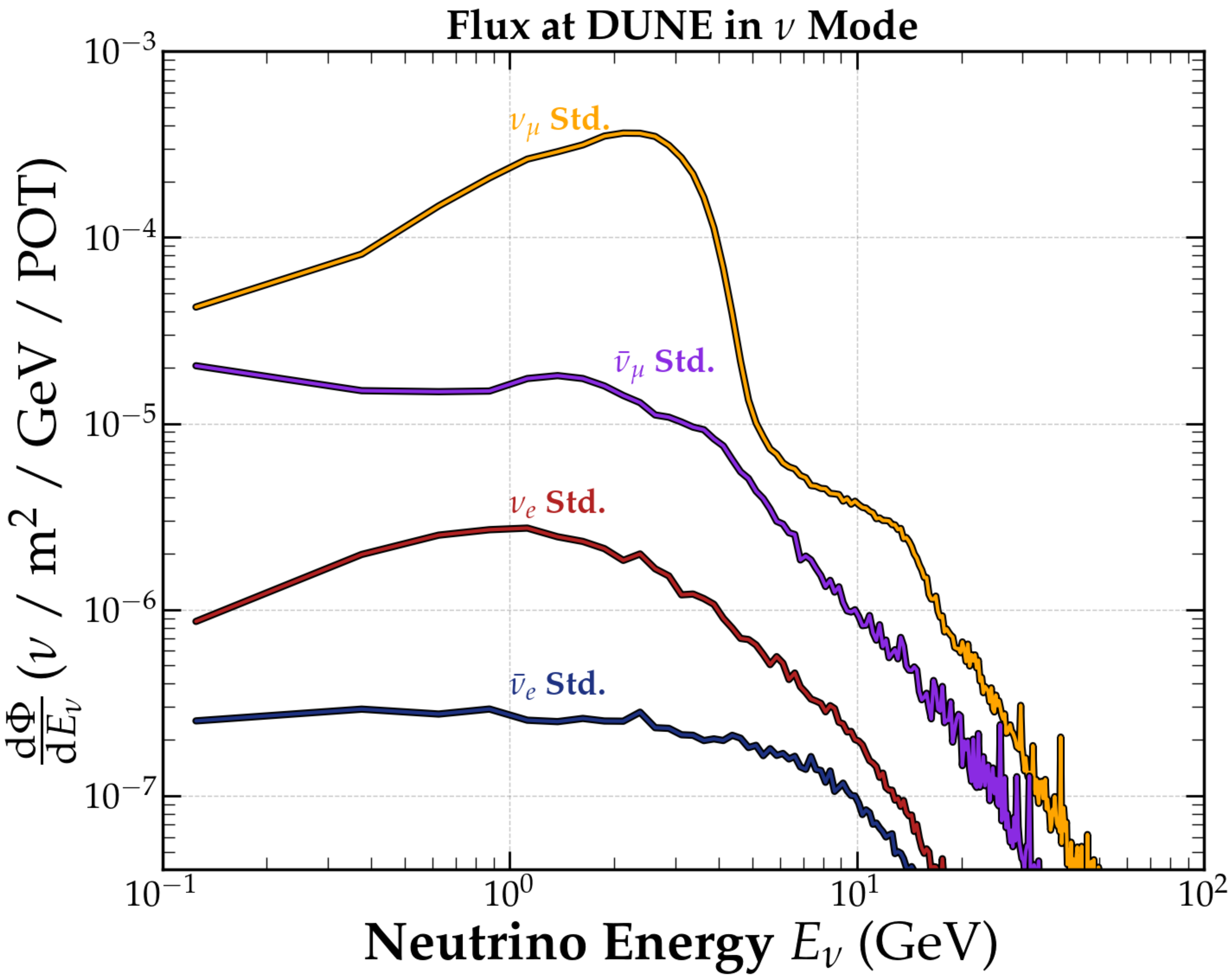

Standard CP-optimized Flux

- ν's mostly in the $1-5$ GeV range.
- Peak at ~ 2 GeV.
- Better for δ_{CP} measurements.

DUNE ND Flux

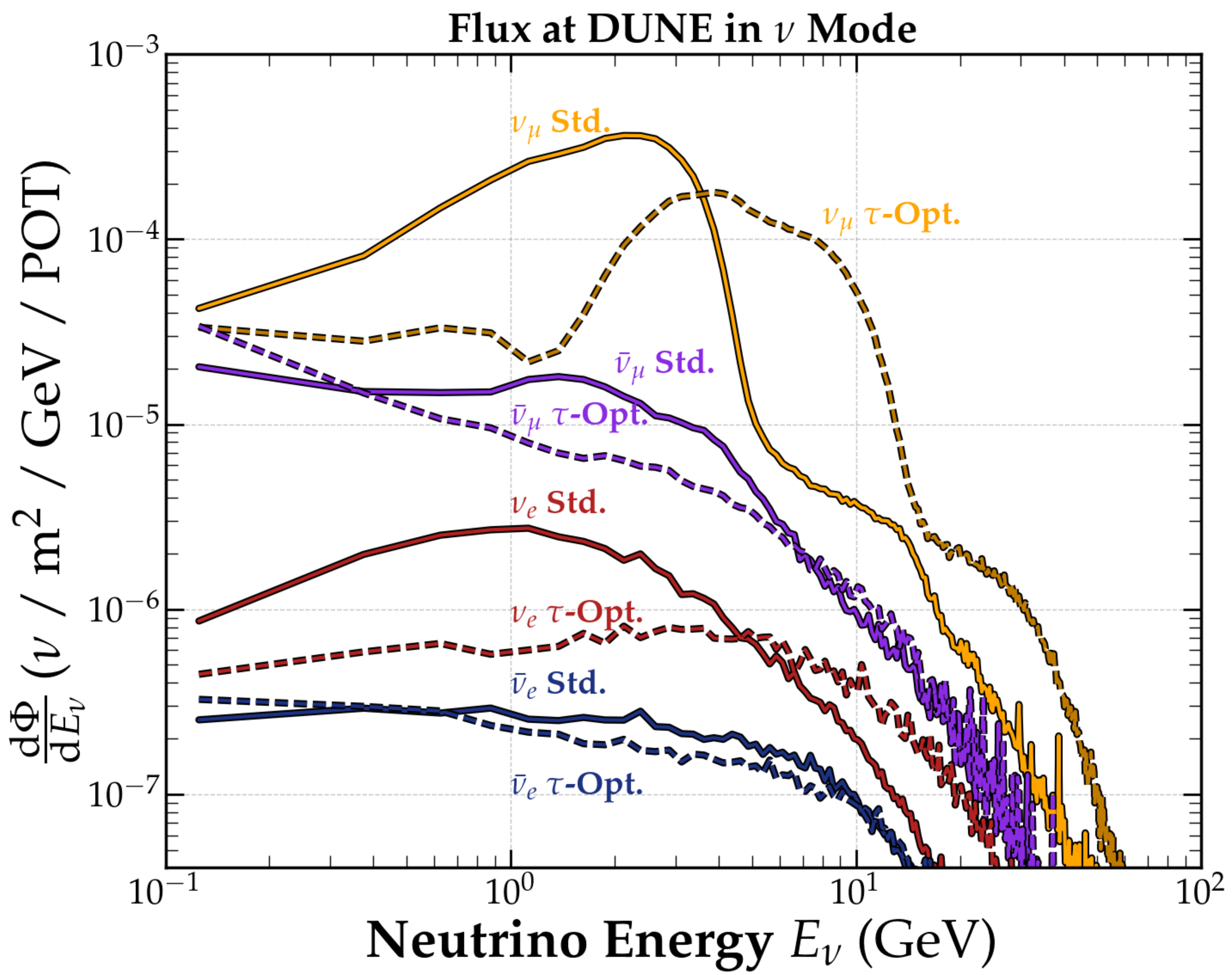

Standard CP-optimized Flux

- ν's mostly in the $1-5$ GeV range.
- Peak at ~ 2 GeV.
- Better for δ_{CP} measurements.

Tau-optimized Flux

- Higher energy ν flux.
- Peak at ~ 4 GeV.
- Better for ν_τ measurements.

Tridents at DUNE ND

Tridents at DUNE ND

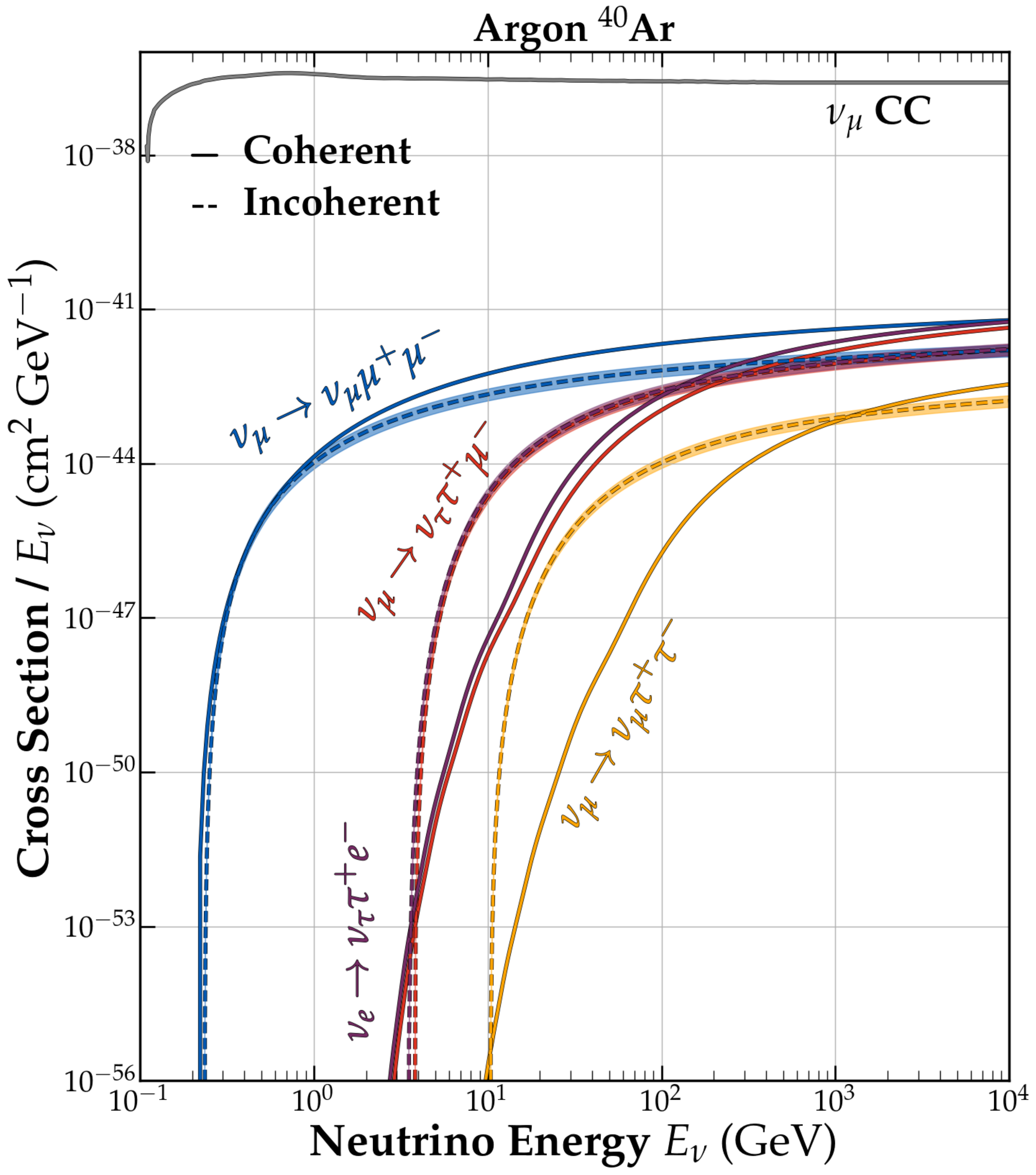

Tridents at DUNE ND

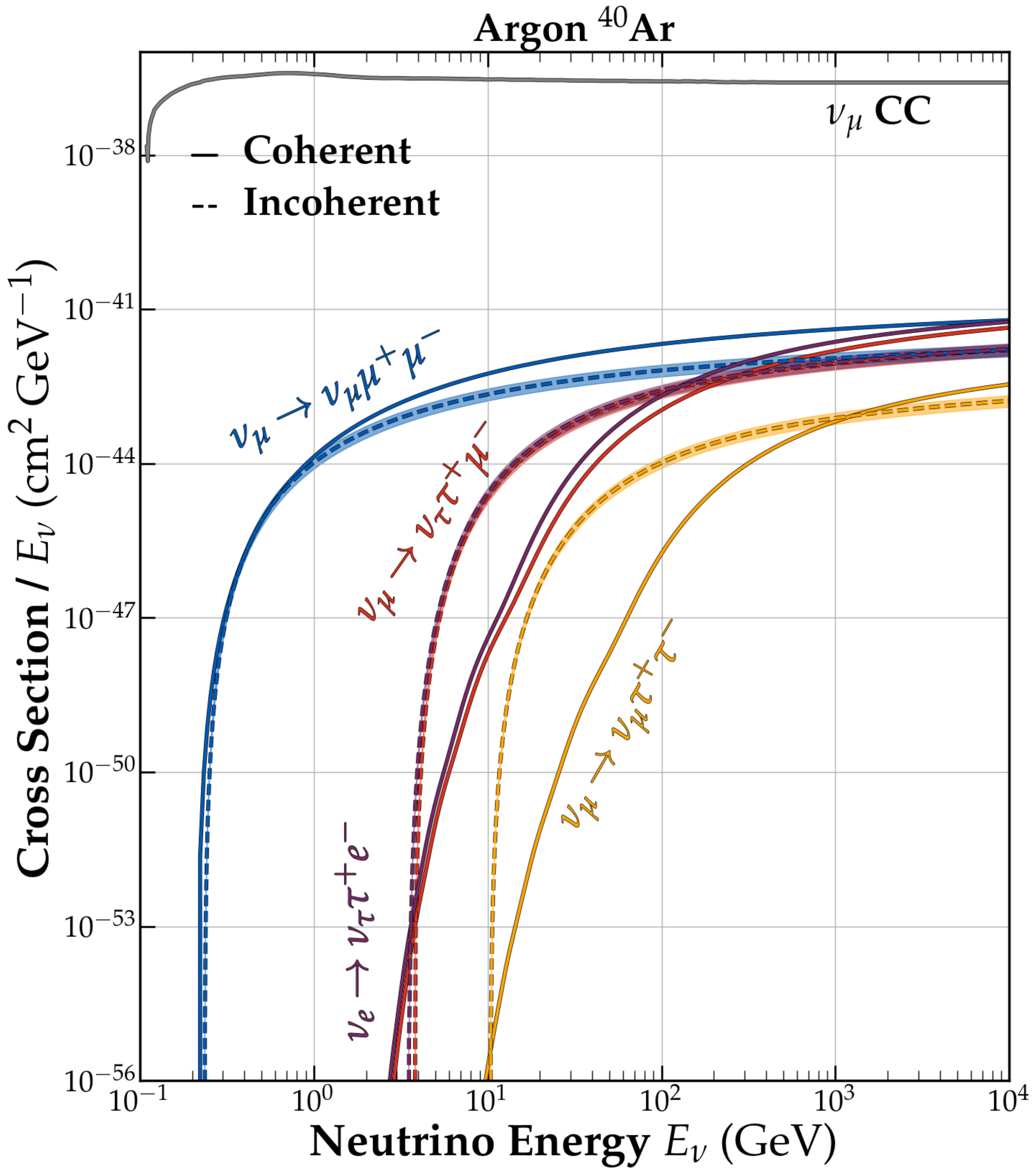

+

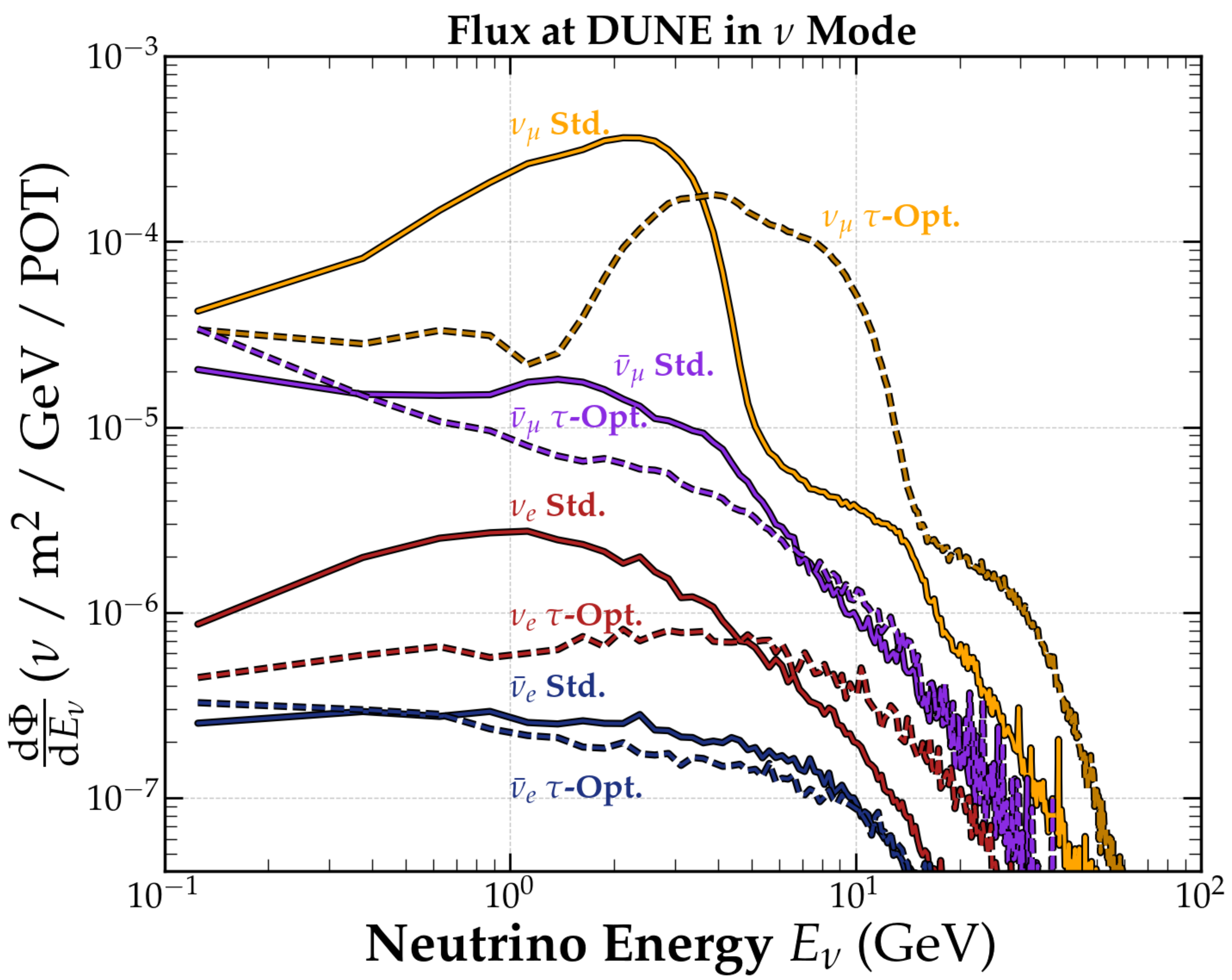

Tridents at DUNE ND

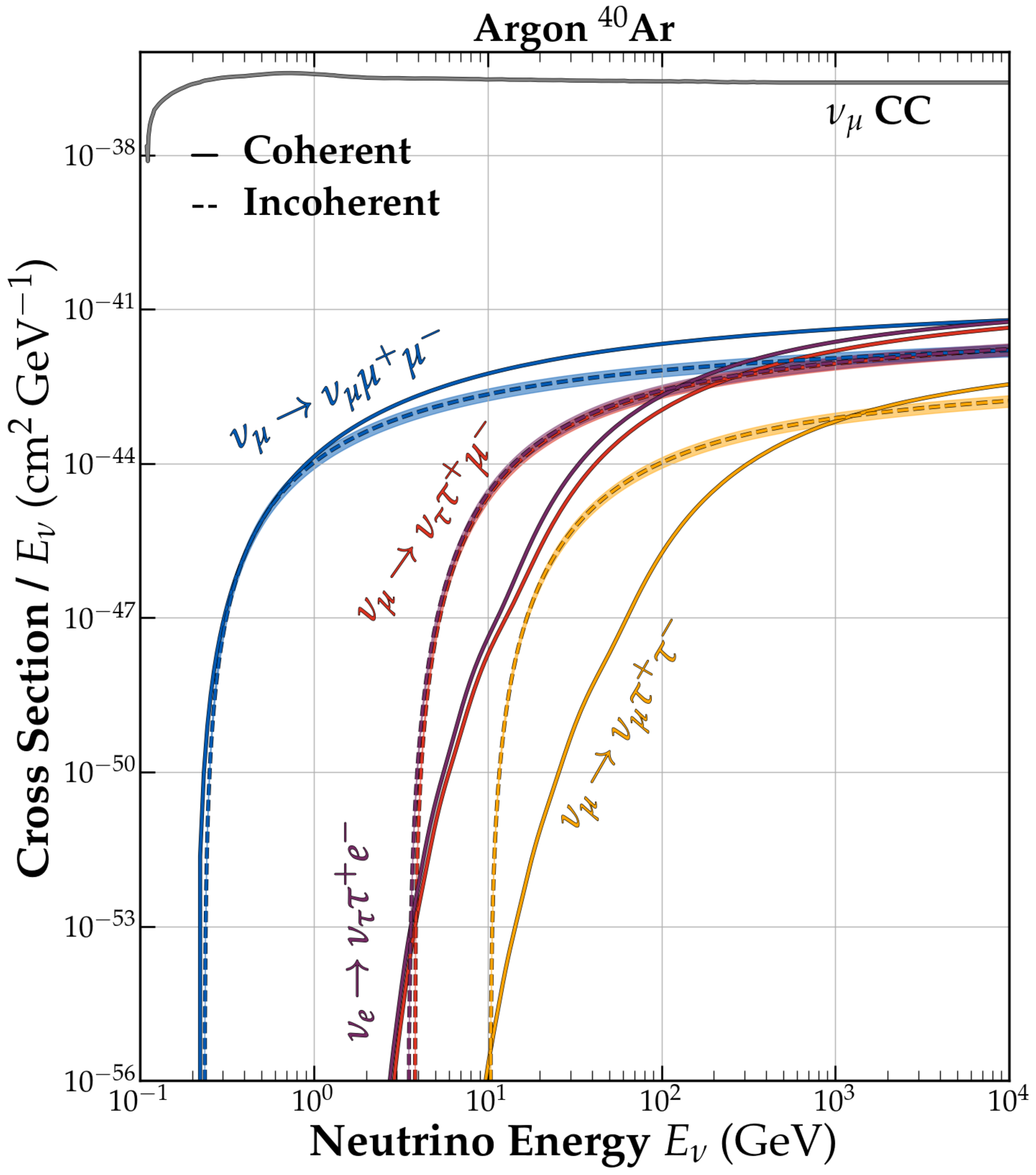

+

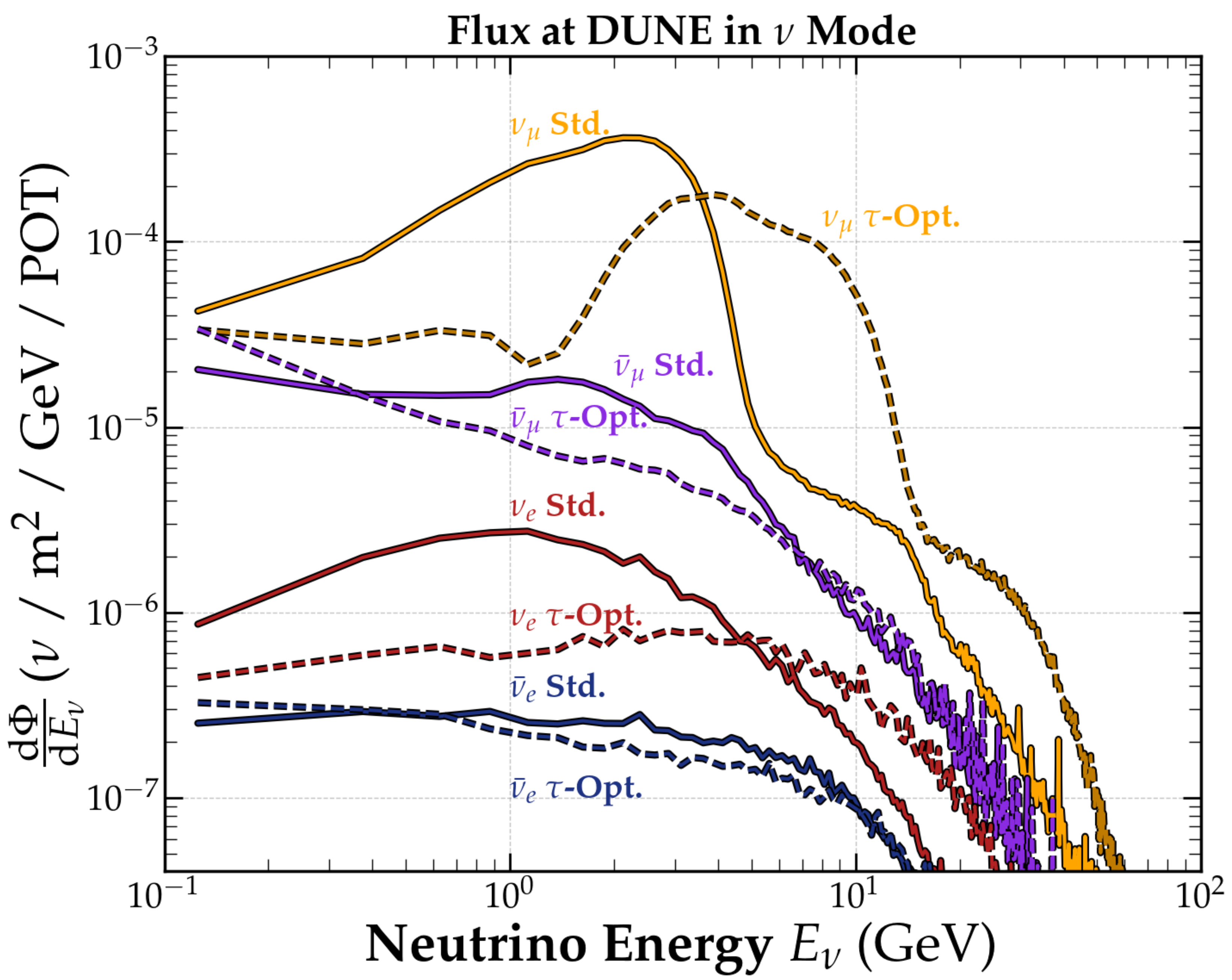

+

DUNE ND

- M_{det}: 67 tonnes of ^{40}Ar
- N_{POT}: 3.3×10^{21} POT

Tridents at DUNE ND

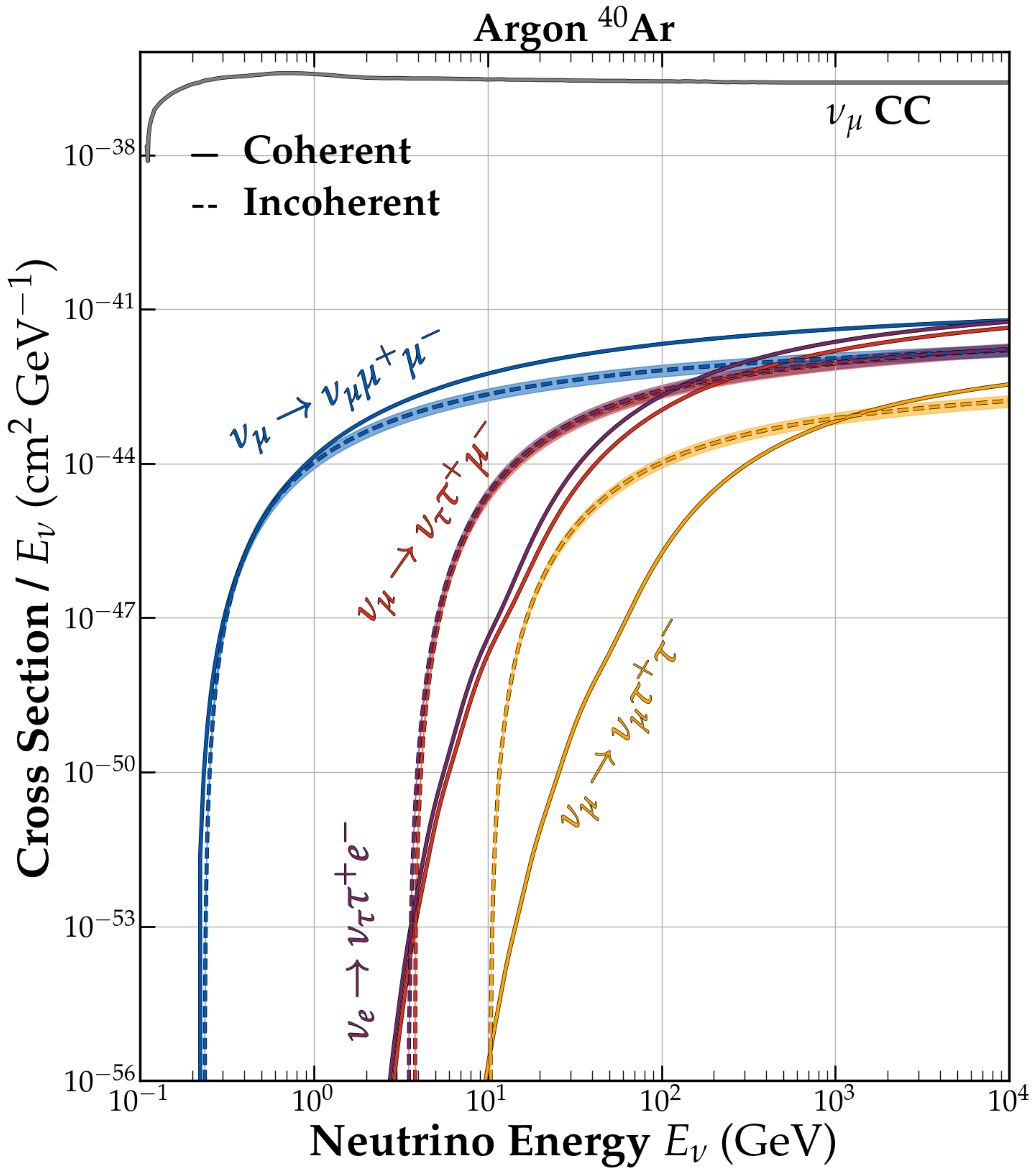

+

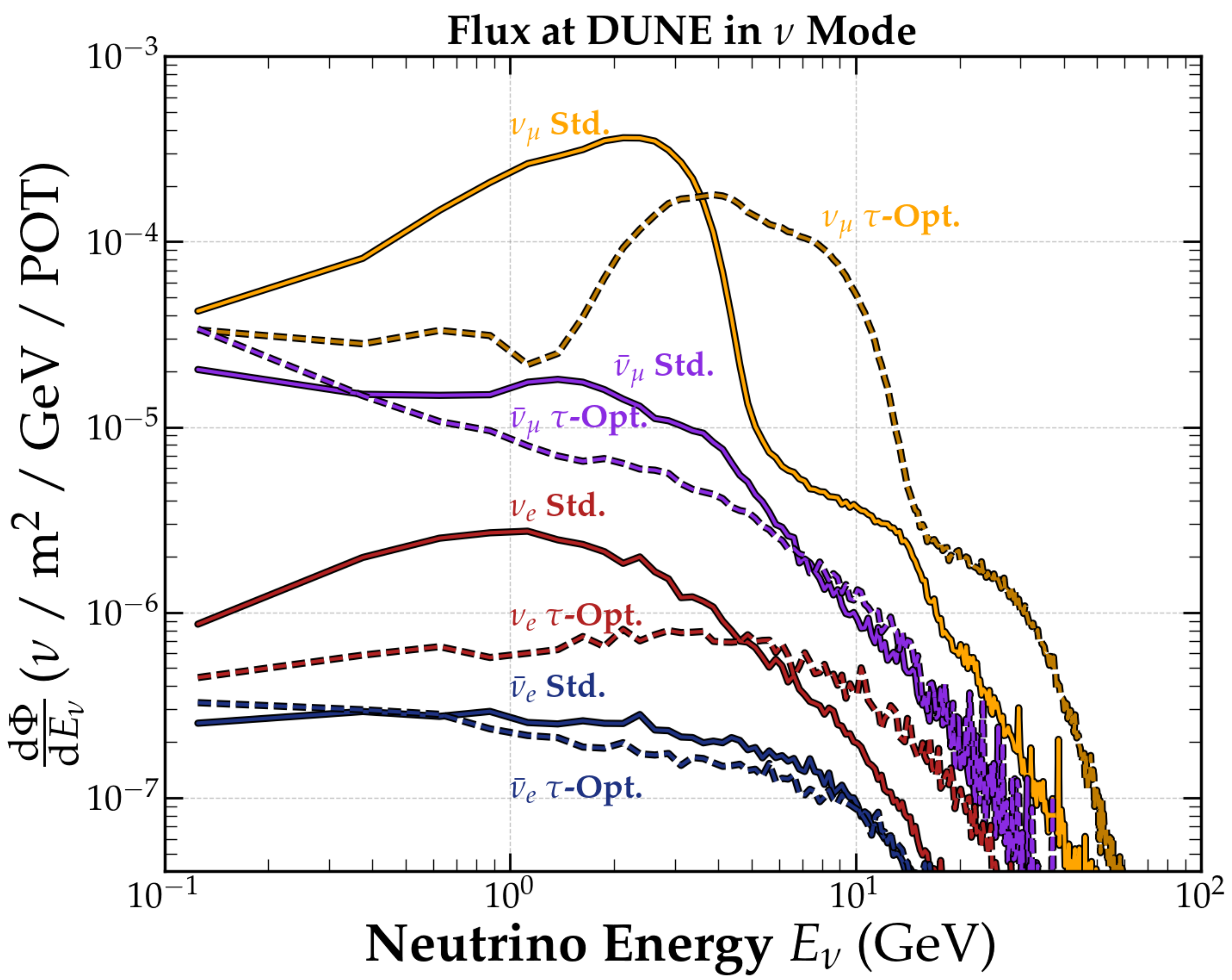

+

DUNE ND

- M_{det}: 67 tonnes of ^{40}Ar
- N_{POT}: 3.3×10^{21} POT

$$N_{\text{trident}} = \frac{M_{\text{det}}}{M_{\text{Ar}}} N_{\text{POT}} \int \frac{d\Phi}{dE_\nu} \sigma(E_\nu) dE_\nu$$

Neutrino Mode - Coherent scattering

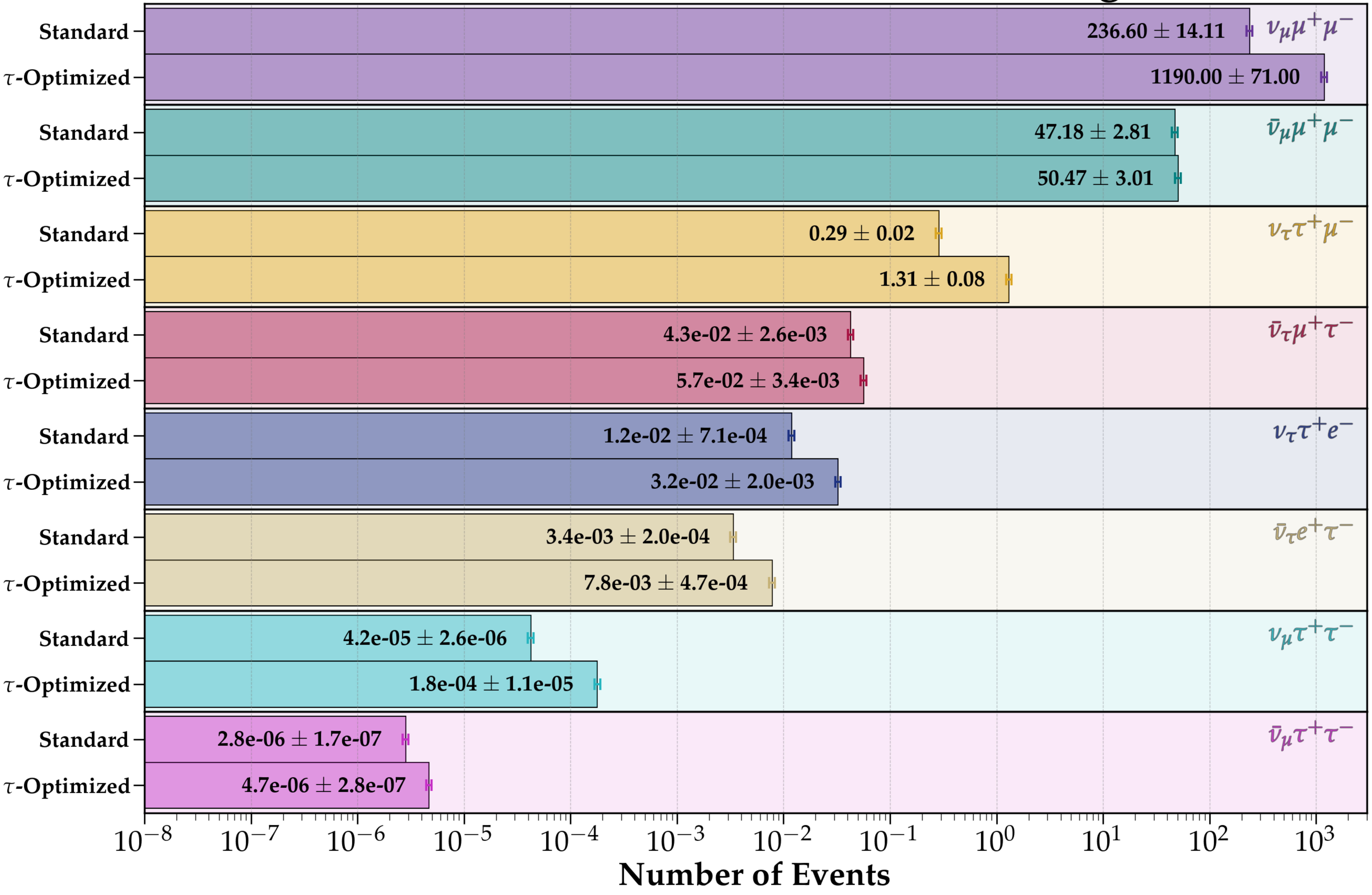

Neutrino Mode - Incoherent scattering

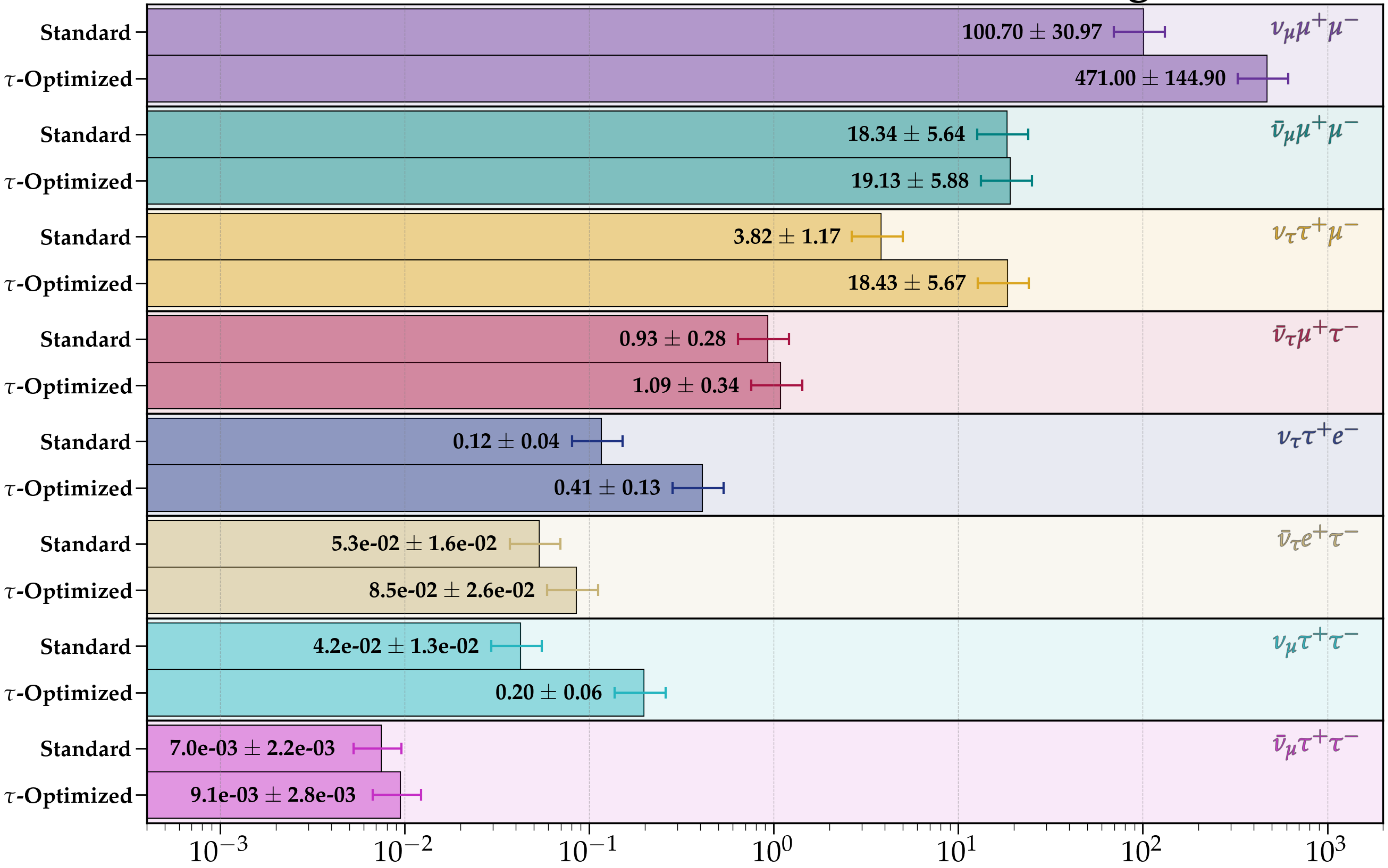

Is there hope of detecting tau tridents ($\nu_\mu \to \nu_\tau \tau^+ \mu^-$)?

Tau Reconstruction at DUNE

Tau Reconstruction at DUNE

τ

- Short-lived
- Low cross sections
- Copious backgrounds

Tau Reconstruction at DUNE

τ

- Short-lived
- Low cross sections
- Copious backgrounds

Tau Reconstruction at DUNE

τ

- Short-lived
- Low cross sections
- Copious backgrounds

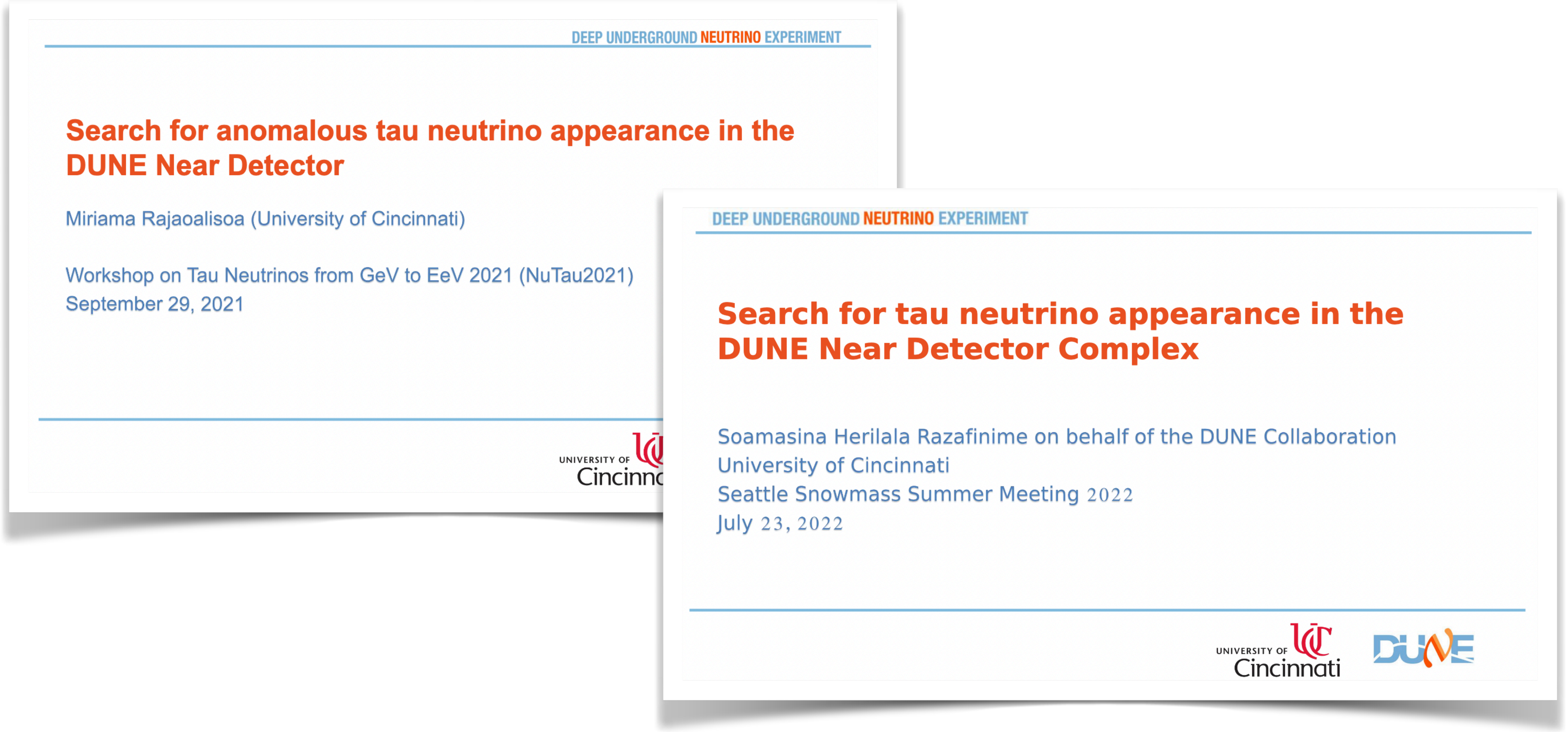

Tau Reconstruction at DUNE

τ

- Short-lived
- Low cross sections
- Copious backgrounds

DEEP UNDERGROUND NEUTRINO EXPERIMENT

Search for anomalous tau neutrino appearance in the DUNE Near Detector

Miriama Rajaoalisoa (University of Cincinnati)

Workshop on Tau Neutrinos from GeV to EeV 2021 (NuTau2021)
September 29, 2021

DEEP UNDERGROUND NEUTRINO EXPERIMENT

Search for tau neutrino appearance in the DUNE Near Detector Complex

Soamasina Herilala Razafinime on behalf of the DUNE Collaboration
University of Cincinnati
Seattle Snowmass Summer Meeting 2022
July 23, 2022

- Signal vs background based on kinematic differences using a BDT.
- Short-baseline $\nu_s \rightarrow \nu_\tau$

Rank-1 Discriminator

$$R^T_{\text{Miss}} = \frac{p^T_{\text{Miss}}}{p^T_{\text{Miss}} + p^T_\mu}$$

Tau Trident Reconstruction at DUNE

τ

- Short-lived
- Low cross sections
- Copious backgrounds

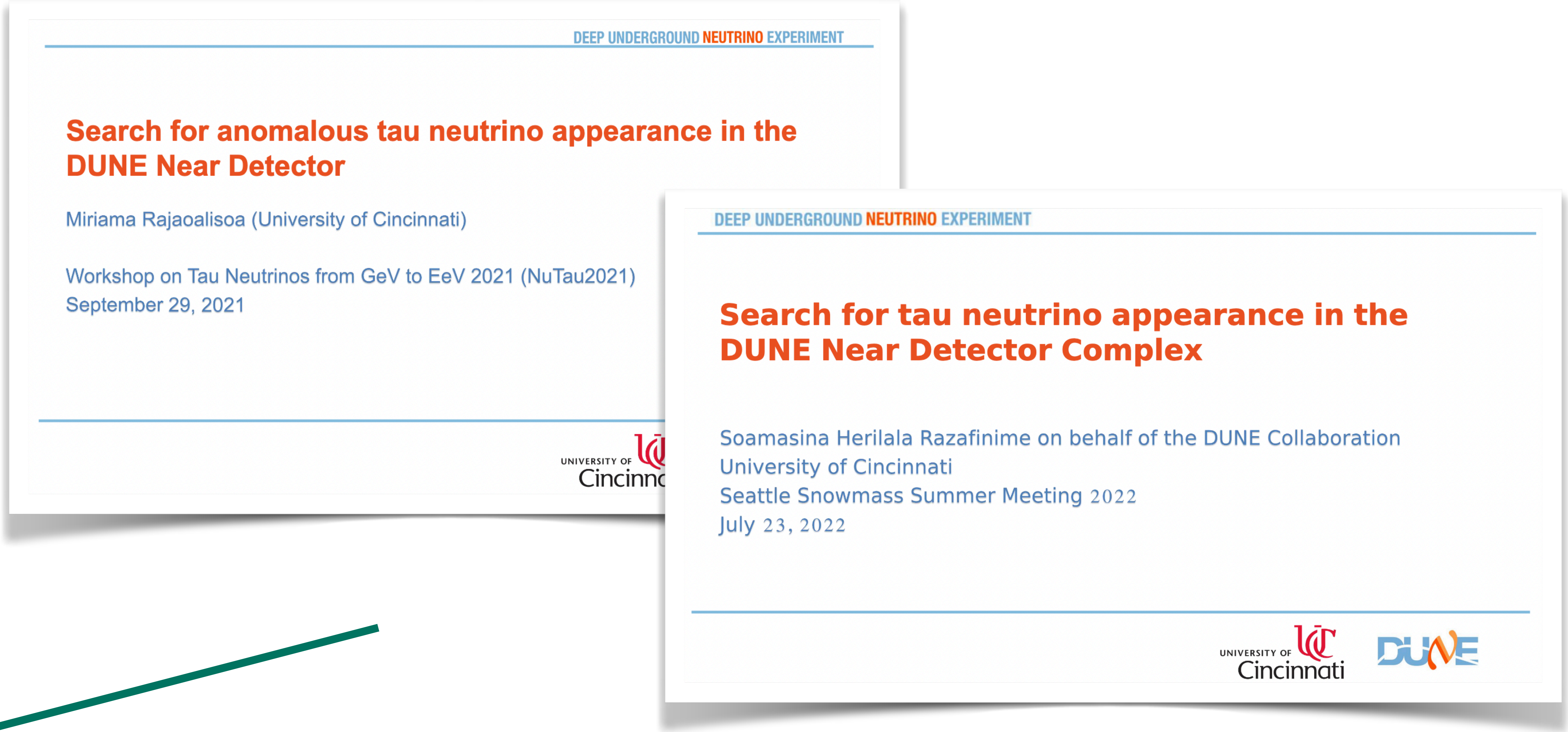

- Signal vs background based on kinematic differences using a BDT.
- Short-baseline $\nu_s \to \nu_\tau$

Rank-1 Discriminator

$$R^T_{\text{Miss}} = \frac{p^T_{\text{Miss}}}{p^T_{\text{Miss}} + p^T_\mu}$$

+

$$\nu_\mu \to \nu_\tau \tau^+ \mu^-$$

- Hadronic τ decays
- Momentum and angular smearing

τ Hadronic Decay Channels

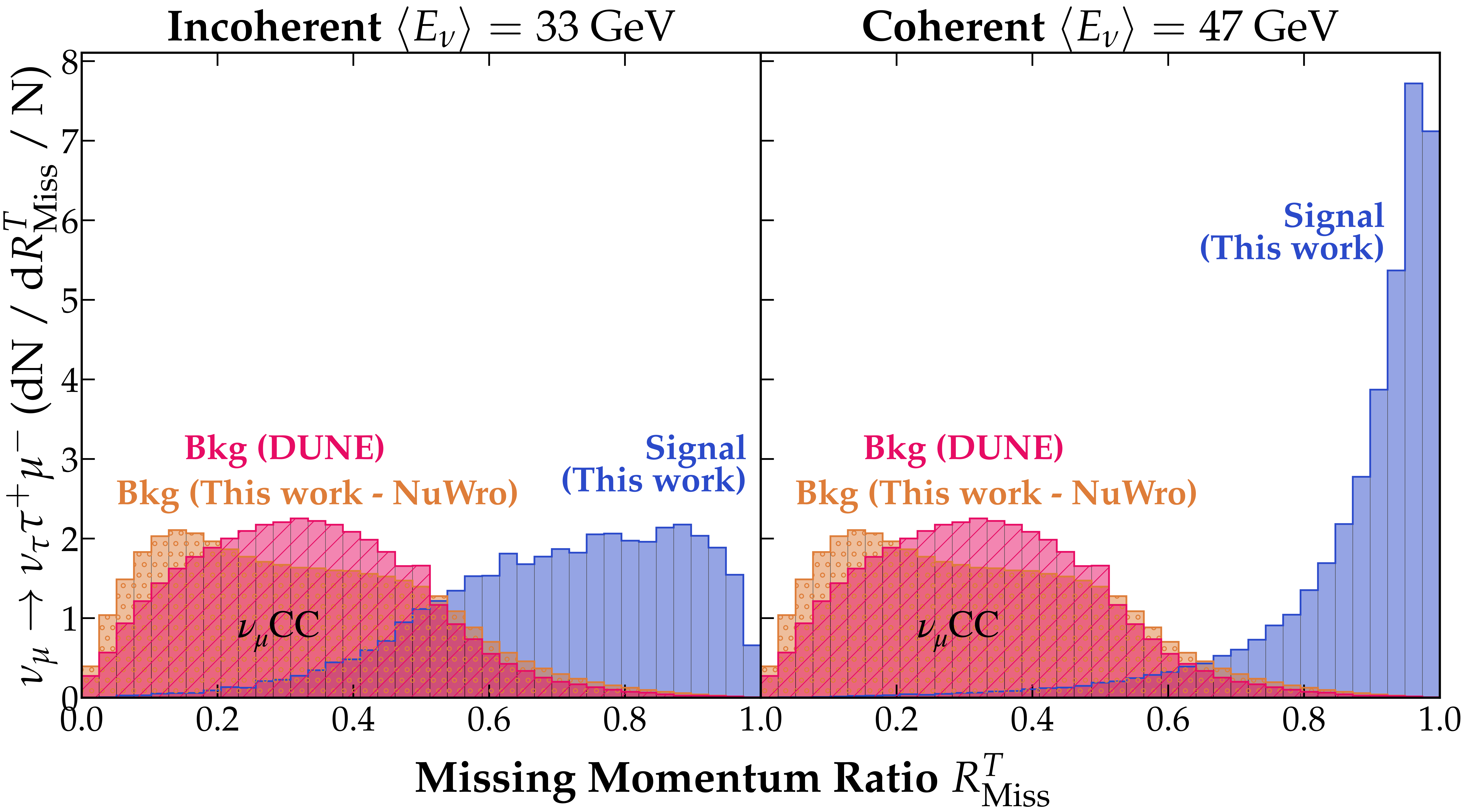

τ Hadronic Decay Channels

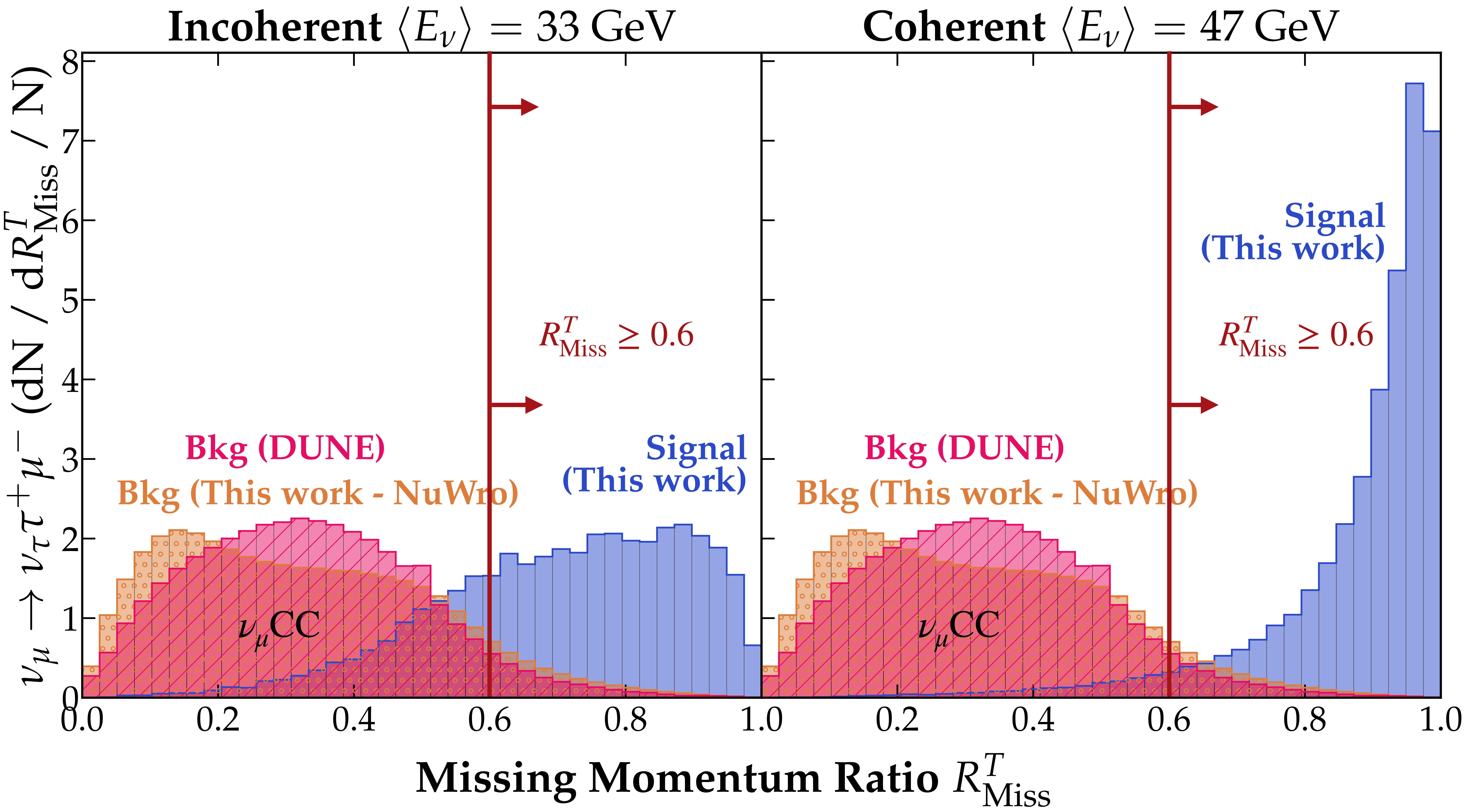

τ Hadronic Decay Channels

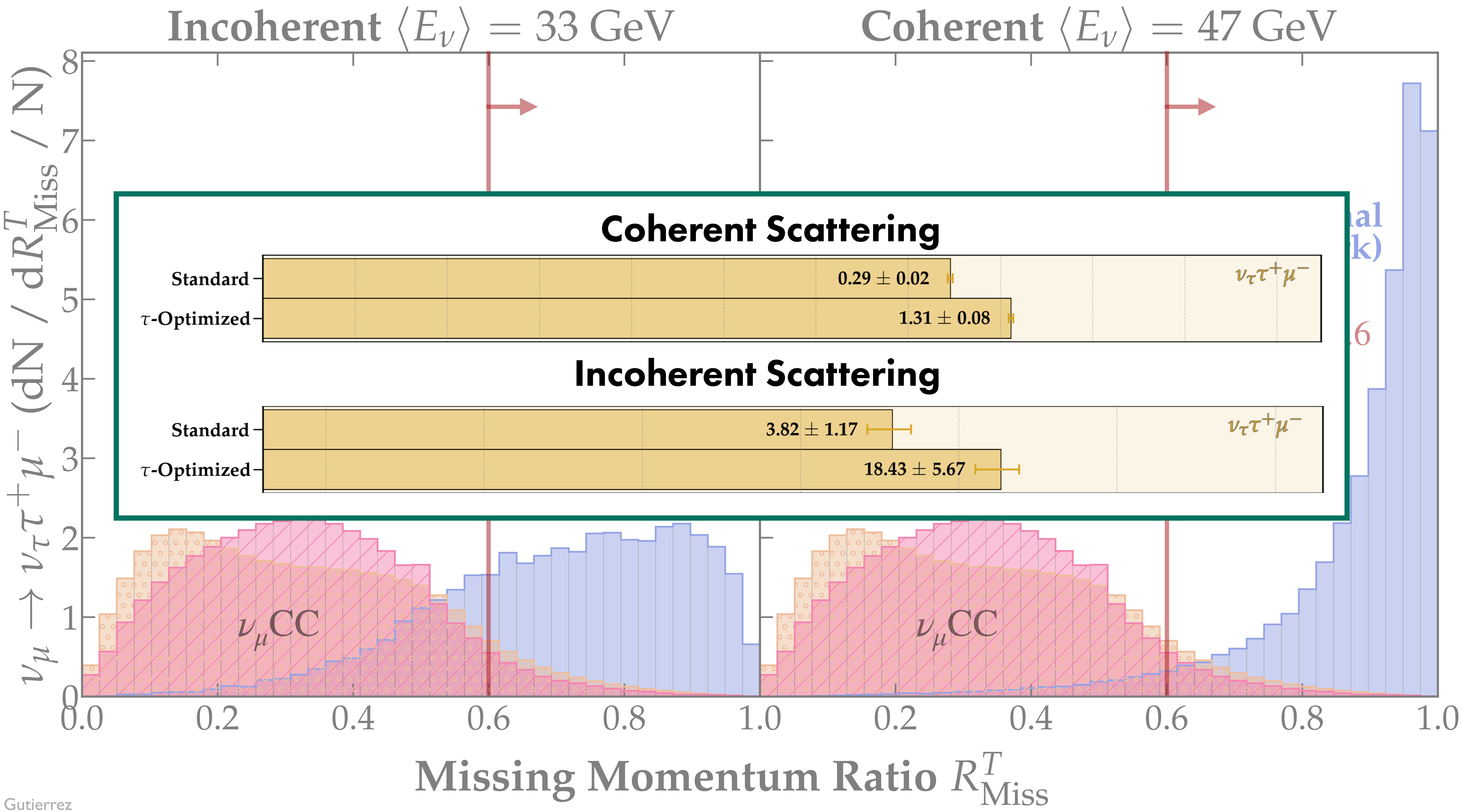

τ Hadronic Decay Channels

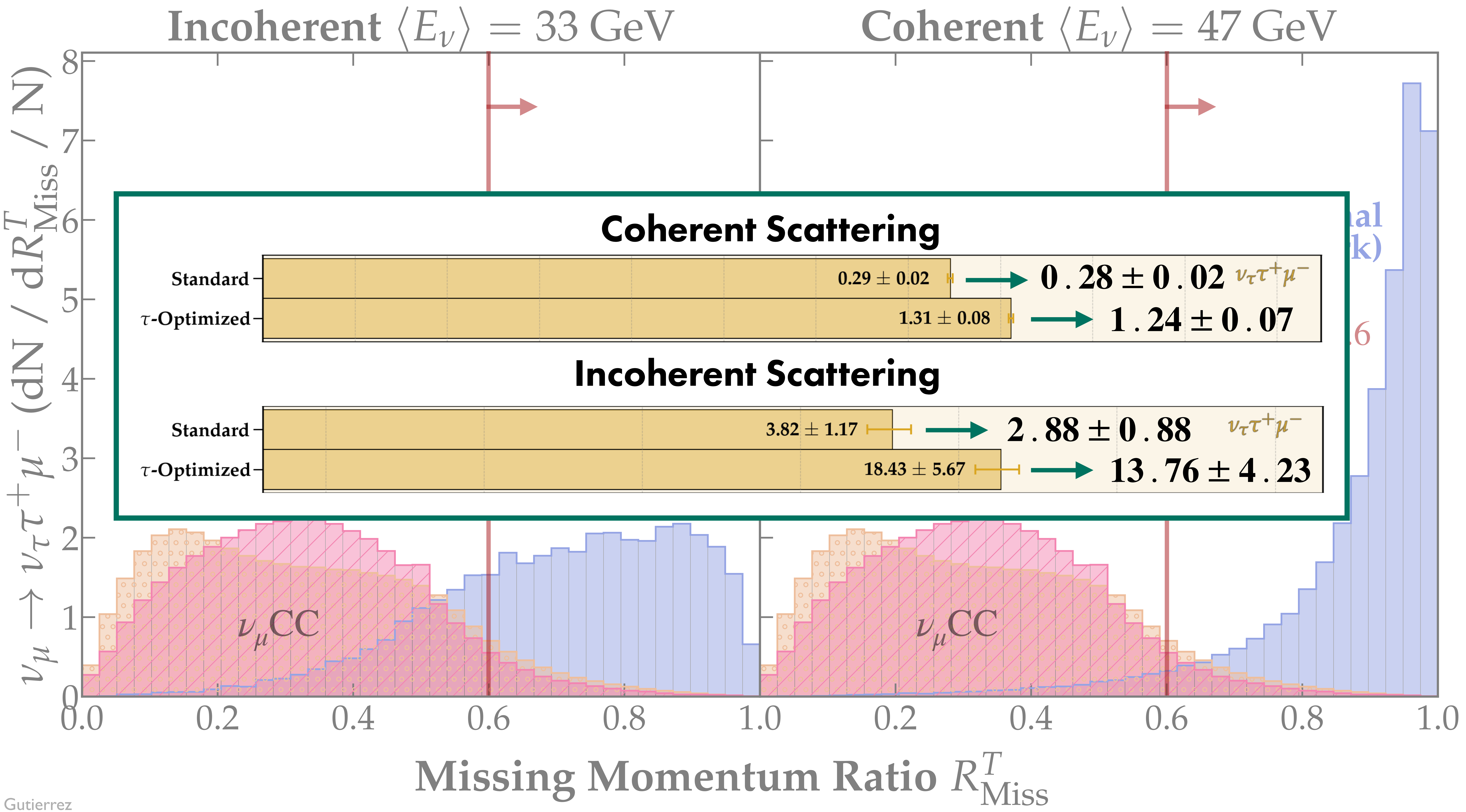

Comparing Form Factors

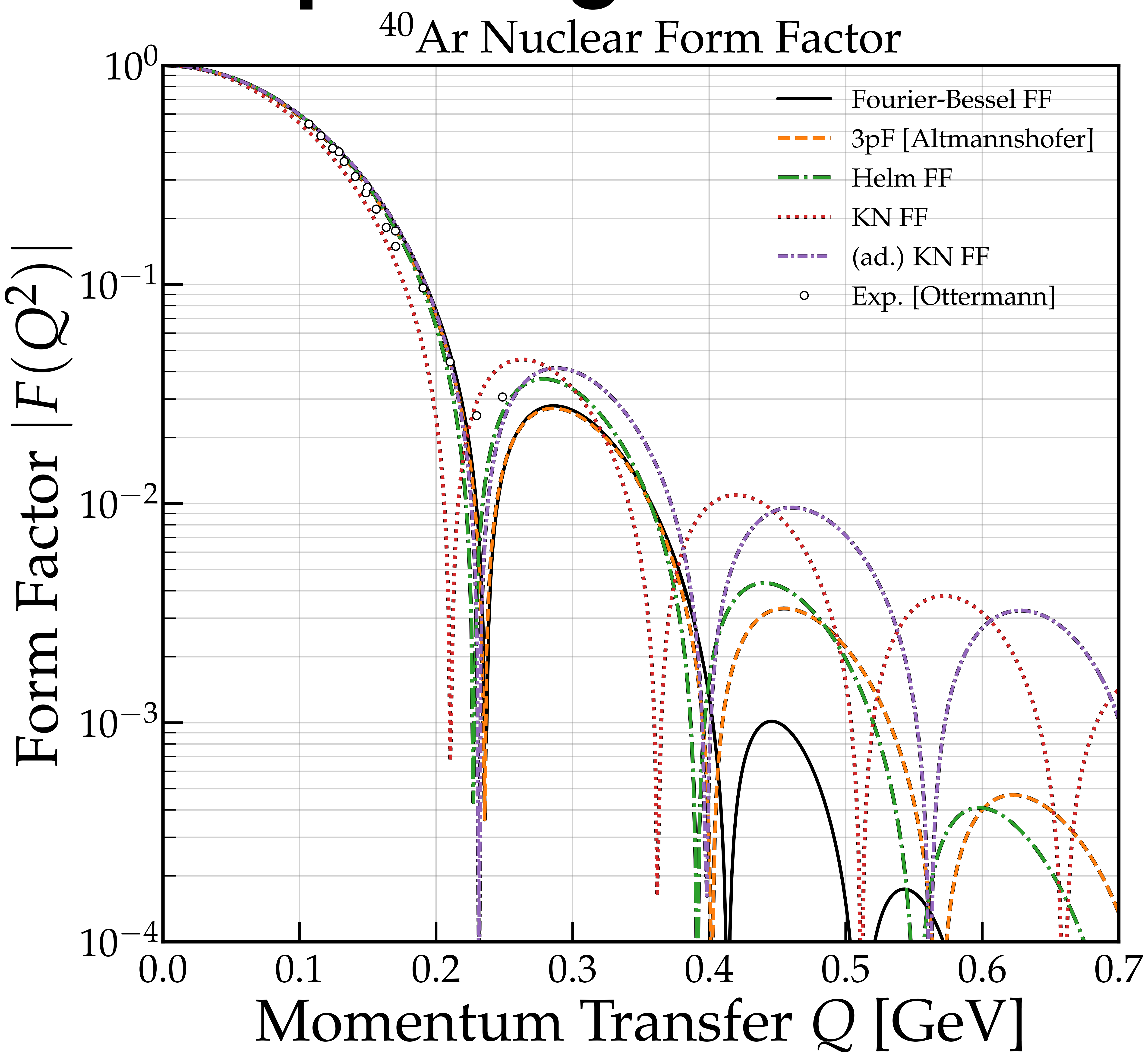

Comparing Form Factors

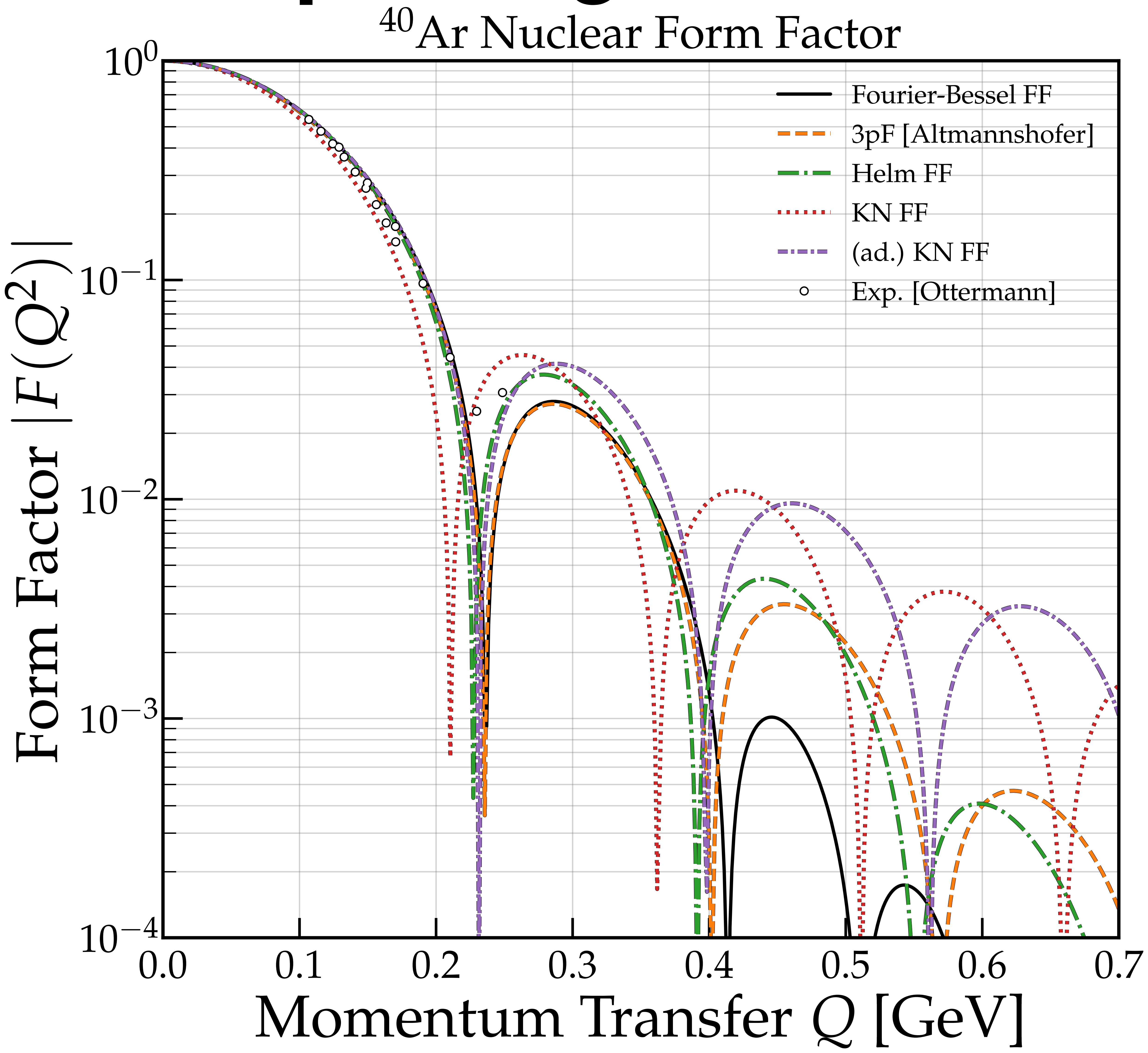

- No experimental data since 1982! And current data only available for $Q \sim 0.11 - 0.26$ GeV.

ELSEVIER

Nuclear Physics A
Volume 379, Issue 3, 10 May 1982, Pages 396-406

Elastic electron scattering from ^{40}Ar

C.R. Ottermann *, CH. Schmitt **, G.G. Simon **, F. Borkowski **, V.H. Walther

Institut für Kernphysik, Johannes Gutenberg-Universität, D-6500 Mainz, Federal Republic of Germany

Abstract

Cross sections for elastic electron scattering from ^{40}Ar have been measured for the momentum transfer range from 0.59 to 1.31 fm^{-1}. We have analyzed with the Fourier-Bessel ansatz our data as well as the data of former experiments. The rms charge radius we have found is 3.423(14) fm. The results are in excellent agreement with latest muonic data. Furthermore, we have reanalyzed former ^{40}Ca data and have discussed the ^{40}Ca-^{40}Ar charge distribution.

Comparing Form Factors

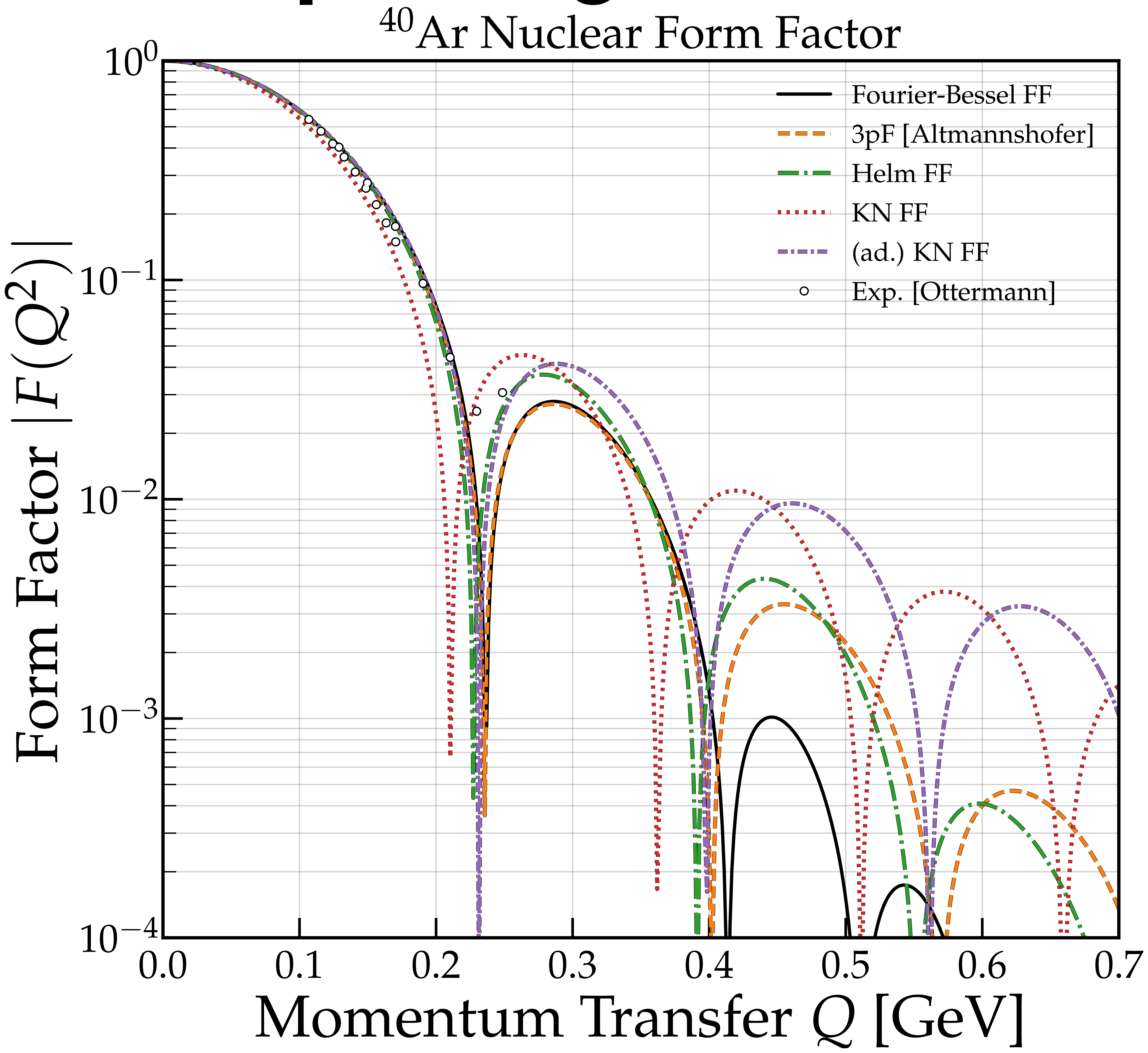

- No experimental data since 1982! And current data only available for $Q \sim 0.11 - 0.26$ GeV.

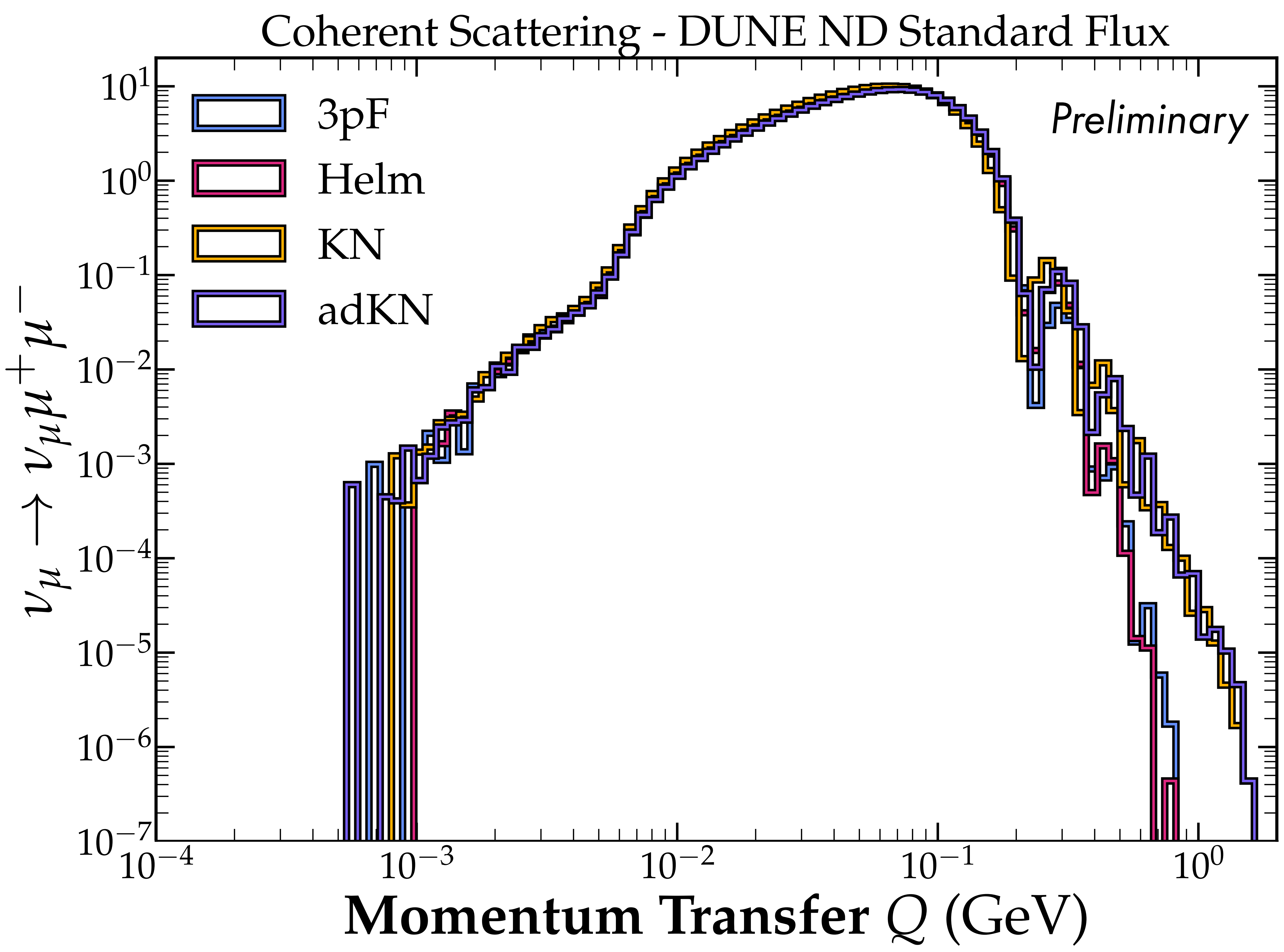

Form Factor Uncertainty

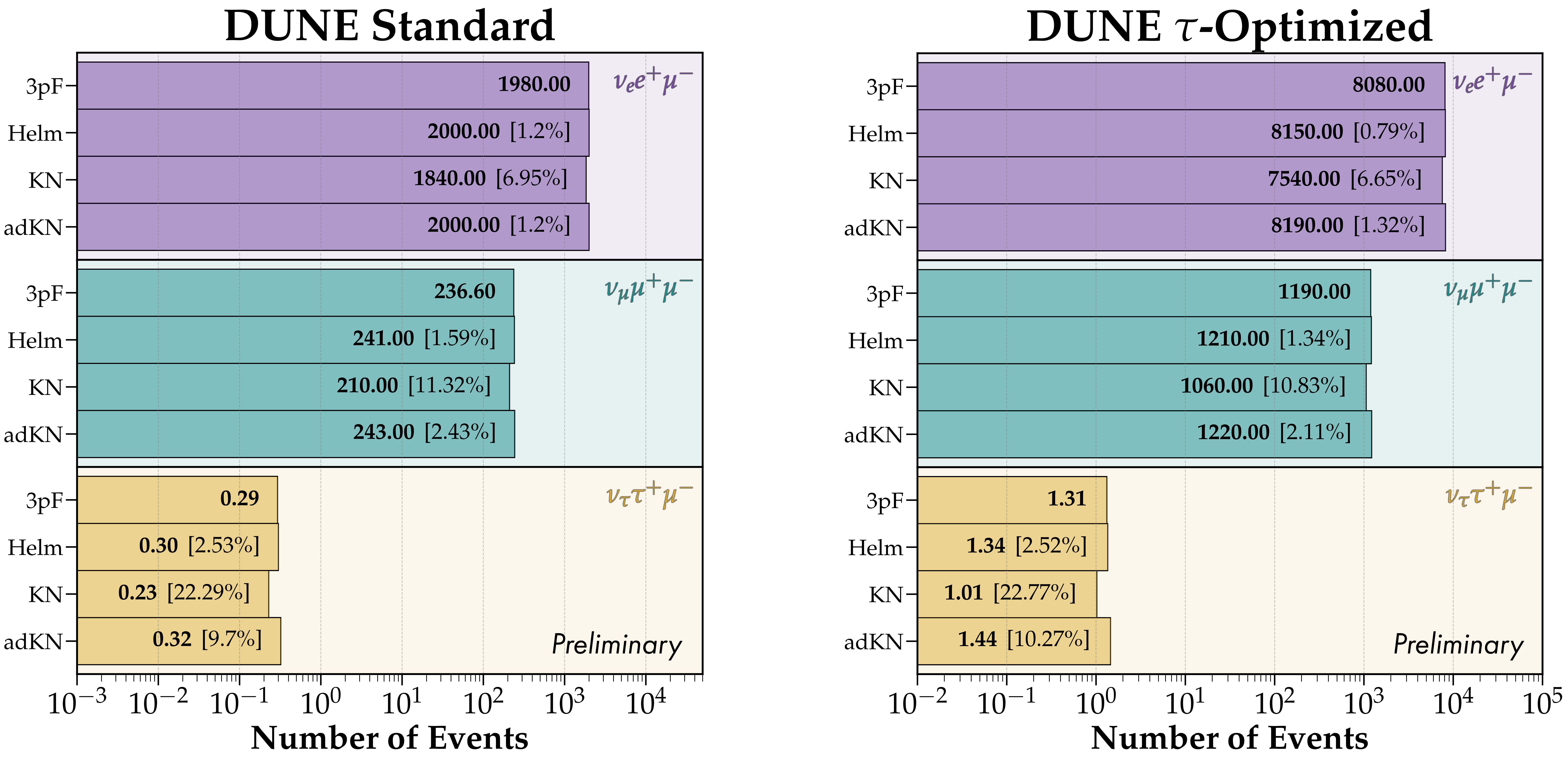

Summary

Summary

What are neutrino tridents and why do we care?

- Precision tests of the SM electroweak sector (both W and Z channels for same-flavored charged leptons).
- τ tridents are **SM processes** that constitute a new source of τ/ν_τ for SM physics and a new background for BSM searches.

Summary

What are neutrino tridents and why do we care?

- Precision tests of the SM electroweak sector (both W and Z channels for same-flavored charged leptons).
- τ tridents are **SM processes** that constitute a new source of τ/ν_τ for SM physics and a new background for BSM searches.

Can we see tridents at DUNE?

- Yes for electron and muon tridents, even after accounting for nuclear modeling uncertainties.
- DUNE ND, particularly when running in τ-optimized mode, will probe τ tridents with a potential detection of $\nu_\mu \to \nu_\tau \tau^+ \mu^-$ after 3 years of running.

Summary

What are neutrino tridents and why do we care?

- Precision tests of the SM electroweak sector (both W and Z channels for same-flavored charged leptons).
- τ tridents are **SM processes** that constitute a new source of τ/ν_τ for SM physics and a new background for BSM searches.

Can we see tridents at DUNE?

- Yes for electron and muon tridents, even after accounting for nuclear modeling uncertainties.
- DUNE ND, particularly when running in τ-optimized mode, will probe τ tridents with a potential detection of $\nu_\mu \to \nu_\tau \tau^+ \mu^-$ after 3 years of running.

Is there hope of detecting $\nu_\mu \to \nu_\tau \tau^+ \mu^-$?

- Possible with ML optimization tools. Systematic uncertainties, e.g. flux, can similarly be reduced to appropriate levels.
- Discriminants like R^T_{Miss} mitigate the copious ν_μCC background while retaining most signal events, suggesting feasible tau trident reconstruction.

Summary

What are neutrino tridents and why do we care?

- Precision tests of the SM electroweak sector (both W and Z channels for same-flavored charged leptons).
- τ tridents are **SM processes** that constitute a new source of τ/ν_τ for SM physics and a new background for BSM searches.

Can we see tridents at DUNE?

- Yes for electron and muon tridents, even after accounting for nuclear modeling uncertainties.
- DUNE ND, particularly when running in τ-optimized mode, will probe τ tridents with a potential detection of $\nu_\mu \to \nu_\tau \tau^+ \mu^-$ after 3 years of running.

Is there hope of detecting $\nu_\mu \to \nu_\tau \tau^+ \mu^-$?

- Possible with ML optimization tools. Systematic uncertainties, e.g. flux, can similarly be reduced to appropriate levels.
- Discriminants like R^T_{Miss} mitigate the copious ν_μCC background while retaining most signal events, suggesting feasible tau trident reconstruction.

Thank you!

Back-up Slides

$\nu_\mu \to \nu_\tau \tau^+ \mu^-$ Event Distribution

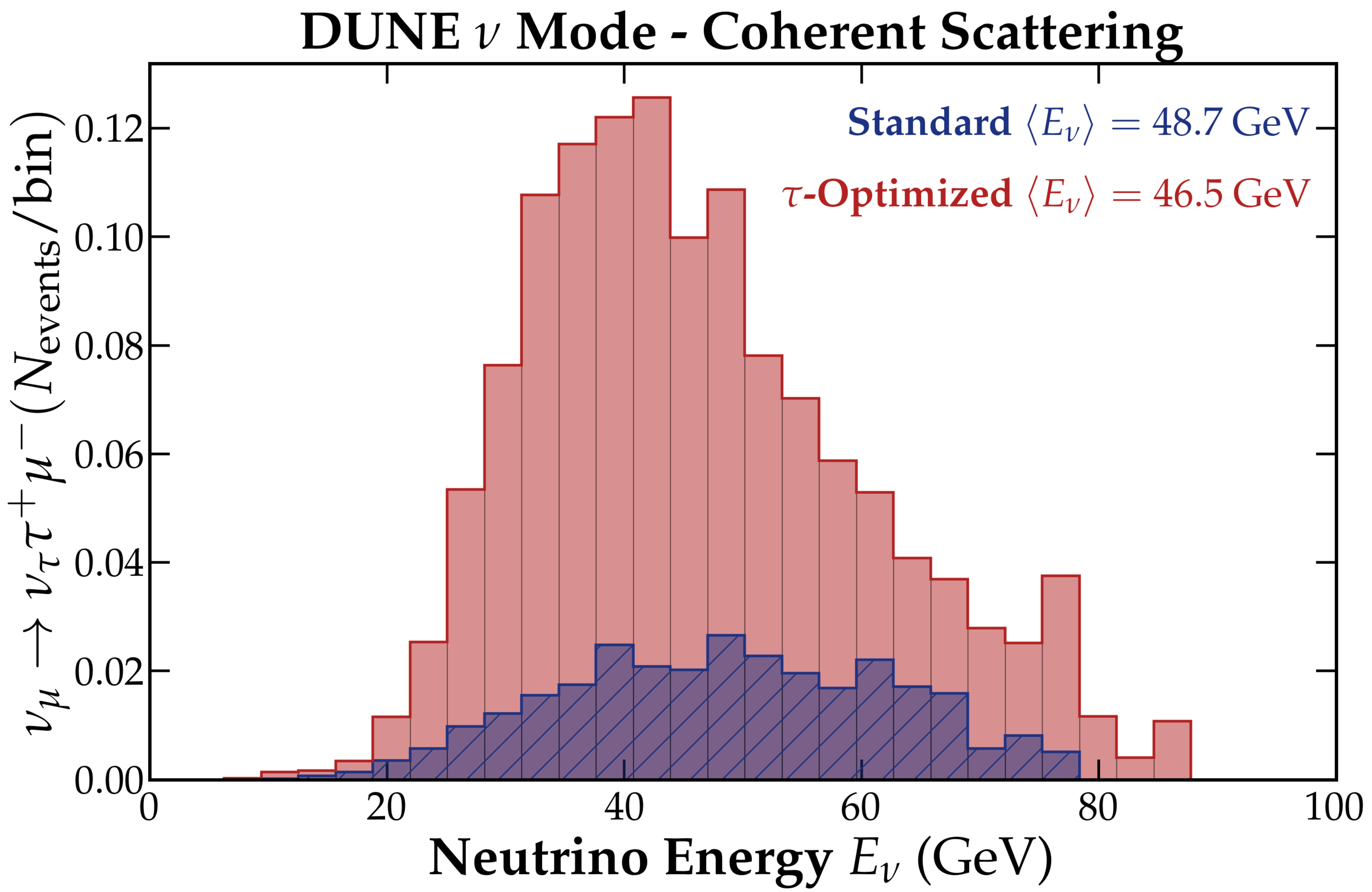

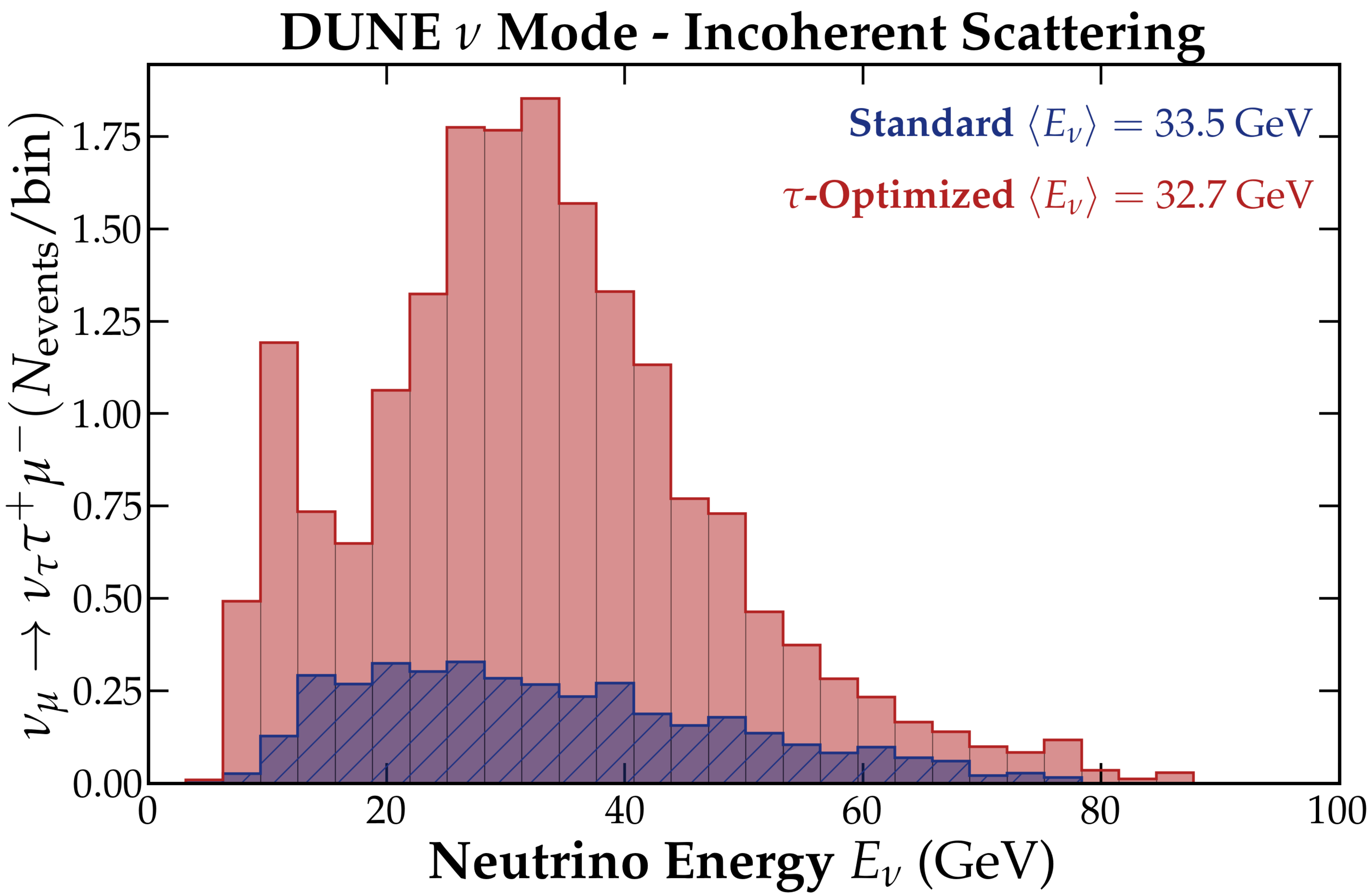

Cross Sections

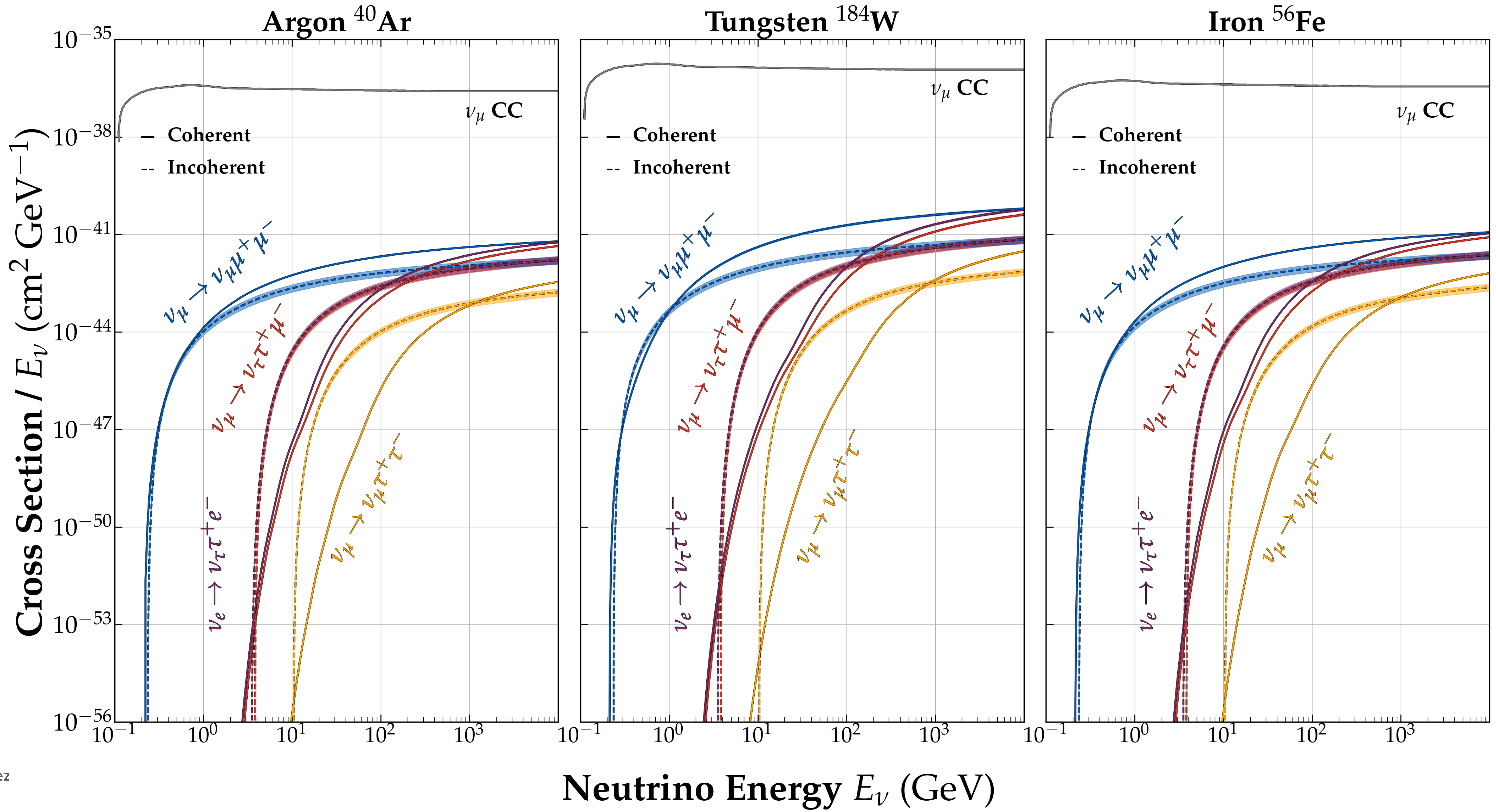

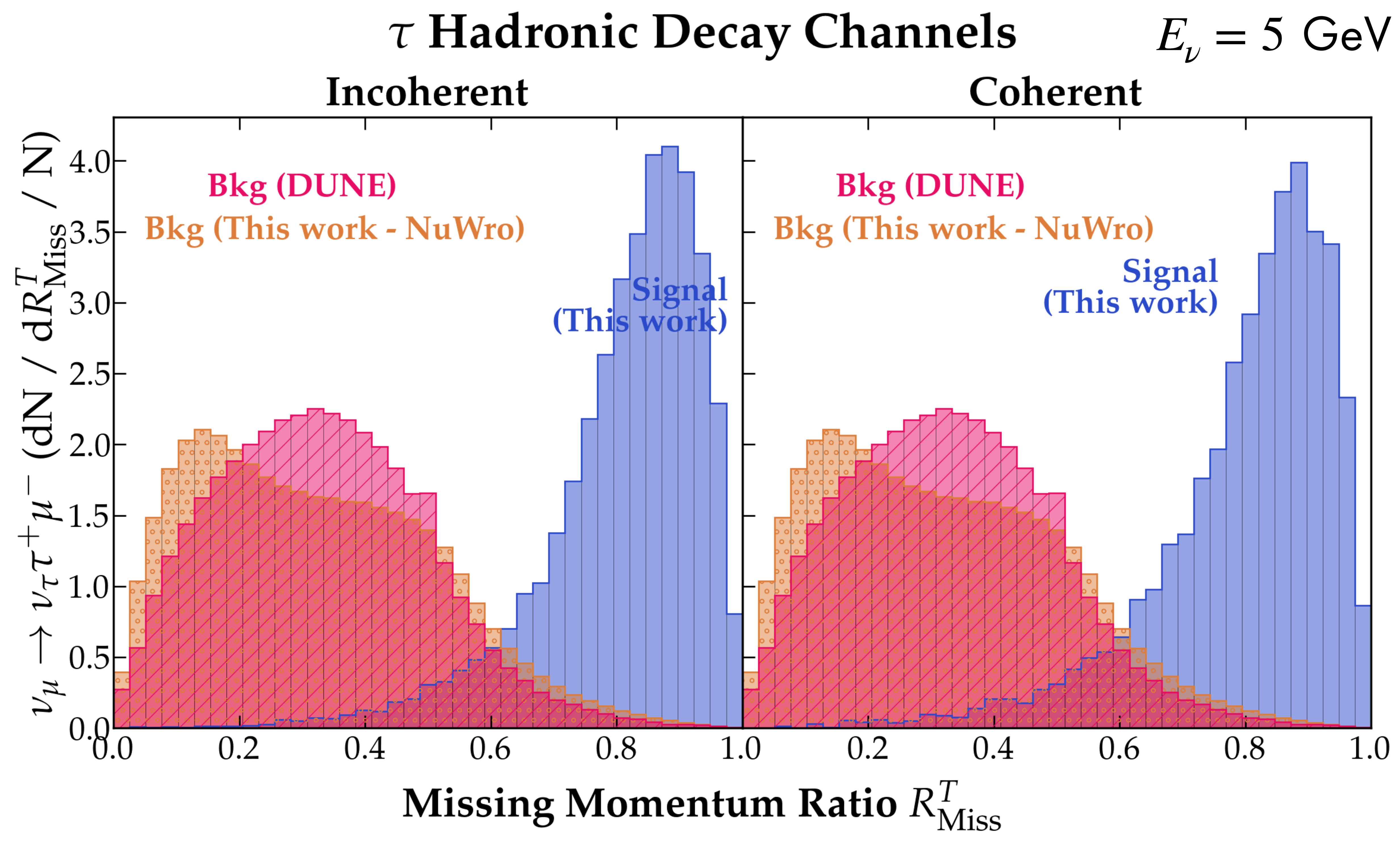

τ Hadronic Decay Channels
$E_\nu = 5$ GeV
Incoherent
Coherent
Bkg (DUNE)
Bkg (This work - NuWro)
Signal
(This work)
$\nu_\mu \to \nu_\tau \tau^+ \mu^-$ (dN / d$R^T_{\rm Miss}$ / N)
Missing Momentum Ratio $R^T_{\rm Miss}$

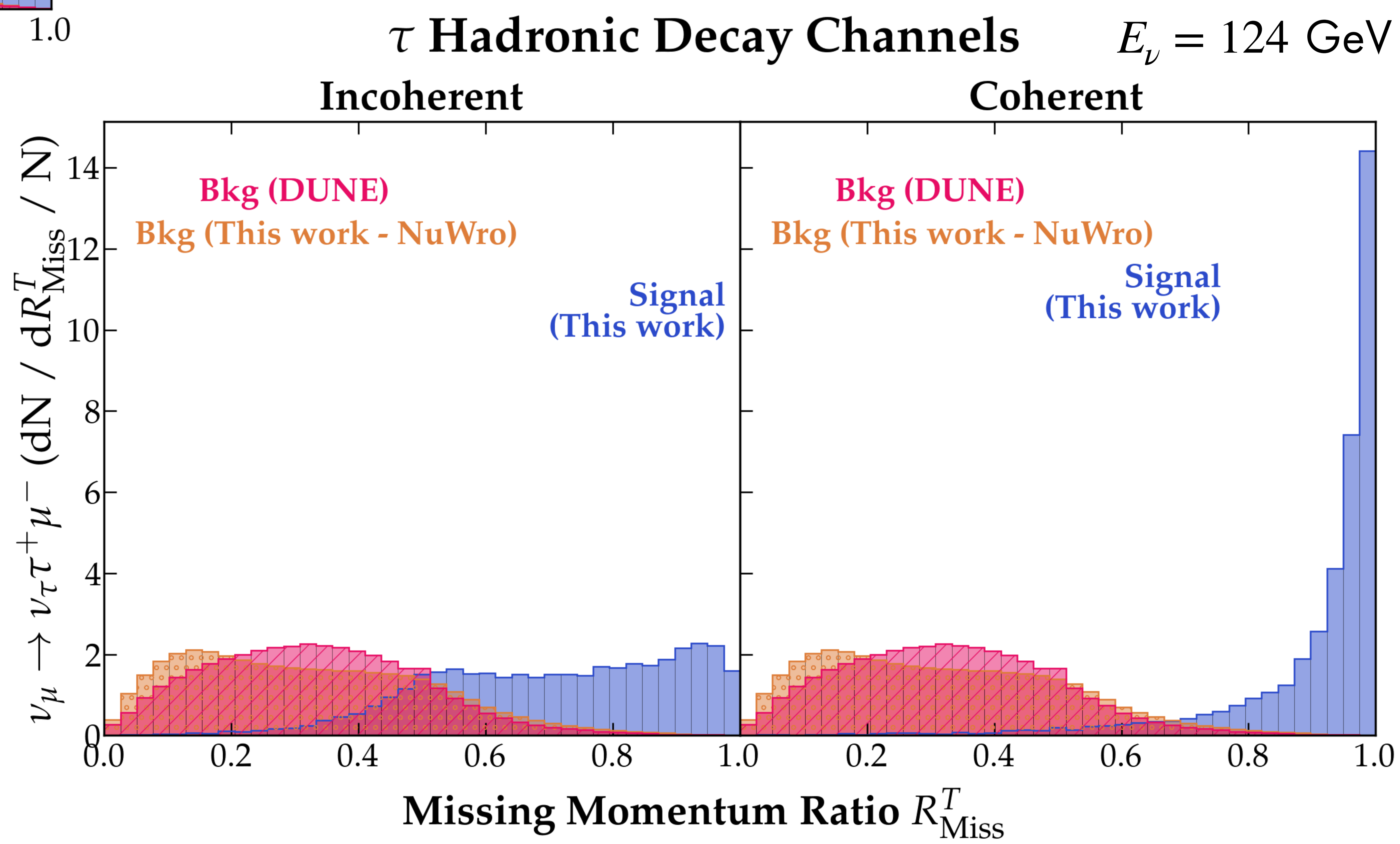

τ Hadronic Decay Channels
$E_\nu = 124$ GeV
Incoherent
Coherent
Bkg (DUNE)
Bkg (This work - NuWro)
Signal
(This work)
$\nu_\mu \to \nu_\tau \tau^+ \mu^-$ (dN / d$R^T_{\rm Miss}$ / N)
Missing Momentum Ratio $R^T_{\rm Miss}$

DUNE

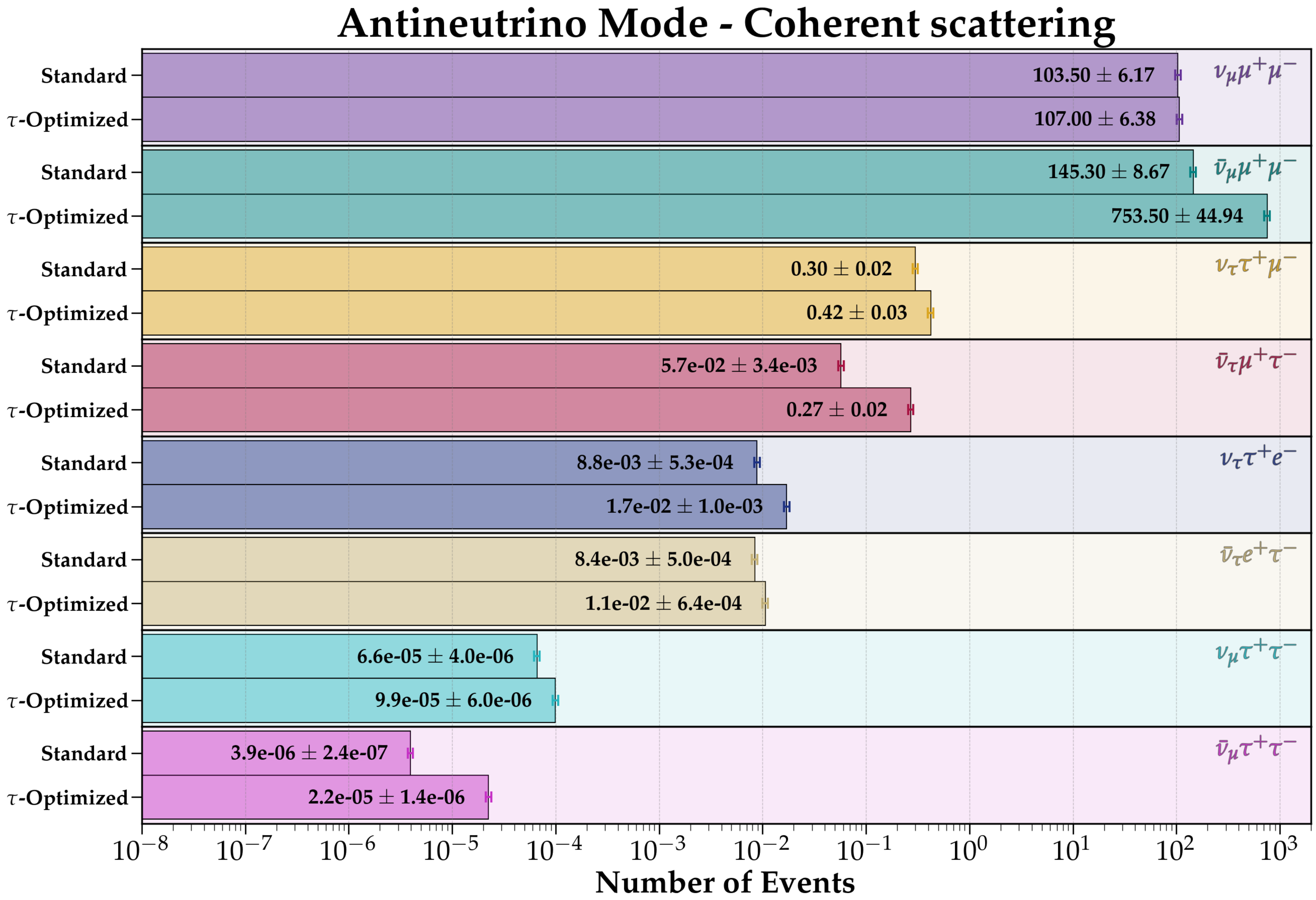

D. Lopez Gutierrez

DUNE

Antineutrino Mode - Incoherent scattering

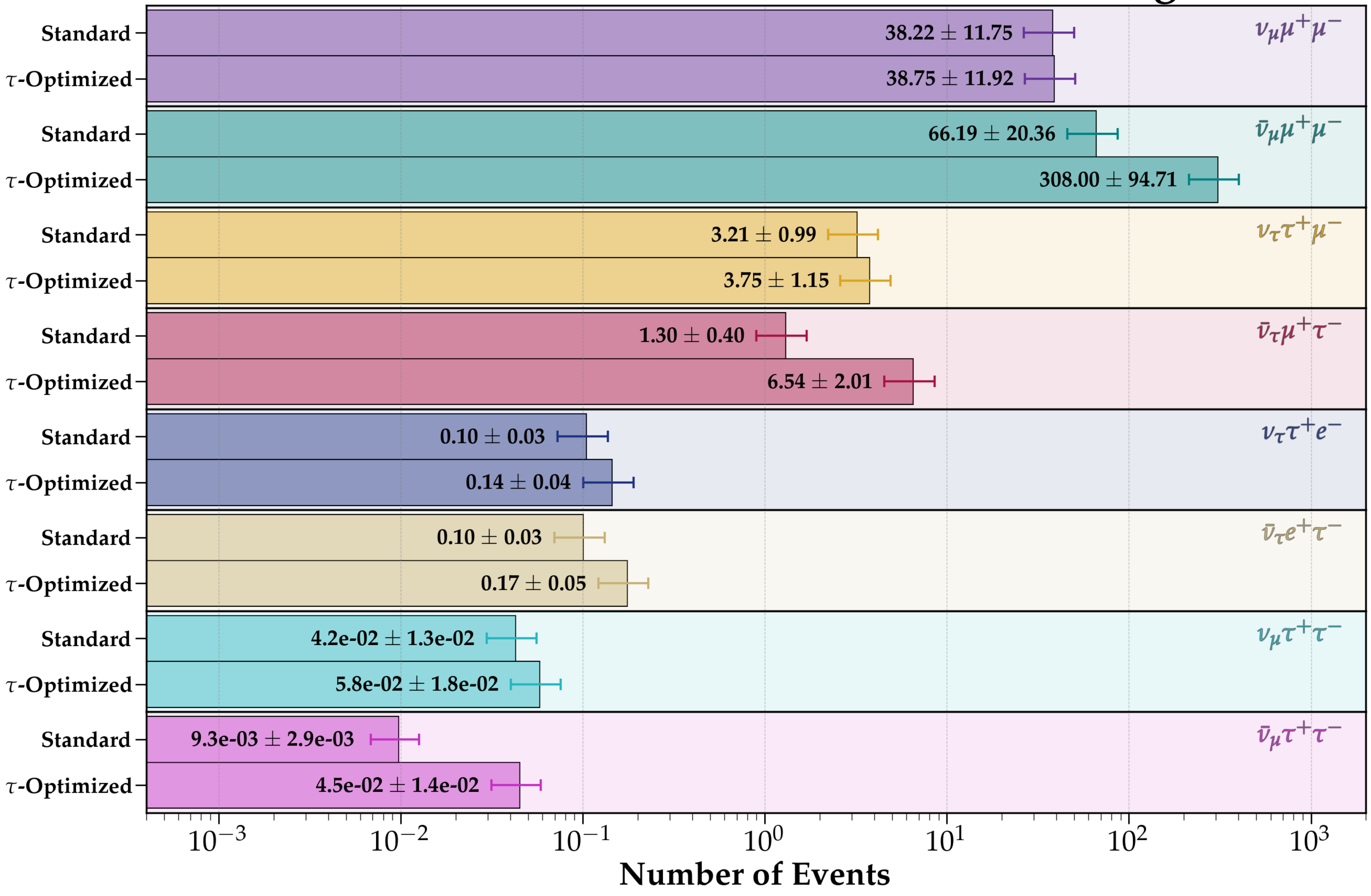

FASERν

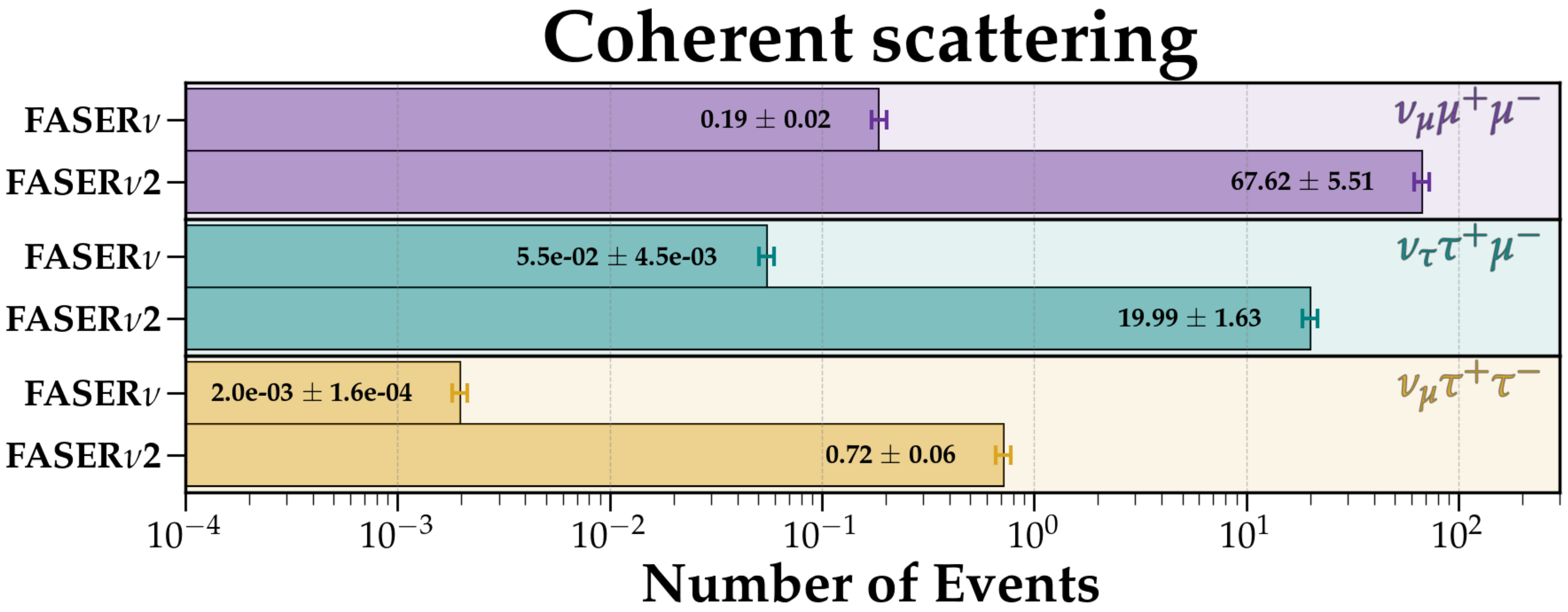

Coherent scattering
FASERν
FASERν2
0.19 ± 0.02
67.62 ± 5.51
$\nu_\mu \mu^+ \mu^-$
5.5e-02 ± 4.5e-03
19.99 ± 1.63
$\nu_\tau \tau^+ \mu^-$
2.0e-03 ± 1.6e-04
0.72 ± 0.06
$\nu_\mu \tau^+ \tau^-$
10^{-4} 10^{-3} 10^{-2} 10^{-1} 10^{0} 10^{1} 10^{2}
Number of Events

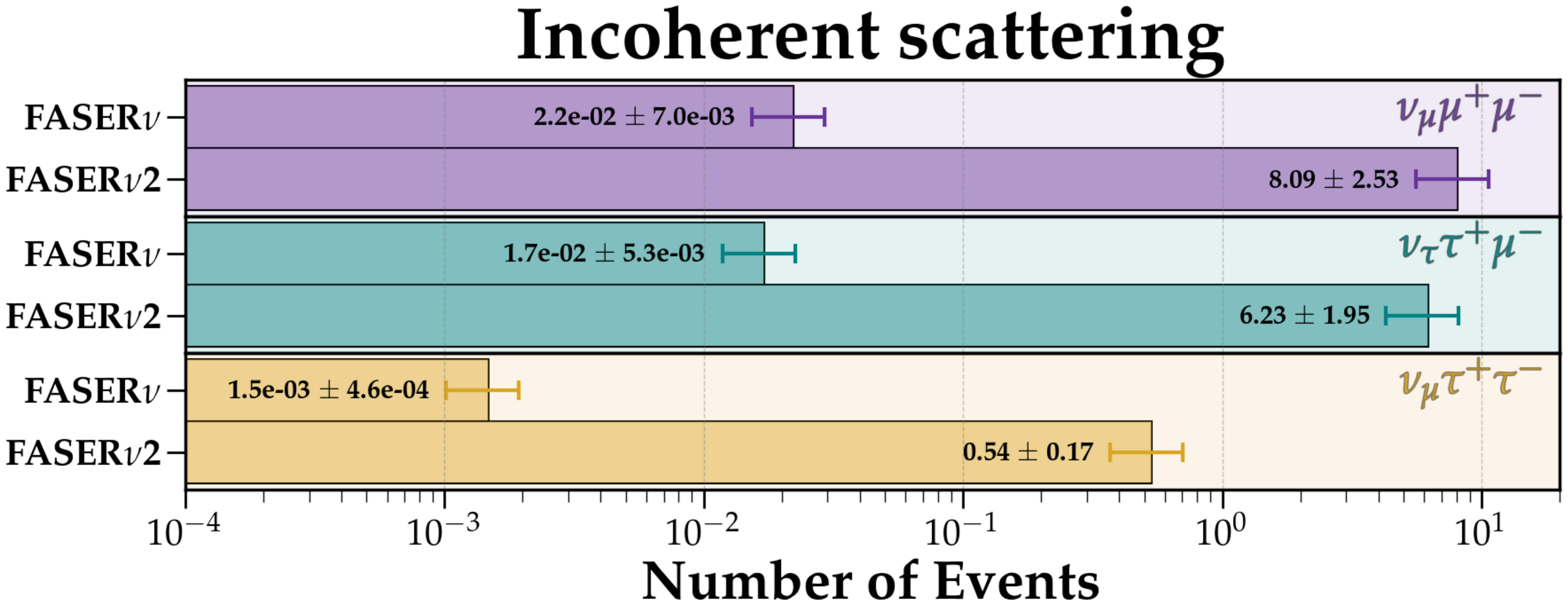

Incoherent scattering
FASERν
FASERν2
2.2e-02 ± 7.0e-03
8.09 ± 2.53
$\nu_\mu \mu^+ \mu^-$
1.7e-02 ± 5.3e-03
6.23 ± 1.95
$\nu_\tau \tau^+ \mu^-$
1.5e-03 ± 4.6e-04
0.54 ± 0.17
$\nu_\mu \tau^+ \tau^-$
10^{-4} 10^{-3} 10^{-2} 10^{-1} 10^{0} 10^{1}
Number of Events

T2K-INGRID

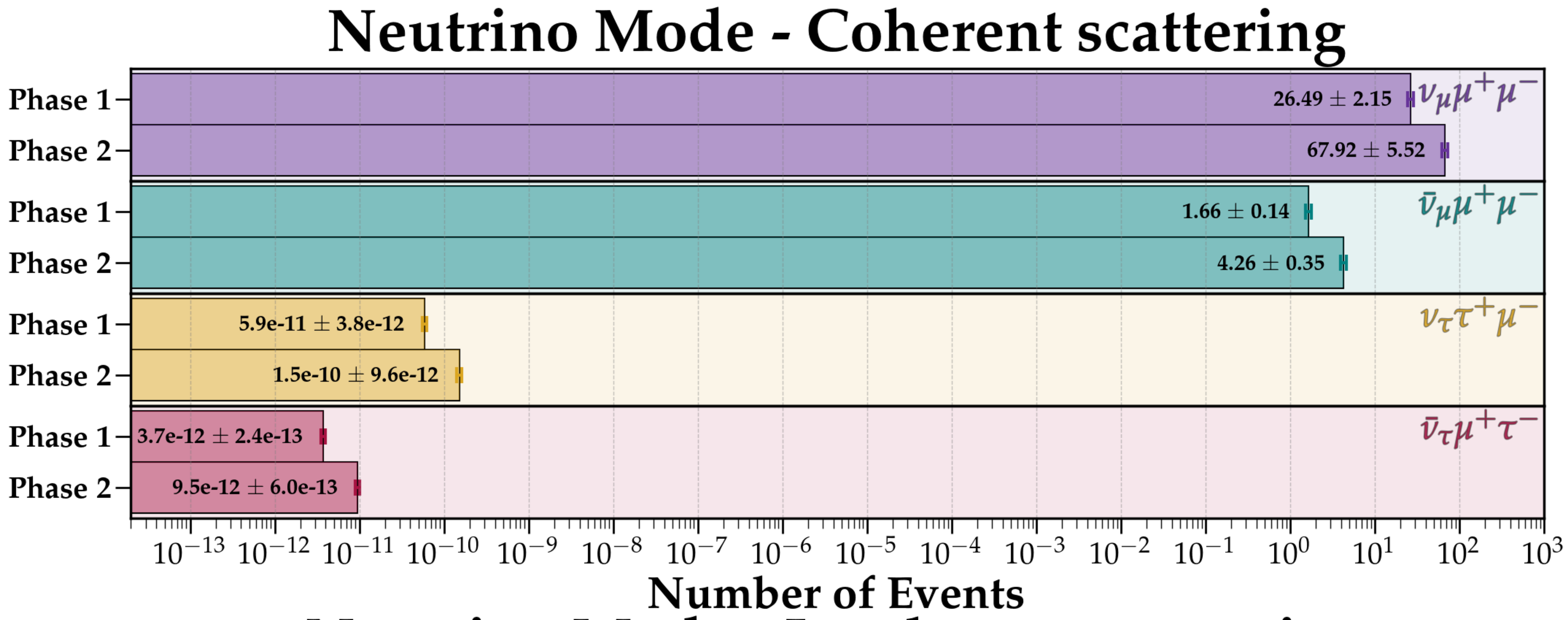

Neutrino Mode - Coherent scattering
Phase 1
Phase 2
26.49 ± 2.15
67.92 ± 5.52
$\nu_\mu \mu^+ \mu^-$
1.66 ± 0.14
4.26 ± 0.35
$\bar{\nu}_\mu \mu^+ \mu^-$
5.9e-11 ± 3.8e-12
1.5e-10 ± 9.6e-12
$\nu_\tau \tau^+ \mu^-$
3.7e-12 ± 2.4e-13
9.5e-12 ± 6.0e-13
$\bar{\nu}_\tau \mu^+ \tau^-$
Number of Events

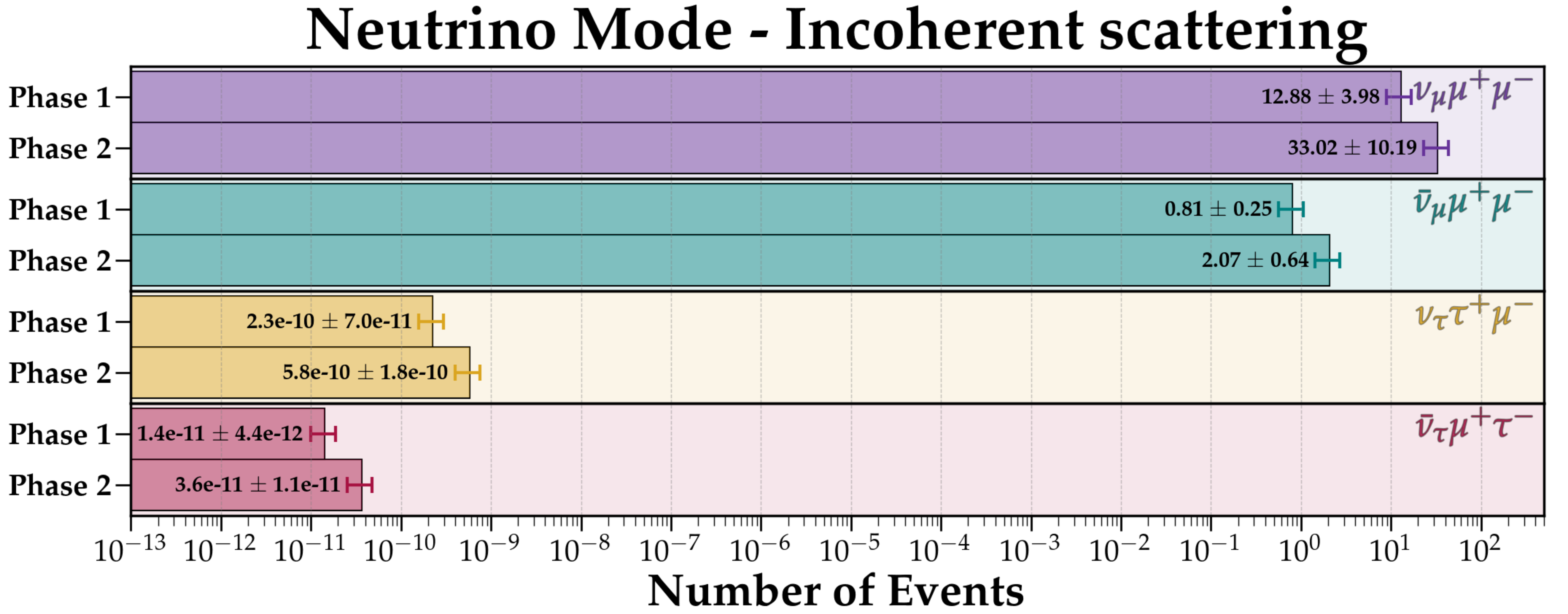

Neutrino Mode - Incoherent scattering
Phase 1
Phase 2
12.88 ± 3.98
33.02 ± 10.19
$\nu_\mu \mu^+ \mu^-$
0.81 ± 0.25
2.07 ± 0.64
$\bar{\nu}_\mu \mu^+ \mu^-$
2.3e-10 ± 7.0e-11
5.8e-10 ± 1.8e-10
$\nu_\tau \tau^+ \mu^-$
1.4e-11 ± 4.4e-12
3.6e-11 ± 1.1e-11
$\bar{\nu}_\tau \mu^+ \tau^-$
Number of Events

MINOS

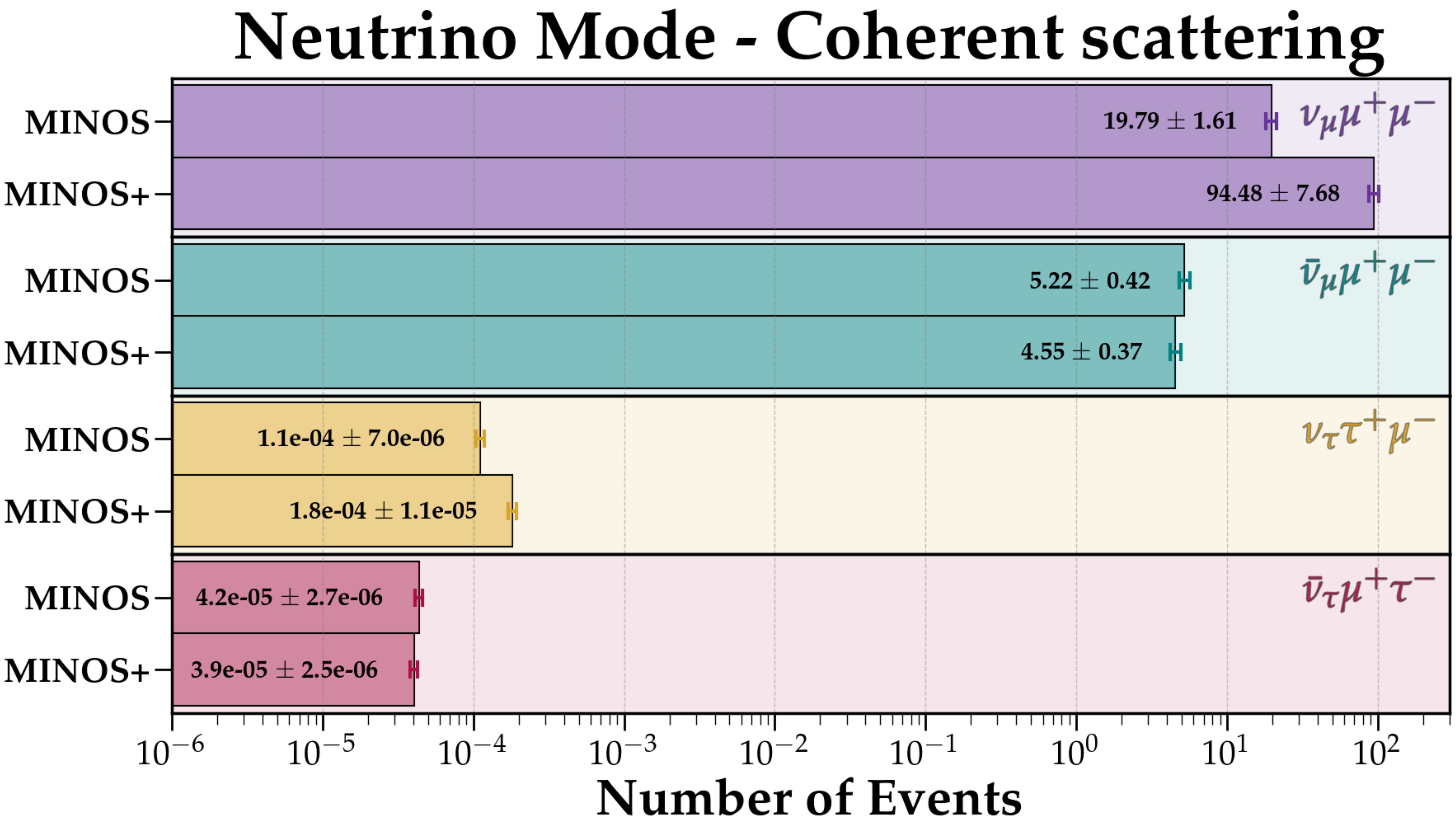

Neutrino Mode - Coherent scattering
MINOS
MINOS+
MINOS
MINOS+
MINOS
MINOS+
MINOS
MINOS+
19.79 ± 1.61
94.48 ± 7.68
$\nu_\mu \mu^+ \mu^-$
5.22 ± 0.42
4.55 ± 0.37
$\bar{\nu}_\mu \mu^+ \mu^-$
1.1e-04 ± 7.0e-06
1.8e-04 ± 1.1e-05
$\nu_\tau \tau^+ \mu^-$
4.2e-05 ± 2.7e-06
3.9e-05 ± 2.5e-06
$\bar{\nu}_\tau \mu^+ \tau^-$
10^{-6} 10^{-5} 10^{-4} 10^{-3} 10^{-2} 10^{-1} 10^{0} 10^{1} 10^{2}
Number of Events

MINOS

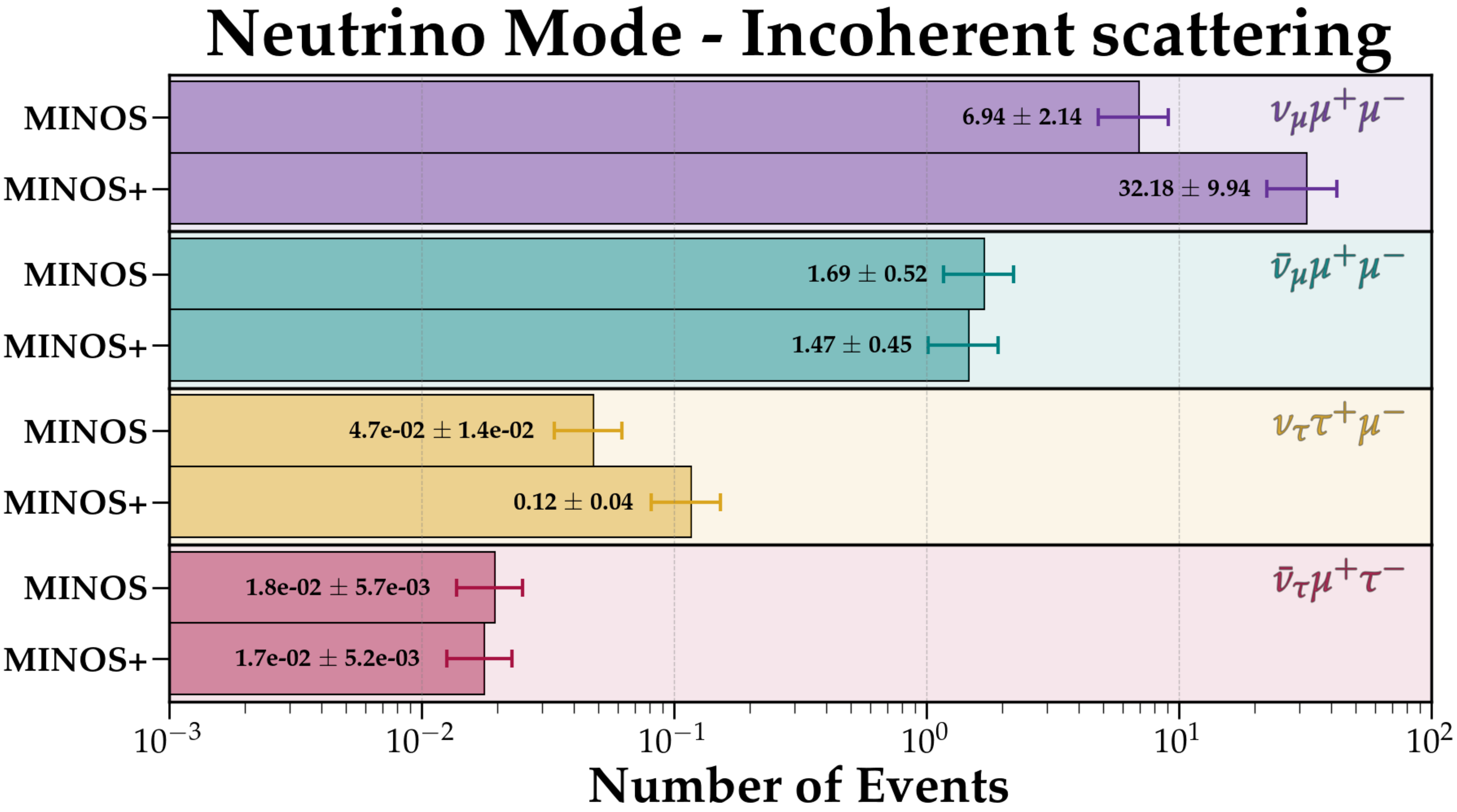

Neutrino Mode - Incoherent scattering
MINOS
MINOS+
6.94 ± 2.14
32.18 ± 9.94
$\nu_\mu \mu^+ \mu^-$
1.69 ± 0.52
1.47 ± 0.45
$\bar{\nu}_\mu \mu^+ \mu^-$
4.7e-02 ± 1.4e-02
0.12 ± 0.04
$\nu_\tau \tau^+ \mu^-$
1.8e-02 ± 5.7e-03
1.7e-02 ± 5.2e-03
$\bar{\nu}_\tau \mu^+ \tau^-$
10^{-3} 10^{-2} 10^{-1} 10^{0} 10^{1} 10^{2}
Number of Events

MINOS

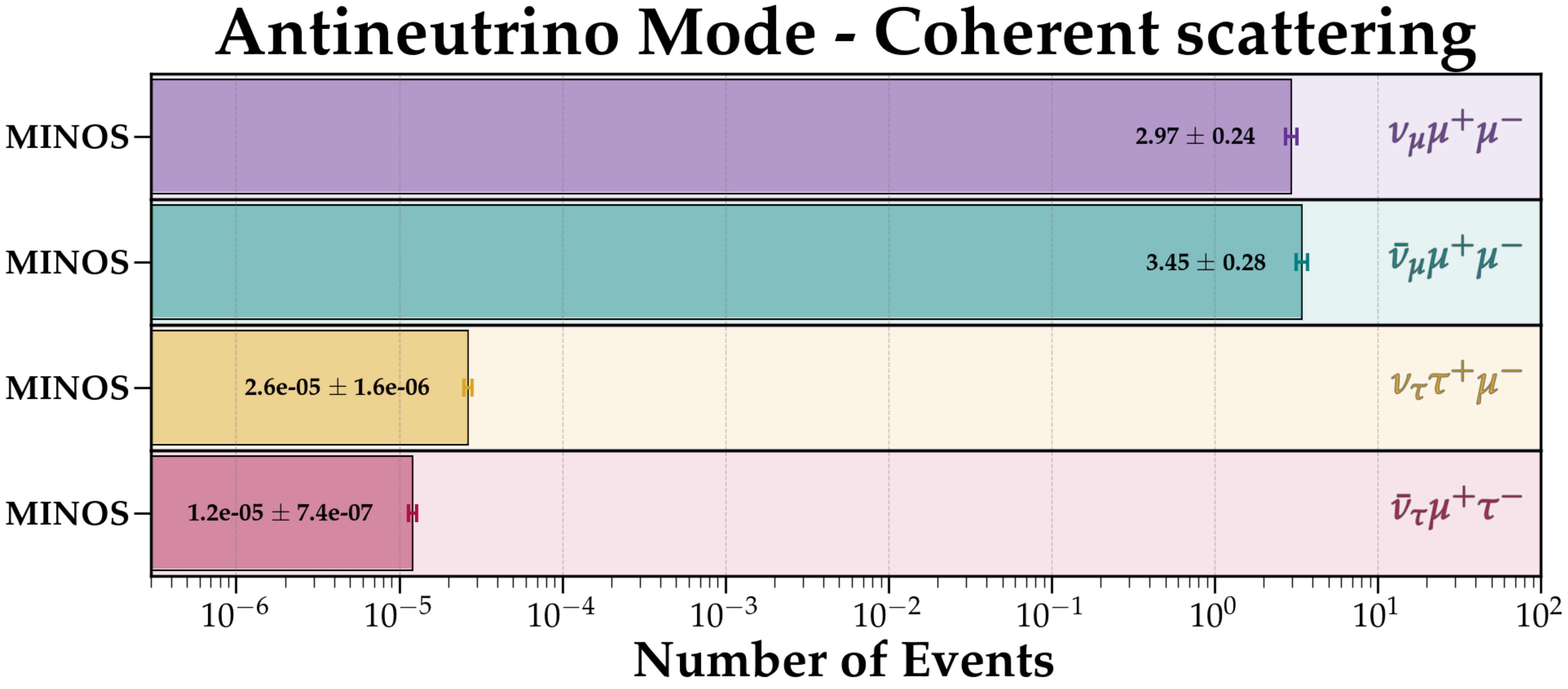
Antineutrino Mode - Coherent scattering
MINOS
MINOS
MINOS
MINOS
2.97 ± 0.24
3.45 ± 0.28
2.6e-05 ± 1.6e-06
1.2e-05 ± 7.4e-07
$\nu_\mu \mu^+ \mu^-$
$\bar{\nu}_\mu \mu^+ \mu^-$
$\nu_\tau \tau^+ \mu^-$
$\bar{\nu}_\tau \mu^+ \tau^-$
10^{-6} 10^{-5} 10^{-4} 10^{-3} 10^{-2} 10^{-1} 10^{0} 10^{1} 10^{2}
Number of Events

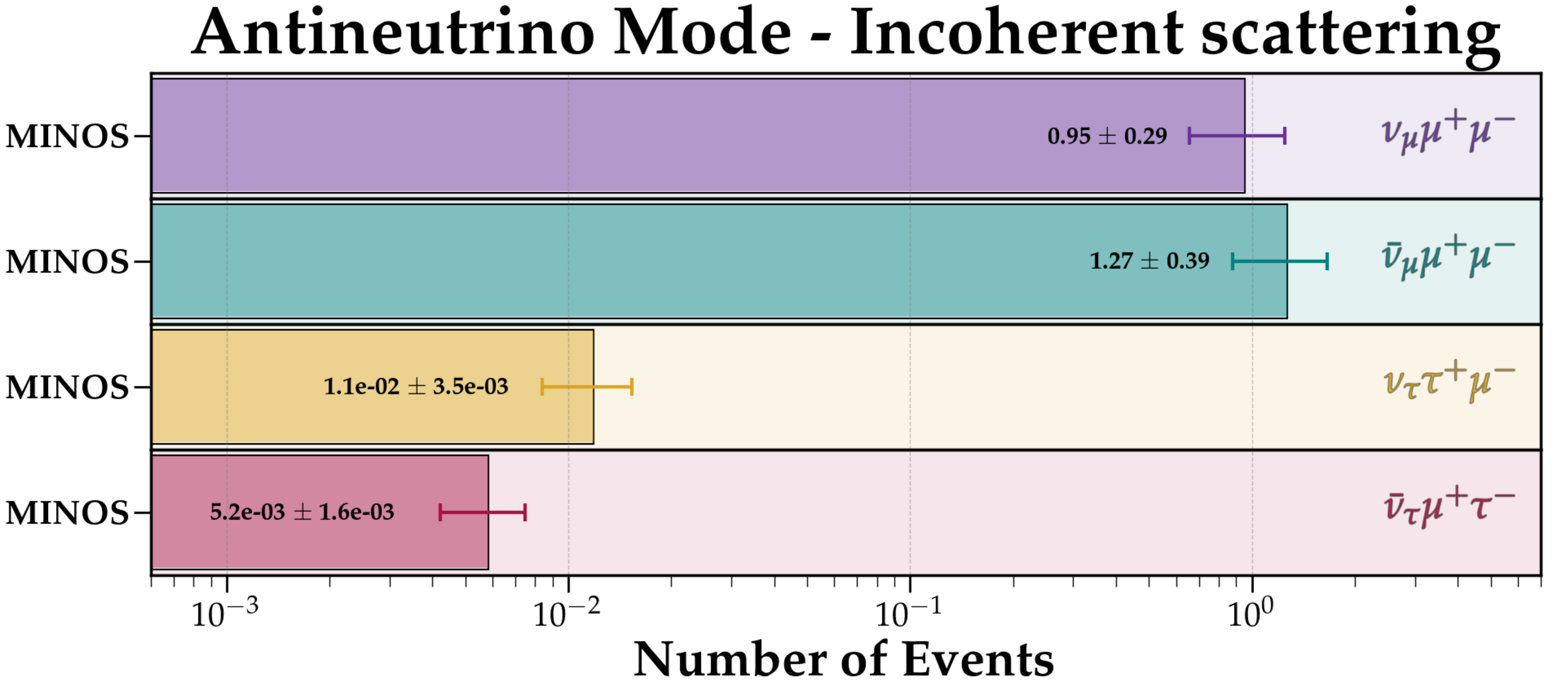
Antineutrino Mode - Incoherent scattering
MINOS
MINOS
MINOS
MINOS
0.95 ± 0.29
1.27 ± 0.39
1.1e-02 ± 3.5e-03
5.2e-03 ± 1.6e-03
$\nu_\mu \mu^+ \mu^-$
$\bar{\nu}_\mu \mu^+ \mu^-$
$\nu_\tau \tau^+ \mu^-$
$\bar{\nu}_\tau \mu^+ \tau^-$
10^{-3} 10^{-2} 10^{-1} 10^{0}
Number of Events